

## **Distribution Agreement**

In presenting this dissertation as a partial fulfillment of the requirements for an advanced degree from Emory University, I hereby grant to Emory University and its agents the non-exclusive license to archive, make accessible, and display my thesis or dissertation in whole or in part in all forms of media, now or hereafter known, including display on the world wide web. I understand that I may select some access restrictions as part of the online submission of this thesis or dissertation. I retain all ownership rights to the copyright of the thesis or dissertation. I also retain the right to use in future works (such as articles or books) all or part of this thesis or dissertation.

Signature:

---

Kate L. Stokes

---

Date

**IDENTIFYING MECHANISMS OF RESPIRATORY SYNCYTIAL VIRUS-  
INDUCED MUCUS**

By  
Kate L. Stokes  
Doctor of Philosophy

Graduate Division of Biological and Biomedical Science  
Immunology and Molecular Pathogenesis

---

Martin L. Moore  
Advisor

---

Timothy L. Denning  
Committee Member

---

Paul A. Rota  
Committee Member

---

David A. Steinhauer  
Committee Member

---

Ifor R. Williams  
Committee Member

Accepted:

---

Lisa A. Tedesco, Ph.D.  
Dean of the James T. Laney School of Graduate Studies

---

Date

**IDENTIFYING MECHANISMS OF RESPIRATORY SYNCYTIAL VIRUS-  
INDUCED MUCUS**

By

Kate L. Stokes

B.S., Rutgers, the State University of New Jersey, 2007

Advisor: Martin L. Moore, Ph.D.

An abstract of a dissertation submitted to the Faculty of the  
James T. Laney School of Graduate Studies of Emory University in partial  
fulfillment of the requirements for the degree of Doctor of Philosophy in  
Graduate Division of Biological and Biomedical Science,  
Immunology and Molecular Pathogenesis

2013

## **ABSTRACT**

### **IDENTIFYING MECHANISMS OF RESPIRATORY SYNCYTIAL VIRUS-INDUCED MUCUS**

**By Kate L. Stokes**

Respiratory syncytial virus (RSV) is the most important cause of bronchiolitis in infants. Viral infection of the bronchiolar epithelium results in destruction of epithelial cells and mucus production, leading to plugs that block airways and cause breathing difficulty. Disease severity has been correlated with RSV genotype; however, the impact of strain differences remains unclear.

We hypothesized that the pathogenesis of RSV disease is strain specific and used low-passage clinical isolates to examine differences in the BALB/cJ mouse model. Infection with isolate A2001/2-20 (2-20) induced higher lung IL-13 levels, airway mucin expression, and airway dysfunction than the genetically related isolate A2001/3-12 (3-12). It was previously shown that the fusion (F) protein of a mucus-inducing strain, line 19, is a factor in RSV mucin induction. We hypothesized that the F protein of 2-20 plays a role in RSV-induced mucin expression. We generated a chimeric RSV harboring the F gene of 2-20 in the genetic background of the non-mucogenic A2 strain. A2-2-20F infection resulted in early airway necrotic cell debris and lung mucin production. We also observed more neutrophil infiltration in the lungs of A2-2-20F-infected mice compared to mock- and A2-infected mice. This data indicates that F is a factor in RSV 2-20-induced mucus expression.

Neutrophils are abundant in the lungs of infants with severe RSV disease. Thus, we hypothesized that they play a role in 2-20 pathogenesis. Anti-Ly6G antibody was used to deplete neutrophils in RSV-infected mice. We observed lower lung mucin expression, less TNF- $\alpha$ , and less IL-13-expressing CD4<sup>+</sup> T cells in neutrophil-depleted, RSV-infected mice compared to controls. Our findings demonstrated a novel role of neutrophils in virus-induced mucin response.

This body of data suggests that viral strain differences play a role in RSV severity. Sequence differences within F resulted in increased fusion activity and subsequent epithelial damage, followed by a robust neutrophil response that mediated lung mucin expression. Elucidating factors in RSV-associated airway pathology may have implications for treatment of severe RSV disease.

**IDENTIFYING MECHANISMS OF RESPIRATORY SYNCYTIAL VIRUS-  
INDUCED MUCUS**

By  
Kate L. Stokes  
B.S., Rutgers, the State University of New Jersey, 2007

Advisor: Martin L. Moore, Ph.D.

A dissertation submitted to the Faculty of the  
James T. Laney School of Graduate Studies of Emory University in partial  
fulfillment of the requirements for the degree of Doctor of Philosophy in  
Graduate Division of Biological and Biomedical Science,  
Immunology and Molecular Pathogenesis

2013

## **ACKNOWLEDGEMENTS**

The work described below would have been impossible without my excellent mentor, Marty Moore. I appreciate all the support and guidance he provided me with throughout my PhD. Thank you for believing in me even when I didn't believe in myself. I would also like to thank current and past members of the Moore lab for their help and encouragement over the years.

Thank you to my wonderful, inspiring science teachers who have fostered a love of science in me, especially Mrs. Vicki Robertson and Mrs. Kate DeSantis at Lenape High School and Dr. Barbara Zilinskas, my undergraduate research mentor.

I do not know if I would have made it without my friends and family. Thank you to them for always being there and supporting and encouraging me during both my triumphs and breakdowns. I am especially thankful to Nick for all the support and encouragement he has given to me. Thank you for always being on my side.

## TABLE OF CONTENTS

Abstract	
Acknowledgements	
Table of Contents	
List of Figures and Tables	
<b>CHAPTER 1: INTRODUCTION</b>	<b>1</b>
Introduction	1
1.1 RSV Classification	1
1.2 RSV Virus Structure	2
1.3 RSV Antigenic Diversity	7
1.4 RSV Reverse Genetics System	9
1.5 RSV Pathogenesis in Infants	11
1.6 RSV Infection Models	13
1.7 RSV Infection in BALB/c Mice	16
1.8 Infection of the Airway Epithelium	18
1.9 Mucus Regulation and Production	20
1.10 Neutrophils In Respiratory Infection	21
1.11 T Cells in RSV Infection	25
1.12 RSV and Asthma	27
1.13 RSV Vaccines	28
1.14 Current Study	30
References	32
<b>CHAPTER 2: DIFFERENTIAL PATHOGENESIS OF RESPIRATORY SYNCYTIAL VIRUS CLINICAL ISOLATES IN BALB/C MICE</b>	<b>66</b>
Abstract	68
Introduction	69
Materials and Methods	70
Results	78
Discussion	98
Acknowledgements	102
References	103
<b>CHAPTER 3: THE RESPIRATORY SYNCYTIAL VIRUS FUSION PROTEIN AND NEUTROPHILS MEDIATE THE AIRWAY MUCIN RESPONSE TO PATHOGENIC RSV INFECTION</b>	<b>117</b>
Abstract	119
Introduction	120
Materials and Methods	122
Results	130

Discussion	147
Acknowledgements	154
References	155

**CHAPTER 4: DISCUSSION** 167

References	182
------------	-----

**LIST OF FIGURES AND TABLES**

**Chapter 1:**

<b>Figure 1:</b> Schematic of RSV genome	3
------------------------------------------	---

<b>Figure 2:</b> RSV reverse genetics system	10
----------------------------------------------	----

**Chapter 2:**

<b>Figure 1:</b> Differential weight loss patterns with RSV clinical isolates	79
-------------------------------------------------------------------------------	----

<b>Figure 2:</b> Weight loss after infection with UV-inactivated RSV 2-20	80
---------------------------------------------------------------------------	----

<b>Figure 3:</b> IL-13 levels in RSV-infected mice	81
----------------------------------------------------	----

<b>Figure 4:</b> Gob-5 Western blotting	82
-----------------------------------------	----

<b>Figure 5:</b> In vitro growth of RSV strains A2, 2-20, and 3-12	85
--------------------------------------------------------------------	----

<b>Figure 6:</b> Viral load of RSV strains A2, 2-20, and 3-12	86
---------------------------------------------------------------	----

<b>Figure 7:</b> RSV antigen in bronchiolar epithelium	88
--------------------------------------------------------	----

<b>Figure 8:</b> Early histopathologic lesions of RSV 2-20 and 3-12 infection	90
-------------------------------------------------------------------------------	----

<b>Figure 9:</b> RSV 2-20 induced high levels of pulmonary mucin expression	92
-----------------------------------------------------------------------------	----

<b>Figure 10:</b> RSV 2-20 induced mucin expression is IL-13-dependent	93
------------------------------------------------------------------------	----

<b>Figure 11:</b> Lung dysfunction caused by RSV 2-20	95
-------------------------------------------------------	----

<b>Figure 12:</b> RSV A2 and 3-12 induced higher levels of IFN- $\gamma$ producing CD8 <sup>+</sup> T cells than 2-20 and line 19	96
-----------------------------------------------------------------------------------------------------------------------------------	----



**Figure 13:** IFN- $\gamma$ -producing CD8<sup>+</sup>T cells in 2-20 infected BALB/cJ and IL-13 KO mice 97

**Chapter 3:**

**Figure 1:** *In vitro* growth and *in vivo* viral load of RSV strains A2, 2-20, and A2-2-20F 131

**Figure 2:** RSV A2-2-20F infection resulted in early lung lesions in BALB/cJ mice 133

**Figure 3:** 2-20 F is a mucogenic factor in RSV infection 135

**Figure 4:** 2-20 F is more fusogenic than A2 F when co-expressed with RSV G protein 137

**Figure 5:** A2-2-20F causes neutrophil infiltration in the lungs of BALB/cJ mice 139

**Figure 6:** Anti-Ly6G treatment results in depletion of neutrophils in the blood and lungs of RSV-infected mice 141

**Figure 7:** 1A8 administration does not affect macrophage numbers in mock- or RSV-infected mice 142

**Figure 8:** Viral load after neutrophil depletion 143

**Figure 9:** Neutrophil depletion decreased mucin production 144

**Figure 10:** Neutrophil depletion results in decreased TNF- $\alpha$  levels during RSV infection 145

**Figure 11:** Neutrophil depletion reduces IL-13 producing CD4<sup>+</sup> T cells in lungs of RSV-infected BALB/cJ mice 147

**Figure 12:** Side-view ribbon representation of the prefusion RSV F protein trimer (PDB 4JHW), colored by monomer 151

**Chapter 4:**

**Table 1:** Comparison of RSV clinical isolates 171

**Table 2:** Comparison of chimeric and parent RSV strains 172

**Figure 1:** Sequence alignment of A2 and 2-20 F proteins 174

**Figure 2:** Thermostability of RSV Strains 177



## CHAPTER 1: INTRODUCTION

Respiratory syncytial virus (RSV) is the major cause of bronchiolitis and viral pneumonia in infants worldwide (1, 2). By age 2, most children have been infected at least once and many have experienced two infections (3). RSV hospitalizes three times more children than influenza or parainfluenza viruses and results in significantly more outpatient visits for children under six months (4). Annually, RSV virus is estimated to infect 64 million people worldwide, result in 160,000 deaths (5), and cost the US \$300,000,000 (6). Despite the global burden of RSV disease, there is no vaccine or effective treatment. RSV targets the bronchiolar epithelium resulting in necrosis and destruction of ciliated epithelial cells. Mucus secretion increases during RSV infection, forming thick plugs mixed with cell debris, fibrin, and lymphocytes (7). These plugs block smaller bronchioles, thereby obstructing airways and increasing airway hyperresponsiveness (AHR) (8). An understanding of how RSV causes epithelial desquamation and mucus production leading to lung dysfunction may aid the development of approaches to prevent severe respiratory illness.

### 1.1 RSV CLASSIFICATION

Human respiratory syncytial virus (RSV) was isolated from a laboratory chimpanzee displaying illness resembling the common cold in 1956 (9). RSV is a member of the *Paramyxoviridae* family of viruses. Additional members of the *Paramyxoviridae* family include measles, parainfluenza, mumps, and metapneumovirus. These viruses are all non-segmented, negative-sense single-

stranded RNA viruses (10). Negative-sense RNA viruses encode and package their own RNA polymerase (RNAP) and use their genome as both a template for synthesis of the antigenome which serves as a template for (-) strand genomic RNA, as well synthesis of mRNAs (11).

*Paramyxoviridae* are traditionally defined by having a fusion protein that can act at a neutral pH, though some members may require low pH for fusogenicity (12). This family is classified into two subfamilies: the *Paramyxovirinae* and the *Pneumovirinae*. Viruses in the *Paramyxovirinae* are the *Respirovirus*, *Rubulavirus*, *Avulavirus*, *Morbillivirus*, and *Henipavirus* genera. The *Pneumovirinae* genus contains only two genera: *Pneumovirus* and *Metapneumovirus*. This classification is based on morphological criteria, the organization of the genome, biological activity of the proteins, and the sequence relationship of the encoded proteins. RSV is a member of the *Pneumovirinae* genus. *Pneumovirinae* can be morphologically distinguished from *Paramyxovirinae* by a narrower nucleocapsid. The number of encoded proteins as well as the attachment protein are also distinct between the genera (10, 13).

## **1.2 RSV VIRUS STRUCTURE**

The *Paramyxoviridae* contain a lipid bilayer envelope derived from the plasma membrane of the host cell. These viruses are generally spherical but can be pleomorphic and filamentous. RSV particles are round, filamentous, and kidney-shaped when grown *in vitro* (14). Glycoprotein spikes extend out from the

membrane, while a nucleocapsid core containing the genome exists within the membrane (10).

The genome of RSV is 15.2 kilobases (kb) in length and comprises 10 genes: nonstructural protein 1 (NS1), nonstructural protein 2 (NS2), nucleocapsid (N), phosphoprotein (P), matrix (M), small hydrophobic (SH), attachment (G), fusion (F), M2, and L (large polymerase). Each mRNA transcript encodes a single polypeptide except for M2, which encodes M2-1 and M2-2 proteins through the use of 2 overlapping open reading frames (ORF). Translation of this second ORF depends upon re-initiation by ribosomes as they exit the M2-1 ORF. The NS1 and NS2 proteins inhibit the induction of type I interferons during viral infection (15). The N protein binds to genomic and antigenomic RNA to form RNase-resistant nucleocapsids (13). The P protein is part of the polymerase complex and forms a complex with free N protein that allows N to be available for nucleocapsid assembly (16). The M protein, which lines the inner surface of the viral envelope, plays a central role in budding and may also silence RNA synthesis in preparation for packaging (17).

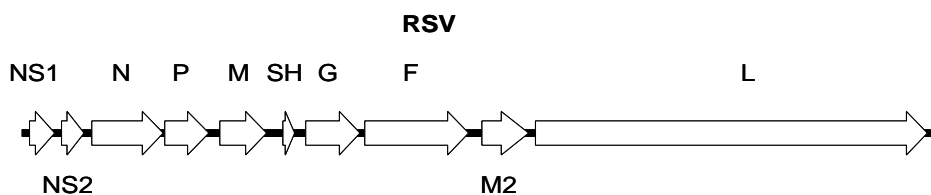


**Figure 1.** Schematic of RSV genome.

The F, G, and SH proteins are glycoproteins lining the surface of the RSV particle. The precise function of SH, or small hydrophobic, protein is unknown. A virus in which the SH protein was deleted was fully viable in cell culture and only slightly attenuated *in vivo* (18). Molecular modeling has suggested that SH may be a channel-forming viroporin, but the role of this function in RSV infection is unclear (19). The SH protein of parainfluenza virus 5 inhibits tumor necrosis factor alpha (TNF- $\alpha$ ) signaling and research suggests RSV SH may have a similar function (20).

The Pneumovirus G protein is structurally distinct from that of Paramyxovirinae. The RSV G has neither hemagglutinin nor neuraminidase activity (21). The central region of G is characterized by a cysteine-rich area termed a “cysteine noose” (22). This central domain also contains a CX<sub>3</sub>C motif that has limited sequence relatedness with the CX<sub>3</sub>C domain of the chemokine fractalkine (23). Fractalkine functions as a chemoattractant and cell adhesion molecule that mediates the influx of CX<sub>3</sub>CR<sub>1</sub><sup>+</sup> leukocytes such as NK cells, CD4<sup>+</sup> T cells, and CD8<sup>+</sup> T cells. Wildtype RSV infection is associated with increased CXCR1<sup>+</sup> cells compared to a mutant virus in which the CX<sub>3</sub>C domain was deleted (24). The CX<sub>3</sub>C motif dampens the antiviral response to RSV infection by diminishing the CX<sub>3</sub>CR<sub>1</sub><sup>+</sup> cell response (24). In another, however, the G protein enhanced the pulmonary RSV-specific CD8<sup>+</sup> T cell response in mice. This activity was dependent on the central conserved region (25). The deletion of either the cysteine noose or CX<sub>3</sub>C motif from RSV had little effect on replication (26).

These conflicting reports indicate that the exact role of these conserved domains is unclear.

RSV G is not absolutely necessary for RSV infection because a virus lacking the G protein is infectious in cell culture and infectious to a lesser degree in mice (27). A secreted form of the G protein (sG) is shed prior to virion release. This form arises from initiation of translation at the second AUG in the ORF, downstream of the transmembrane domain (28, 29). The membrane form of G can be heavily glycosylated. For example, laboratory-adapted strain RSV A2 has an estimated four N-linked sugar side chains that are added cotranslationally (30). G assembles into oligomers in the ER and O-linked sugars are added in the trans-Golgi compartment or network, further increasing the relative molar mass ( $M_r$ ) of G (30).

The F, or fusion, protein is responsible for viral entry into infected cells and facilitating the spread of virus between neighboring cells by syncytia formation. Both the F and G proteins have been shown to interact with glycosaminoglycans (GAGs) (31), however, the G protein is not necessary for fusion. Expression of F by recombinant vesicular stomatitis virus conferred the ability to fuse to and enter cells (32). The F protein is therefore able to mediate fusion independent of the other RSV proteins. Recent research also shows that the F protein plays an important role in viral attachment through interaction with the host protein nucleolin. RSV infection was decreased compared to control when anti-nucleolin

antibodies were used, and RNA-mediated knockdown of lung nucleolin in mice also reduced RSV infection (33).

The F protein is a type I transmembrane surface protein with an N-terminal cleaved signal peptide and a membrane anchor near the C-terminus (34). The inactive 67-kD F<sub>0</sub> precursor is cleaved by furin at two closely-spaced sites to generate F<sub>1</sub> and F<sub>2</sub> chains, and the F<sub>1</sub> subunit's N-terminus inserts directly into the target membrane to initiate fusion. This subunit contains heptad repeats that associate and drive a conformational shift that brings the viral and cellular membranes into close proximity (35). Cleavage at both furin sites results in a short peptide of 27 amino acids (pep27). In bovine RSV (BRSV), pep27 is secreted by infected cells. BRSV pep27 has function similar to tachykinins, a family of neuropeptides that promote airway hypersensitivity and inflammation (36), but this sequence similarity is not found in human RSV. The function of this peptide in human RSV is unknown. The F protein may have other immunomodulatory functions. For example, the F protein has also been shown to bind to toll-like receptor 4 (TLR4), activating the immune response by driving nuclear factor kappa B- (NF-κB) mediated cytokine expression (37).

Multiple studies have shown that the fusion and attachment glycoproteins of paramyxoviruses can interact with each other (38, 39). Activation of most *Paramyxovirinae* subfamily F proteins involves interaction with the attachment protein (40). In Sendai virus, the interaction of the attachment protein with the fusion protein promotes cell fusion (41). The attachment and fusion-promoting



activities of the Newcastle disease virus (NDV) attachment protein were shown to be separate through use of deletion mutants (42). Additionally, the attachment protein of Newcastle NDV was shown to be necessary for triggering of membrane fusion (43). As stated above, the G protein is not absolutely necessary for RSV infection. One hint as to why G is not necessary for fusion comes from the insertion of these the two furin cleavage sites into the fusion protein of Sendai virus, which resulted in increased cell-to-cell fusion in the absence of the attachment protein (44). The presence of these cleavage sites may explain the lack of need for G in RSV infection.

M2-1 and M2-2 are RNA synthesis factors. In the absence of M2-1, transcription prematurely terminates within several hundred nucleotides. M2-2 enhances read-through transcription at gene junctions to generate polycistronic RNAs. M2-2 also has a role in shifting RNA transcription to RNA replication. The L protein acts as the polymerase and also performs mRNA capping (45). This protein is composed of separate domains that require molecular compatibility for bioactivity. The N-terminal fragment contains P binding, polymerase, and polynucleotidyltransferase activities, while the C-terminal domain contains methyltransferase and guanylyltransferase motifs, contributing to the generation of a proper mRNA cap (46).

### **1.3 RSV ANTIGENIC DIVERSITY**

RSV has a single serotype and is divided into two antigenic subgroups A and B. Distinct viral clades have been identified in each subgroup. Subgroup A and B

viruses can circulate either separately or together during a given RSV season (47). There are extensive differences between the G proteins in these two subgroups, but fewer differences in other proteins. F proteins are 50% antigenically related, and the G proteins are 1% to 7% antigenically related (48). The two subgroups share 81% nucleotide identity. M2-2, SH, and G are the most divergent proteins in terms of nucleotide sequence (49). The diversity in G is concentrated in the two hypervariable “mucin-like” regions in the ectodomain (50). It is hypothesized that the host exerts immune pressure on the virus to cause amino acid substitutions. Analysis of RSV isolated over several decades shows that amino acid changes in G are associated with differences in reactivity to monoclonal antibodies (mAbs) (51, 52). The F protein is relatively antigenically stable. Vaccination with F conferred protection against both subgroups of RSV in cotton rats while vaccination with G resulted in protection against homologous (A or B) subgroups (53).

RSV, as well as other respiratory viruses such as human rhinovirus (HRV) and influenza virus, shows strict seasonality. This seasonality depends on factors such as the effects of cold weather and humidity on virus particles, human physiology, and human behavior (54-56). The RSV season is initiated in the fall, peaks in the winter, and ends in late spring (57). In countries with temperate climates, RSV causes epidemics of acute lower respiratory tract infections in children throughout this winter season. Some studies of RSV epidemics in temperate climates have detected a biannual pattern of RSV infections and hospitalization rates. RSV is seen with equal frequency in tropical and semitropical climates, but

the pattern of seasonality is different. These patterns are linked to changes in temperature and rainfall depending on the location (58). In northern tropical areas, RSV seasonality is associated with a decrease in temperature and an increase in rainfall while in southern tropical climates, decreases in both rainfall and temperature are linked to RSV epidemics (59, 60). In equatorial countries, lower respiratory tract infections are observed year-round with a slight increase in prevalence during the dry months (61). Multiple strains of RSV can circulate in the same area during an epidemic. Similar strains can appear at the same time in noncontiguous geographic locations, suggesting rapid global spread. On the other hand, more detailed strain sequencing studies have shown that strains in specific communities are often distinct (62, 63). Conversely, there is also evidence of spread between communities (62). Interestingly, it has been observed that low levels of RSV are present year-round in patients with chronic obstructive pulmonary disease (64). In addition to equatorial populations, these patients may act as RSV reservoirs, and factors such as climate may cause epidemics to spread to the community.

#### **1.4 RSV REVERSE GENETICS SYSTEM**

Infectious recombinant RSV (rRSV) can be recovered from transfected cDNA. Co-expression of RSV proteins N, P, L, and M2-1 as well as the antigenomic RNA is necessary and sufficient for RSV replication (65, 66). In order to generate rRSV, plasmids encoding N, P, L, and M2-1 proteins and the antigenome under control of the T7 promoter are transfected into BHK-21 cells that stably express T7 RNA polymerase (BSR-T7/5 cells). Cell supernatants are passaged onto HEp-2

cells for generation of recombinant RSV (67, 68). This system has been used in development of RSV vaccines (69). The reverse genetics system allows for the addition of small genes expressing immunomodulatory proteins such as cytokines and chemokines (70). It has also may be possible to alter RSV using this recombinant system in order to achieve greater immunogenicity or reduced pathogenesis. The P, NS1, NS2, SH, M2-1, and M2-2 genes have been deleted from RSV using the reverse genetics system to generate attenuated vaccine candidates (71).

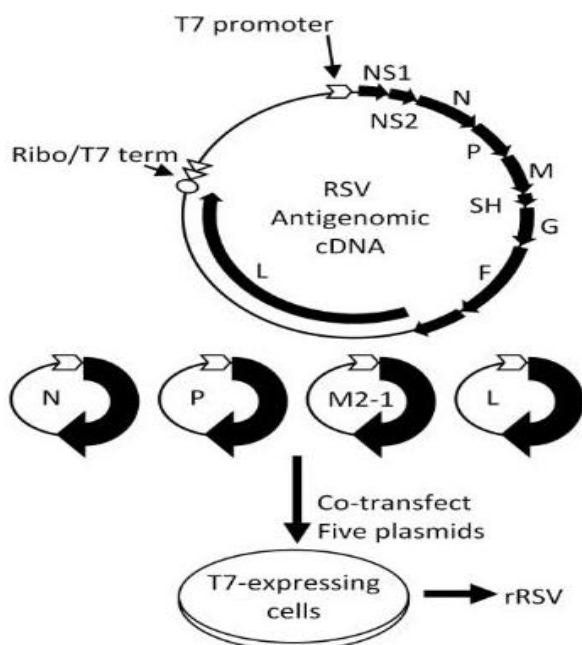


**Figure 2.** RSV reverse genetics system. Antigenomic RSV RNA is expressed under the control of a T7 promoter. The 3' end is generated by the hepatitis delta virus hammerhead ribozyme. The antigenomic plasmid and plasmids expressing N, P, M2-1, and L proteins are also under control of the T7 promoter. All plasmids are co-transfected in T7-expressing cells.

Plasmid-based virus rescue systems for *Pneumovirinae*, such as the one described above, are plagued by instability (67, 72). Additionally, the proteins expressed from the helper plasmids as well as the antigenome cDNA plasmid are based on the RSV A2 strain (73). A bacterial artificial chromosome (BAC) recombination-mediated system has recently been established for the rescue of RSV (74). This system allows for the stabilization of RSV antigenomic cDNA in the BAC vector. The BAC rescue system also permits the use of antigenomic cDNA plasmids based on other RSV strains, including those that induce mucus (74). Overall, this system provides a stable and efficient mutagenesis method for reverse genetics of a negative strand RNA virus.

### **1.5 RSV PATHOGENESIS IN INFANTS**

RSV infection results in the hospitalization of approximately 100,000 infants per year in the US, including an estimated 500 deaths (75). The disease manifests in a spectrum of clinical disease ranging from mild upper respiratory tract (URTI) symptoms to more severe lower respiratory tract symptoms and respiratory failure. URTI with RSV can result in rhinitis, cough, and low-grade fever (76). Acute otitis media develops in one third of RSV-infected children (77). Conversely, RSV can also lead to a more severe lower respiratory tract infection (LRTI). RSV is the most common cause of bronchiolitis, infecting the lower respiratory tract in 20-40% of RSV cases in children under one year of age (3, 78). Overall, bronchiolitis hospital admissions cost more than \$500 million annually (79). Bronchiolitis is characterized by acute inflammation, edema, necrosis of epithelial cells lining small airways, increased mucus production, and

bronchospasm. These symptoms lead to chest tightness and breathing difficulty (80). Interestingly, a 2010 study demonstrated that RSV bronchiolitis, compared to non-RSV bronchiolitis was independently associated with severe outcomes (81). This implies that RSV infections themselves may be more serious than other winter viral infections in children.

RSV infection in human infants results in a predominance of neutrophils in airways (82), bronchiolar epithelial damage, and the plugging of small airways with lung debris. Lung injury is usually manifested by the loss of alveolar epithelial cells, hemorrhage, hyaline membrane formation, intraalveolar hemorrhage, and inflammation in alveolar spaces and airways (83). Though many infections are confined to the upper airways, some viral infections can result in infection of the lower respiratory tract, occurring most often in young children, the elderly, and the immunocompromised (84). In infants, RSV generally causes a more severe LRTI than influenza viruses. Some studies have examined fatal RSV cases in infants. In all fatal cases examined by Johnson and colleagues, acute bronchiolitis was prominent in mostly medium and small bronchioles. Airways were plugged with debris composed of sloughed epithelial cells, macrophages, fibrin, and mucin. Interstitial inflammation and hyperplasia of bronchiolar-associated lymphoid tissue and (BALT) were also observed in the lungs of all four patients (85). Macrophages and neutrophils were abundant in the lungs of fatal bronchiolitis cases in a second study (86). Viral antigen was detected in the airway epithelia in subjects infected with both influenza and RSV, but antigen was more prominent in RSV-infected infants (86). Johnson and

colleagues observed RSV antigen in both bronchiolar and bronchial epithelial cells, as well as in alveolar spaces and exudates (85). CD8 T cells, however, were not found in autopsy tissues of infants with fatal bronchiolitis in a study by Welliver and colleagues (87). Conversely, Johnson et al. observed some CD8 T cells but saw that they were outnumbered by CD3+ double-negative (negative staining for CD8 and CD4) T cells (85). These findings suggest that severe bronchiolitis is not characterized by enhanced CD8 response but by inefficient viral clearance. Infants with the mildest bronchiolitis cases (those surviving influenza infections) had the most interferon gamma (IFN- $\gamma$ ) expression. Overall, cytokine responses were greater among subjects with milder cases of influenza than in those with RSV infection. Therefore, epithelial destruction in RSV infection may play more of a role in disease pathogenesis than production of inflammatory cytokines (86). According to these two retrospective autopsy studies, severe, primary RSV bronchiolitis in infants is a viral and lung disease and neither apparently immune-mediated disease nor associated with a “cytokine storm.”

## **1.6 RSV INFECTION MODELS**

Immortalized lung epithelial cell-derived cell lines such as A549 and HEp-2 cells have been used to model RSV host infection (88-90). These cell lines, however, fails to take into account the complexities of the human lung. The ability to culture primary human epithelial cells into authentic pseudostratified airway epithelial (HAE) cultures provides a more physiologic model. Primary pediatric bronchial epithelial cells in air-liquid interface (ALI) cultures have been used to

model both Sendai virus and RSV infections as well as asthma (91-93). For this culture system, cells were derived from bronchial brushings of children undergoing elective surgery and cultured on collagen-coated, 12-mm filters in transwells at ALI. Resulting cultures were named “well-differentiated pediatric bronchial epithelial cells” (WD-PBECs). RSV infected mainly ciliated and occasionally nonciliated epithelial cells but not goblet cells in these cultures. Syncytia were consistently observed in addition to cell sloughing within apical washes. Goblet cell hyperplasia and metaplasia similar to infant RSV bronchiolitis was also seen in this culture system. Additionally, increased levels of chemokines RANTES (CCL5), CXCL8, CXCL10, interleukin-6 (IL-6), and TNF-related apoptosis-inducing ligand (TRAIL) were observed (92). It has also been shown the RSV F and G proteins alone will induce a similar chemokine response in primary normal human bronchial epithelial cells grown at ALI (94). Overall, RSV infection in WD-PBECs showed similar histopathology and chemokine responses to severe RSV cases and represent a useful *ex vivo* model. Relevant to my dissertation work on RSV strain-specific phenotypes, differences in cytopathic effect between the laboratory strain A2 and a clinical isolate (B2a) were observed in the WD-PBEC system (92).

A suitable animal model of RSV infection is necessary for gaining insight into lung pathogenesis. Cotton rats, mice, ferrets, guinea pigs, hamsters, marmosets, lambs, and some species of nonhuman primates are semi-permissive to RSV infection (95, 96). Chimpanzees are permissive to RSV and have been used in studies of efficacy and immunogenicity of candidate RSV vaccines (97-99).



However, chimpanzees are expensive and increasingly difficult to obtain and maintain. The lack of inbreeding and reagents for non-human primate species is also a challenge for immunologic studies. Cotton rats are 100-fold more permissive to laboratory strain RSV infection than BALB/c mice (100) and RSV is able to infect both the upper and lower respiratory tracts of cotton rats (101). One limitation in the use of cotton rats, however, is the lack of reagents for immunologic characterization as well as transgenic and knockout strains. Some inbred cotton rat strains are available but transgenic or knockout strains have not yet been established. Furthermore, despite exhibiting higher RSV viral loads than mice, cotton rats have not been shown to exhibit airway mucin expression and pulmonary dysfunction, parameters of disease I focused on in my dissertation work (see section 1.14).

RSV has also been tested in a human challenge model. Volunteer subjects were inoculated with RSV intranasally and viral shedding and neutralizing antibody levels were measured (102-104). These studies, however, were performed on healthy adults that were mostly likely previously exposed to RSV. Consequently, only an upper respiratory tract infection is observed in this model. It is hypothesized that existing neutralizing antibodies in subjects prevent infection of the lower respiratory tract. Adult subjects also do not harbor as high of a peak nasal viral load as infected infants. Overall, the adult nasal challenge model does not mirror RSV pathogenesis in infants. This model is very useful for investigating efficacy of antivirals to inhibit replication in the context of human

infection, or vaccines to prevent RSV URTI, although most RSV candidate vaccines are targeted to prevent LTRI.

### **1.7 RSV INFECTION IN BALB/C MICE**

Semi-permissive replication of RSV in mice is a drawback. Traditionally used laboratory RSV strains replicate to low levels in the nasal turbinates and lungs of mice. Despite this limitation, there are several advantages to the mouse model of RSV. Various reagents for immunology, as well as knockout and transgenic strains are available. BAL/c mice exhibit RSV strain-dependent induction of airway mucus expression (105, 106). The mucus production in BALB/c mouse infection makes them more advantageous for pathogenesis studies.

The RSV A2 strain was first isolated in Australia in 1961 (107) and has been used to examine the role of T cells in RSV clearance, immunopathology, and immune modulation. Infection of BALB/c mice with RSV A2 results in high levels of IFN- $\gamma$  in the lung and bronchoalveolar lavage fluid (BALF) and T cell-mediated clearance and immunopathology (96). Graham and colleagues showed that CD4+ and CD8+ lymphocytes are both involved in viral clearance and both contribute to illness (weight loss). CD8+ cells, however, appeared to make a greater contribution to viral-induced illness than CD4+ T cells (108). Epitope studies show that specific CD4+ T cells regulate the CD8 T cell response to RSV infection, reducing the magnitude and effector cytokine production but not affecting their clearance kinetics (109). The peak viral load of RSV in BALB/c mouse lung is at approximately day four post-infection and the peak of lymphocytic inflammation

is one week post-infection (96). Studies using RSV A2 focus on lymphocyte-associated inflammation and airway damage as well as weight loss (110-112). Infection with RSV strain A2, however, does not result in airway epithelial destruction or airway mucin expression, both hallmarks of severe RSV infection in infants. Rather, RSV A2 infection results in a predominately lymphocytic (T cells) inflammation manifesting as alveolitis and perivascular cuffing.

Some RSV clinical isolates have shown differential pathogenesis in BALB/c mice. RSV line 19 is an antigenic subgroup A strain derived from a clinical case in 1967 at the University of Michigan Hospital by passage through SPAFAS primary chick lung (SCL) and kidney (SCK) cells (113). In BALB/c mice, line 19 induces detectable airway hyperreactivity (AHR) to methacholine (a bronchoconstrictor) whereas RSV A2 does not. Additionally, line 19 produced considerable goblet cell hyperplasia as well as increases in mucus markers gob5 and MUC5AC mRNA levels. The mucus-associated cytokine IL-13 was also produced in response to RSV line 19 infection but not A2, and the observed AHR was shown to be IL-13 dependent (105). Further studies have also shown that the fusion protein of RSV line 19 is a factor in its IL-13 and mucus production in BALB/c mice. Infection with a chimeric virus expressing the F protein of line 19 in an A2 backbone (RSV rA2-line19F) resulted in lower IFN- $\alpha$  lung levels 24 h post-infection, higher lung viral load, higher lung IL-13 levels, greater airway mucin expression levels, and greater airway hyperresponsiveness than infection with a similarly made virus expressing A2 F (rA2-A2F). The mucus effects seen following RSV line 19 infection may be due to early immune modulation. Infection with RSV rA2-

line19F also lead to increased IFN- $\alpha$  compared to RSV rA2-A2F (67). The RSV strain used to study RSV pathogenesis in human tissues is important (92).

Mucus-inducing strains provide a more accurate mouse model of severe RSV infection. Further study of strains recapitulating severe RSV disease is important to elucidate the pathway of RSV infection in severe infant disease.

### **1.8 INFECTION OF THE AIRWAY EPITHELIUM**

The airway epithelium is the first line of defense of the lung against pathogens such as RSV. The lungs work to clear pathogens through the function of ciliated epithelial and secretory cells (114). Epithelial cells cover the whole mucosal surface in contact with air. The cells are arranged in an impenetrable barrier, connected by junctions such as tight junctions, adherens junctions, gap junctions, and desmosomes (114). These junctions act as a barrier to virus entry and dissemination. There is a high concentration of retinoic acid-inducible gene I (RIG-I), an important regulator of antiviral immunity, at tight junctions (115). RIG-I has been shown to detect RSV, and it has been shown to be essential for signaling that leads to innate immunity (116). Airway epithelial cells play a role in both innate and adaptive immunity. Epithelial cells produce antiviral substances and proinflammatory cytokines, recruiting innate immune cells and initiating the adaptive immune response (117). In RSV-infected children, increased levels of IL-8, RANTES, macrophage inflammatory protein-1 alpha (MIP-1 $\alpha$ ), and monocyte chemoattractant protein-1 (MCP-1) chemokines in both upper and lower airways have been observed (118). TLRs are type I integral membrane glycoproteins which recognize pathogen-associated molecular patterns (119). TLR3 is found in

cytoplasmic endosomes of airway epithelial cells and responds to RSV (120). This receptor mediates inflammatory cytokines and chemokine production in RSV-infected epithelial cells (121). The extracellular TLR4 has been shown to interact with RSV F, causing signaling through MyD88 and activation of immunity (37, 122). TLR7, which detects ssRNA, also mediates the immune response to RSV. TLR7 deficiency results in increases in mucogenic cytokines IL-4, IL-13, and IL-17 as well as mucus production and a decrease in IL-12 production (123). These results suggest TLR7 is important in preventing RSV-associated mucus and pathology. RSV has also been shown to stimulate the extracellular receptors TLR2 and TLR6 resulting in subsequent innate immune activation, although the mechanism is unknown. Cytokines and chemokines secreted by infected epithelial cells attract inflammatory cells such as neutrophils, eosinophils, and macrophages.

RSV can cause widespread damage to the bronchial epithelium *in vitro* and *in vivo*. RSV infection of human epithelial cells results in membrane barrier disruption characterized by a decrease in transepithelial electrical resistance and changes in paracellular permeability mediated by cellular cytoskeletal rearrangement (124). RSV infection may also affect the repair of damaged epithelium. Excess production of fibroblast growth factor basic (FGFb) in response to viral infection leads to remodeling in the airway. Increased FGFb and subsequent airway remodeling is hypothesized to lead to wheezing after RSV infection (125).

## **1.9 MUCUS REGULATION AND PRODUCTION IN RESPIRATORY INFECTIONS**

Pathogen by-products, inflammatory and immune response mediators, and growth factors upregulate mucin genes expression in airway epithelial cells. A hallmark of severe RSV disease is mucus production which obstructs airways and causes breathing difficulty. Mucus obstruction is the culmination of several complex processes including mucin (*MUC*) gene regulation, mucin secretion and goblet cell hyperplasia. *MUC* genes are regulated by transcription factors NF- $\kappa$ B and/or specificity protein 1 (Sp1). Infection of human airway epithelial cells with respiratory viruses causes induction of proinflammatory transcription factors including NF- $\kappa$ B, activator protein 1 (AP-1), and signal transducer and activator of transcription 1 and 2 (STAT1 and 2) (126). Cytokines and chemokines secreted by infected epithelial cells attract inflammatory cells such as neutrophils, eosinophils, and macrophages that may further contribute to mucus production (114).

Airway mucus is composed of water, ions, lung secretions, serum protein transudates, and mucin glycoproteins (mucins) (127). Mucins are complex glycoconjugates that share a common structural motif of tandem repeats enriched in serine and/or threonine residues. These repeats are unique in sequence and size for each mucin (127). 11 mucins have been identified in human airways with MUC5AC and MUC5AB predominantly composing sputum (114). Secreted mucins, such as MUC5AC, are large molecules that tend to aggregate with other proteins including other mucins. A second group of

mucins are membrane-tethered. MUC5AC is expressed by surface goblet cells in the upper and lower respiratory tracts and is a marker of mucus expression (128). MUC5AC is expressed during human asthma and in murine models of allergic asthma (129, 130), and RSV infection increases MUC5AC levels (131). Mucus overproduction during inflammatory disease is a consequence of goblet cell metaplasia and hyperplasia. Metaplasia is the transformation of one type of tissue into another while hyperplasia is the abnormal multiplication of cells. The appearance of goblet cells indicates goblet cell metaplasia in mice since murine airways normally do not contain many goblet cells (132). Goblet cell metaplasia is mediated by T<sub>h</sub>2 cytokines such as IL-13. IL-13 has been shown to induce goblet cell hyperplasia *in vitro* and *in vivo* (130, 133). IL-13 also induces MUC5AC mRNA expression (134). Additionally, IL-17 enhances mucus production synergistically with IL-13 by acting directly on epithelial cells (135). Research examining the regulation of mucus production following RSV infection is essential for developing useful therapies.

### **1.10 NEUTROPHILS IN RESPIRATORY INFECTION**

Neutrophils, or polymorphonuclear leukocytes (PMN), are the first cells to migrate from the blood to infection sites. They are named for their lobulated nucleus and granules (136). Neutrophils are the predominant leukocytes in both the upper and lower respiratory tracts during RSV infection (82, 137). They are phagocytic cells that release lytic enzymes from primary and secondary granules. Primary granules contain peroxidase, lysozyme, and various hydrolytic enzymes. Secondary granules contain collagenase, lactoferrin, and lysozyme. Neutrophils

also display TLRs on their surface. Neutrophils also use reactive oxygen species (ROS), generated by the NADPH phagosome oxidase (phox) enzyme complex (138). Neutrophils are recruited to the site of infection by chemokines such as IL-8 and MIP-2 (139). Activated neutrophils produce several cytokines, including IL-9, transforming growth factor beta (TGF- $\beta$ ), and TNF- $\alpha$  (140). Neutrophils may contribute to goblet cell hyperplasia and mucus secretion. PMN are a major source of TNF- $\alpha$ . Intratracheal administration of TNF- $\alpha$  in BALB/c mice induces Gob-5, MUC5AC, and mucus expression in the airways (141). Gob-5 is a marker of mucus production (131). Neutrophil elastase can increase MUC5AC expression *in vitro* (142, 143) and is released in upper respiratory tract during RSV infection (144).

Neutrophils are reported to play an important role in the pathogenesis of RSV as well as other respiratory viruses. Infection of both immortalized and primary epithelial cell cultures with type 2 parainfluenza virus resulted in significantly enhanced neutrophil adherence compared to uninfected controls (145).

Neutrophils have also been shown to bind more frequently to Madin-Darby canine kidney epithelial cells (MDCK) infected with influenza when compared to mock-infected cultures (146). RSV infection of A549 human respiratory epithelial cell monolayers resulted in increased surface expression of the adhesion molecule intercellular adhesion molecular-1 (ICAM-1), as well as major histocompatibility complex I (MHC I), resulting in enhanced neutrophil and eosinophil adhesion (147). RSV infection of epithelial cells *in vitro* has been shown to enhance neutrophil adherence. The addition of neutrophils to RSV-infected cells increased



cell damage and detachment. These data suggest that neutrophils may induce epithelial damage and cell loss that contribute to RSV pathogenesis (148).

Adherence of stimulated neutrophils to epithelial cell monolayers also promotes epithelial cell killing (149).

Neutrophil apoptosis may reduce the potential for tissue injury. Using fluorescence actin staining (FAS) and Annexin V staining, Wang and colleagues showed that RSV causes increased apoptosis of neutrophils (150). Conversely, factors present in the airways of RSV-infected infants such as IL-8, leukotriene-B<sub>4</sub>, and granulocyte-monocyte colony-stimulating factor (GM-CSF) inhibit neutrophil apoptosis. Nasal lavage fluid (NLF) from infants with RSV bronchiolitis resulted in delayed apoptosis of neutrophils compared to NLF from healthy controls. The authors speculated that the extended survival of neutrophils in the airways of infected infants contributed to the observed accumulation of neutrophils (151). The exact role of neutrophil apoptosis in RSV infection remains unclear.

Neutrophil degranulation and chemokine production may play a role in RSV pathogenesis. RSV stimulates the release of IL-8, MIP-1 $\alpha$ , and MIP-1 $\beta$  from neutrophils in addition to neutrophil degranulation. Viable RSV is required for chemokine release but not neutrophil degranulation (152). *In vivo*, neutrophil elastase and IL-8 are released in the upper respiratory tract during RSV infection (144). Therefore, neutrophil degranulation and chemokine release may play a role in RSV infant infections, but the exact function of neutrophil degranulation

remains uncertain. Neutrophils can also be activated by TLR4 signaling. Circulating neutrophils express all human TLRs except TLR3 (153). Wheeler et al. showed that RSV infection of human bronchial epithelial cells caused an increase in Hsp72, which subsequently activates neutrophil-derived cytokine production via TLR4 activation (154). In infants with severe bronchiolitis, both circulating and airway neutrophil TLR4 expression was found to be reduced (155). TLR4 may therefore play an important role in the neutrophil response to RSV infection.

RSV can directly infect neutrophils. RSV genomic RNA as well as F, G, and N gene mRNA have been detected in both blood neutrophils and lung neutrophils from infants infected with RSV, indicating that RSV binds and undergoes transcription in these cells (156). A specific immune response by neutrophils to RSV, however, is unlikely. Another *in vitro* study performed by Kaul et al. suggested RSV initially activates the complement pathway in cells it infects, and these cells are subsequently lysed by neutrophils (157). Welliver and colleagues proposed that neutrophils and macrophages are responsible for viral clearance in infant airways (87). Complement, nonetheless, may play a role in passive protection from RSV (158) or pathology (159). In enhanced RSV disease that resulted from the formalin-inactivated RSV vaccine, immune complexes that fix complement were shown to be important for pathogenesis (160). Taken in concert, these studies show that multiple immune pathways are involved in the host response to RSV infection.

Neutrophils are associated with bronchiolitis in respiratory infection *in vivo*. In influenza infection, neutrophils have been reported to play an important role in the containment and clearance of influenza virus as well as influenza-induced lung pathology (161). Low, intermediate, or high virulence influenza strains differ in their ability to recruit neutrophils to airways. It has been shown that neutrophils are important in limiting disease severity in mice infected with intermediate and high virulence influenza strains but not a relatively avirulent strain (162). In fatal human influenza infections, massive neutrophils infiltration was observed (163). Neutrophils are the predominant airway leukocytes observed in RSV bronchiolitis (82) and are overwhelmingly present in BAL samples from both lower and upper respiratory airways of infants infected with RSV in numerous studies (82, 137, 164). In fatal human RSV infections, neutrophils are seen in alveolar extrudates and peribronchiolar tissues (85). Additionally, neutrophil products such as myeloperoxidase and neutrophil elastase are released into the airways of infected individual (144). These data suggest that neutrophils play an important part in respiratory pathogenesis.

### **1.11 T CELLS IN RSV INFECTION**

Cellular immunity is important for clearance of RSV infection. In BALB/c mice, up to 40% of CD8 T cells are RSV epitope specific at the peak of infection (165). T cells are also implicated in viral clearance in humans. Depletion of both CD4+ and CD8+ T cells in mice suggests that both of these subsets are important for shortening the length of viral shedding (108). Depletion of B cells did not have an effect on viral clearance (166). T cells are also implicated in viral clearance in

humans. Children with an impaired cellular immune response demonstrate prolonged viral shedding and high susceptibility to RSV bronchiolitis (167). In children with severe RSV, CD8<sup>+</sup> antigen-specific T cells are found in the peripheral blood and airways, peaking around 9 days post-symptom onset, but their number does not correlate with disease severity (168).

Conversely, the cellular immune response may also play a detrimental role in RSV infection. Both T<sub>h</sub>1 and T<sub>h</sub>2 responses have been observed in RSV-infected infants. It is hypothesized that RSV infection skews the immune response toward a T<sub>h</sub>2 response in order to evade the adaptive immune system (169). Clinical studies of RSV infection indicate increased T<sub>h</sub>2 cytokines such as IL-4 and increased IgE antibody. It has also been demonstrated that the effector T cell population is predominantly made of oligoclonal CD4<sup>+</sup> T cells (170). IFN- $\gamma$  expression in lymphocyte subsets from RSV-infected infants was significantly lower than in healthy infants. Therefore, it was hypothesized that lower IFN- $\gamma$  expression may contribute to RSV pathogenesis (171). Conversely, humans deficient in STAT1, which is involved in IFN- $\gamma$  signaling, are likely to develop severe RSV infections (172). Plasma from RSV infected infants showed lower IFN- $\gamma$  levels compared to control infants (173). This disparity could, however, be due to the immature infant immune system.

T<sub>h</sub>17 cells contribute to respiratory inflammatory disorders such as asthma and chronic obstructive pulmonary disease (COPD). They may also play an important role in RSV pathophysiology (174, 175). Mice deficient in complement 3a

receptor- (C3aR) did not develop AHR, and production of T<sub>h</sub>17 cytokines was attenuated in these mice compared to wildtype mice. These results indicate that complement activation leads to the production of T<sub>h</sub>17 cytokines and viral-induced AHR (176). In IL-17-deficient mice or in wildtype mice whose IL-17 was neutralized via antibody treatment mucus production and allergic airway responses were diminished during RSV infection. Additionally, IL-17 reduction resulted in decreased viral load and altered cytotoxic T cell marker expression (135). RSV infection of STAT1-deficient mice lacking IFN- $\gamma$  signaling led to elevated IL-13 and IL-17 levels and excess inflammation and mucus production. This was linked to increased IL-23 production (177). This phenomenon is supported by *in vitro* studies that showed IL-17 directly upregulates the mucus gene *MUC5B* in human tracheal and bronchial epithelial cells lines (178). A recent study that profiled cytokines in plasma of RSV infected infants revealed higher IL-17 levels in infants with moderate RSV disease compared to those with severe disease (173). This same pattern was also seen in BAL samples (179). The precise role of IL-17 in the respiratory tract of infected infants requires further exploration.

### **1.12 RSV AND ASTHMA**

An association between lower respiratory tract viral infections in infancy and respiratory abnormalities later in life is widely reported. RSV bronchiolitis during the first year of life is an important risk factor for the development of asthma and allergic sensitization (180). A follow-up study indicated that RSV bronchiolitis significantly elevated the risk for development and asthma at seven and thirteen

years of age (181, 182). This link also held up into early adulthood (183). Seven to 8 year old children with a history of severe RSV bronchiolitis in infancy have increased frequencies of IL-4-secreting  $T_H2$  cells specific to RSV as well as cat antigen (184). Infections with respiratory viruses such as rhinovirus have been established as triggers of asthma exacerbations in children with established asthma (185). RSV infection of neonatal mice causes more aggressive airway inflammation when the mice were reinfected as adults than when the initial virus infection was delayed (2). A direct causative role of RSV in asthma causation, however, has yet to be definitively proven. One hypothesis conjectures that early viral infections damage the developing lung, later causing allergic responses (186). Another hypothesis involves the  $CD4^+$  T cell response to RSV. In a recent study, repeated RSV infections of infant mice tolerized to ovalbumin (OVA) induced allergic airway disease in response to OVA sensitization and challenge. These data suggest that RSV infection induces lung  $T_H2$ -like inflammation, promoting a  $T_H2$ -like effector phenotype in  $T_{reg}$  cells and ablation of tolerance to an unrelated allergen. These data support the hypothesis that asthma development is stimulated by promotion of sensitization to inhaled allergens as a result of  $T_H2$  response skewing.

### **1.13 RSV VACCINES**

There is currently no vaccine available for RSV. The only existing therapy for RSV is a prophylactic antibody called Palivizumab. A formalin-inactivated RSV (FI-RSV) vaccine was developed in 1969, but administration of this vaccine failed to offer protection and additionally exacerbated RSV disease (187, 188). There have

been a number of studies that have attempted to explain observed enhanced RSV disease. FI-RSV vaccination resulted in infiltration of inflammatory cells in the lungs and non-neutralizing antibodies. It has been suggested that these antibodies are of the IgE isotype (189). It has also been implied that enhanced RSV disease is mediated by immune complexes. In children with fatal enhanced RSV disease, there is evidence of complement activation in postmortem lung sections (160). A subsequent study showed that lack of protection from FI-RSV is due to low antibody avidity for protective epitopes. The nonprotective antibody response elicited by FI-RSV is due to lack of affinity maturation due to deficient TLR activation in B cells (190). The failure of the FI-RSV vaccine inhibited vaccine development for decades. A number of challenges to RSV vaccine development remain, including the fact that the undeveloped infant immune system that may not respond well to a vaccine, risk factors such as cardiac or lung disease, and elevated susceptibility of infants to disease (191).

Humoral immunity is thought to be essential in the prevention of RSV infection. Neutralizing antibodies to the RSV F are a clear correlate of immune protection against RSV infection and RSV LRTI (192). Therefore, the aim of a successful, protective RSV vaccine is induction of sufficient humoral immunity. There have been multiple types of RSV vaccines tested, and many are in various stages of development. Several attenuated live vaccine virus candidates have been developed but not pursued further. Attenuation strategies include deleting genes associated with immune response modulation, and passaging cells to induce temperature sensitive mutations (193, 194). Some attenuated viruses, however,

are overattenuated and do not provide protection such as a live, cold-passaged candidate that was found to lack most of the RSV SH and G genes (195). Subunit vaccines have also been developed. Most subunit vaccines have concentrated on the RSV F protein. These vaccines may require yearly reimmunization compared to replication competent vectors that can elicit a sustained immune response (196). An RSV G subunit vaccine that showed promise in animal trials was also developed, but human trials were discontinued due to the rare development of purpura in some subjects (197). A vaccine combining RSV F, G, and M was tested in the elderly and resulted in increased neutralizing antibody titers, but there is reluctance to test a subunit vaccine in infants (198). Virus vectors, gene-based vectors, replicons, DNA plasmids have been developed in order to stimulate the antigen presentation that occurs during live RSV infection (191). A bovine parainfluenza virus 3 expressing RSV-F (MEDI-534) has been studied in infants and young children and does not cause enhanced disease (199). Further trials will have to be carried out to evaluate the safety and efficacy of additional vaccine candidates. Human and animal studies that have examined the immune response to RSV may help in these assessments.

#### **1.14 CURRENT STUDY**

Though RSV genotypes have been correlated with varying disease severity (200), the role of strain differences is still unclear. We sought to study how viral strain sequence differences contribute to differential immune responses during RSV disease. A chimeric virus approach was used to determine if the RSV fusion (F) protein is sufficient for heightened virulence compared to non-mucogenic strains. A



second aim sought to examine the role of neutrophils in a mouse model of RSV pathogenesis. Neutrophils are among the first cells recruited to sites of infection and are seen in large quantities in the airways of RSV-infected infants including fatal RSV cases (82, 85, 137). Based on the involvement of neutrophils in mucin expression in allergic airway disease (201), we hypothesized that the neutrophil response in RSV also affects mucin expression. To our knowledge, neutrophils were not explicitly linked to the RSV mucus response previously. Elucidating specific causes of mucin expression in RSV infection is potentially useful for future RSV therapies aimed at alleviating pulmonary obstruction.

## REFERENCES

1. **Hall, C. B., K. R. Powell, N. E. MacDonald, C. L. Gala, M. E. Menegus, S. C. Suffin, and H. J. Cohen.** 1986. Respiratory syncytial viral infection in children with compromised immune function. *N Engl J Med* **315**:77-81.
2. **Culley, F. J., J. Pollott, and P. J. Openshaw.** 2002. Age at first viral infection determines the pattern of T cell-mediated disease during reinfection in adulthood. *J Exp Med* **196**:1381-1386.
3. **Glezen, W. P., L. H. Taber, A. L. Frank, and J. A. Kasel.** 1986. Risk of primary infection and reinfection with respiratory syncytial virus. *Am J Dis Child* **140**:543-546.
4. **Hall, C. B., G. A. Weinberg, M. K. Iwane, A. K. Blumkin, K. M. Edwards, M. A. Staat, P. Auinger, M. R. Griffin, K. A. Poehling, D. Erdman, C. G. Grijalva, Y. Zhu, and P. Szilagyi.** 2009. The burden of respiratory syncytial virus infection in young children. *N Engl J Med* **360**:588-598.
5. **Hastie, M. L., M. J. Headlam, N. B. Patel, A. A. Bukreyev, U. J. Buchholz, K. A. Dave, E. L. Norris, C. L. Wright, K. M. Spann, P. L. Collins, and J. J. Gorman.** 2012. The human respiratory syncytial virus nonstructural protein 1 regulates type I and type II interferon pathways. *Mol Cell Proteomics* **11**:108-127.
6. **Openshaw, P. J., G. S. Dean, and F. J. Culley.** 2003. Links between respiratory syncytial virus bronchiolitis and childhood asthma: clinical

and research approaches. *Pediatr Infect Dis J* **22**:S58-64; discussion S64-55.

7. **Aherne, W., T. Bird, S. D. Court, P. S. Gardner, and J. McQuillin.** 1970. Pathological changes in virus infections of the lower respiratory tract in children. *J Clin Pathol* **23**:7-18.
8. **Rogers, D. F.** 2004. Airway mucus hypersecretion in asthma: an undervalued pathology? *Curr Opin Pharmacol* **4**:241-250.
9. **Blount, R. E., Jr., J. A. Morris, and R. E. Savage.** 1956. Recovery of cytopathogenic agent from chimpanzees with coryza. *Proc Soc Exp Biol Med* **92**:544-549.
10. **Lamb, R. A. a. P., G.D.** 2007. Paramyxoviridae: The Viruses and Their Replication, p. 1449-1496, *Fields Virology Fifth ed*, vol. 1. Lippincott Williams and Wilkins, Philadelphia.
11. **Neumann, G., M. A. Whitt, and Y. Kawaoka.** 2002. A decade after the generation of a negative-sense RNA virus from cloned cDNA - what have we learned? *J Gen Virol* **83**:2635-2662.
12. **Schwalter, R. M., S. E. Smith, and R. E. Dutch.** 2006. Characterization of human metapneumovirus F protein-promoted membrane fusion: critical roles for proteolytic processing and low pH. *J Virol* **80**:10931-10941.
13. **Collins, P. L. a. C., J. E., Jr.** 2007. Respiratory Syncytial Virus and Metapneumovirus p. 1601-1646. *In* D. M. a. H. Knipe, P. M. (ed.), *Fields Virology, Fifth ed.* Lippincott Williams & Wilkins Philadelphia, PA.

14. **Bachi, T., and C. Howe.** 1973. Morphogenesis and ultrastructure of respiratory syncytial virus. *J Virol* **12**:1173-1180.
15. **Spann, K. M., K. C. Tran, B. Chi, R. L. Rabin, and P. L. Collins.** 2004. Suppression of the induction of alpha, beta, and lambda interferons by the NS1 and NS2 proteins of human respiratory syncytial virus in human epithelial cells and macrophages [corrected]. *J Virol* **78**:4363-4369.
16. **Lu, B., C. H. Ma, R. Brazas, and H. Jin.** 2002. The major phosphorylation sites of the respiratory syncytial virus phosphoprotein are dispensable for virus replication in vitro. *J Virol* **76**:10776-10784.
17. **Ghildyal, R., C. Baulch-Brown, J. Mills, and J. Meanger.** 2003. The matrix protein of Human respiratory syncytial virus localises to the nucleus of infected cells and inhibits transcription. *Arch Virol* **148**:1419-1429.
18. **Bukreyev, A., S. S. Whitehead, B. R. Murphy, and P. L. Collins.** 1997. Recombinant respiratory syncytial virus from which the entire SH gene has been deleted grows efficiently in cell culture and exhibits site-specific attenuation in the respiratory tract of the mouse. *J Virol* **71**:8973-8982.
19. **Kochva, U., H. Leonov, and I. T. Arkin.** 2003. Modeling the structure of the respiratory syncytial virus small hydrophobic protein by silent-mutation analysis of global searching molecular dynamics. *Protein Sci* **12**:2668-2674.

20. **Fuentes, S., K. C. Tran, P. Luthra, M. N. Teng, and B. He.** 2007. Function of the respiratory syncytial virus small hydrophobic protein. *J Virol* **81**:8361-8366.
21. **Graham, B. S., T. R. Johnson, and R. S. Peebles.** 2000. Immune-mediated disease pathogenesis in respiratory syncytial virus infection. *Immunopharmacology* **48**:237-247.
22. **Gorman, J. J., B. L. Ferguson, D. Speelman, and J. Mills.** 1997. Determination of the disulfide bond arrangement of human respiratory syncytial virus attachment (G) protein by matrix-assisted laser desorption/ionization time-of-flight mass spectrometry. *Protein Sci* **6**:1308-1315.
23. **Tripp, R. A., L. P. Jones, L. M. Haynes, H. Zheng, P. M. Murphy, and L. J. Anderson.** 2001. CX3C chemokine mimicry by respiratory syncytial virus G glycoprotein. *Nat Immunol* **2**:732-738.
24. **Harcourt, J., R. Alvarez, L. P. Jones, C. Henderson, L. J. Anderson, and R. A. Tripp.** 2006. Respiratory syncytial virus G protein and G protein CX3C motif adversely affect CX3CR1+ T cell responses. *J Immunol* **176**:1600-1608.
25. **Bukreyev, A., M. E. Serra, F. R. Laham, G. A. Melendi, S. R. Kleeberger, P. L. Collins, and F. P. Polack.** 2006. The cysteine-rich region and secreted form of the attachment G glycoprotein of respiratory syncytial virus enhance the cytotoxic T-lymphocyte response despite lacking major histocompatibility complex class I-restricted epitopes. *J Virol* **80**:5854-5861.

26. **Teng, M. N., and P. L. Collins.** 2002. The central conserved cystine noose of the attachment G protein of human respiratory syncytial virus is not required for efficient viral infection in vitro or in vivo. *J Virol* **76**:6164-6171.
27. **Teng, M. N., S. S. Whitehead, and P. L. Collins.** 2001. Contribution of the respiratory syncytial virus G glycoprotein and its secreted and membrane-bound forms to virus replication in vitro and in vivo. *Virology* **289**:283-296.
28. **Hendricks, D. A., K. McIntosh, and J. L. Patterson.** 1988. Further characterization of the soluble form of the G glycoprotein of respiratory syncytial virus. *J Virol* **62**:2228-2233.
29. **Roberts, S. R., D. Lichtenstein, L. A. Ball, and G. W. Wertz.** 1994. The membrane-associated and secreted forms of the respiratory syncytial virus attachment glycoprotein G are synthesized from alternative initiation codons. *J Virol* **68**:4538-4546.
30. **Wertz, G. W., M. Krieger, and L. A. Ball.** 1989. Structure and cell surface maturation of the attachment glycoprotein of human respiratory syncytial virus in a cell line deficient in O glycosylation. *J Virol* **63**:4767-4776.
31. **Crim, R. L., S. A. Audet, S. A. Feldman, H. S. Mostowski, and J. A. Beeler.** 2007. Identification of linear heparin-binding peptides derived from human respiratory syncytial virus fusion glycoprotein that inhibit infectivity. *J Virol* **81**:261-271.

32. **Kahn, J. S., M. J. Schnell, L. Buonocore, and J. K. Rose.** 1999. Recombinant vesicular stomatitis virus expressing respiratory syncytial virus (RSV) glycoproteins: RSV fusion protein can mediate infection and cell fusion. *Virology* **254**:81-91.
33. **Tayyari, F., D. Marchant, T. J. Moraes, W. Duan, P. Mastrangelo, and R. G. Hegele.** 2011. Identification of nucleolin as a cellular receptor for human respiratory syncytial virus. *Nat Med* **17**:1132-1135.
34. **Collins, P. L., Y. T. Huang, and G. W. Wertz.** 1984. Nucleotide sequence of the gene encoding the fusion (F) glycoprotein of human respiratory syncytial virus. *Proc Natl Acad Sci U S A* **81**:7683-7687.
35. **Zhao, X., M. Singh, V. N. Malashkevich, and P. S. Kim.** 2000. Structural characterization of the human respiratory syncytial virus fusion protein core. *Proc Natl Acad Sci U S A* **97**:14172-14177.
36. **Zimmer, G., M. Rohn, G. P. McGregor, M. Schemann, K. K. Conzelmann, and G. Herrler.** 2003. Virokinin, a bioactive peptide of the tachykinin family, is released from the fusion protein of bovine respiratory syncytial virus. *J Biol Chem* **278**:46854-46861.
37. **Kurt-Jones, E. A., L. Popova, L. Kwinn, L. M. Haynes, L. P. Jones, R. A. Tripp, E. E. Walsh, M. W. Freeman, D. T. Golenbock, L. J. Anderson, and R. W. Finberg.** 2000. Pattern recognition receptors TLR4 and CD14 mediate response to respiratory syncytial virus. *Nat Immunol* **1**:398-401.

38. **Lee, J. K., A. Prussia, T. Paal, L. K. White, J. P. Snyder, and R. K. Plemper.** 2008. Functional interaction between paramyxovirus fusion and attachment proteins. *J Biol Chem* **283**:16561-16572.
39. **Bose, S., A. Zokarkar, B. D. Welch, G. P. Leser, T. S. Jardetzky, and R. A. Lamb.** 2012. Fusion activation by a headless parainfluenza virus 5 hemagglutinin-neuraminidase stalk suggests a modular mechanism for triggering. *Proc Natl Acad Sci U S A* **109**:E2625-2634.
40. **Waning, D. L., C. J. Russell, T. S. Jardetzky, and R. A. Lamb.** 2004. Activation of a paramyxovirus fusion protein is modulated by inside-out signaling from the cytoplasmic tail. *Proc Natl Acad Sci U S A* **101**:9217-9222.
41. **Tanabayashi, K., and R. W. Compans.** 1996. Functional interaction of paramyxovirus glycoproteins: identification of a domain in Sendai virus HN which promotes cell fusion. *J Virol* **70**:6112-6118.
42. **Sergel, T., L. W. McGinnes, M. E. Peeples, and T. G. Morrison.** 1993. The attachment function of the Newcastle disease virus hemagglutinin-neuraminidase protein can be separated from fusion promotion by mutation. *Virology* **193**:717-726.
43. **Takimoto, T., G. L. Taylor, H. C. Connaris, S. J. Crennell, and A. Portner.** 2002. Role of the hemagglutinin-neuraminidase protein in the mechanism of paramyxovirus-cell membrane fusion. *J Virol* **76**:13028-13033.
44. **Rawling, J., B. Garcia-Barreno, and J. A. Melero.** 2008. Insertion of the two cleavage sites of the respiratory syncytial virus fusion protein in



- Sendai virus fusion protein leads to enhanced cell-cell fusion and a decreased dependency on the HN attachment protein for activity. *J Virol* **82**:5986-5998.
45. **Liuzzi, M., S. W. Mason, M. Cartier, C. Lawetz, R. S. McCollum, N. Dansereau, G. Bolger, N. Lapeyre, Y. Gaudette, L. Lagace, M. J. Massariol, F. Do, P. Whitehead, L. Lamarre, E. Scouten, J. Bordeleau, S. Landry, J. Rancourt, G. Fazal, and B. Simoneau.** 2005. Inhibitors of respiratory syncytial virus replication target cotranscriptional mRNA guanylation by viral RNA-dependent RNA polymerase. *J Virol* **79**:13105-13115.
46. **Dochow, M., S. A. Krumm, J. E. Crowe, Jr., M. L. Moore, and R. K. Plemper.** 2012. Independent structural domains in paramyxovirus polymerase protein. *J Biol Chem* **287**:6878-6891.
47. **Akerlind, B., and E. Norrby.** 1986. Occurrence of respiratory syncytial virus subtypes A and B strains in Sweden. *J Med Virol* **19**:241-247.
48. **Hendry, R. M., J. C. Burns, E. E. Walsh, B. S. Graham, P. F. Wright, V. G. Hemming, W. J. Rodriguez, H. W. Kim, G. A. Prince, K. McIntosh, and et al.** 1988. Strain-specific serum antibody responses in infants undergoing primary infection with respiratory syncytial virus. *J Infect Dis* **157**:640-647.
49. **Collins, P. L., R. A. Olmsted, and P. R. Johnson.** 1990. The small hydrophobic protein of human respiratory syncytial virus: comparison between antigenic subgroups A and B. *J Gen Virol* **71 ( Pt 7)**:1571-1576.

50. **Johnson, P. R., M. K. Spriggs, R. A. Olmsted, and P. L. Collins.** 1987. The G glycoprotein of human respiratory syncytial viruses of subgroups A and B: extensive sequence divergence between antigenically related proteins. *Proc Natl Acad Sci U S A* **84**:5625-5629.
51. **Zlateva, K. T., P. Lemey, A. M. Vandamme, and M. Van Ranst.** 2004. Molecular evolution and circulation patterns of human respiratory syncytial virus subgroup a: positively selected sites in the attachment g glycoprotein. *J Virol* **78**:4675-4683.
52. **Cane, P. A., and C. R. Pringle.** 1995. Evolution of subgroup A respiratory syncytial virus: evidence for progressive accumulation of amino acid changes in the attachment protein. *J Virol* **69**:2918-2925.
53. **Johnson, P. R., Jr., R. A. Olmsted, G. A. Prince, B. R. Murphy, D. W. Alling, E. E. Walsh, and P. L. Collins.** 1987. Antigenic relatedness between glycoproteins of human respiratory syncytial virus subgroups A and B: evaluation of the contributions of F and G glycoproteins to immunity. *J Virol* **61**:3163-3166.
54. **Lowen, A. C., S. Mubareka, J. Steel, and P. Palese.** 2007. Influenza virus transmission is dependent on relative humidity and temperature. *PLoS Pathog* **3**:1470-1476.
55. **Dowell, S. F.** 2001. Seasonal variation in host susceptibility and cycles of certain infectious diseases. *Emerg Infect Dis* **7**:369-374.
56. **Lofgren, E., N. H. Fefferman, Y. N. Naumov, J. Gorski, and E. N. Naumova.** 2007. Influenza seasonality: underlying causes and modeling theories. *J Virol* **81**:5429-5436.

57. **Sloan, C., M. L. Moore, and T. Hartert.** 2011. Impact of pollution, climate, and sociodemographic factors on spatiotemporal dynamics of seasonal respiratory viruses. *Clin Transl Sci* **4**:48-54.
58. **Stensballe, L. G., J. K. Devasundaram, and E. A. Simoes.** 2003. Respiratory syncytial virus epidemics: the ups and downs of a seasonal virus. *Pediatr Infect Dis J* **22**:S21-32.
59. **Weber, M. W., E. K. Mulholland, and B. M. Greenwood.** 1998. Respiratory syncytial virus infection in tropical and developing countries. *Trop Med Int Health* **3**:268-280.
60. **McAnerney, J. M., S. Johnson, and B. D. Schoub.** 1994. Surveillance of respiratory viruses. A 10-year laboratory-based study. *S Afr Med J* **84**:473-477.
61. **Chew, F. T., S. Doraisingham, A. E. Ling, G. Kumarasinghe, and B. W. Lee.** 1998. Seasonal trends of viral respiratory tract infections in the tropics. *Epidemiol Infect* **121**:121-128.
62. **Peret, T. C., C. B. Hall, K. C. Schnabel, J. A. Golub, and L. J. Anderson.** 1998. Circulation patterns of genetically distinct group A and B strains of human respiratory syncytial virus in a community. *J Gen Virol* **79 ( Pt 9)**:2221-2229.
63. **Peret, T. C., C. B. Hall, G. W. Hammond, P. A. Piedra, G. A. Storch, W. M. Sullender, C. Tsou, and L. J. Anderson.** 2000. Circulation patterns of group A and B human respiratory syncytial virus genotypes in 5 communities in North America. *J.Infect.Dis.* **181**:1891-1896.

64. **Seemungal, T., R. Harper-Owen, A. Bhowmik, I. Moric, G. Sanderson, S. Message, P. Maccallum, T. W. Meade, D. J. Jeffries, S. L. Johnston, and J. A. Wedzicha.** 2001. Respiratory viruses, symptoms, and inflammatory markers in acute exacerbations and stable chronic obstructive pulmonary disease. *Am J Respir Crit Care Med* **164**:1618-1623.
65. **Collins, P. L., M. G. Hill, E. Camargo, H. Grosfeld, R. M. Chanock, and B. R. Murphy.** 1995. Production of infectious human respiratory syncytial virus from cloned cDNA confirms an essential role for the transcription elongation factor from the 5' proximal open reading frame of the M2 mRNA in gene expression and provides a capability for vaccine development. *Proc Natl Acad Sci U S A* **92**:11563-11567.
66. **Collins, P. L., and B. R. Murphy.** 2005. New generation live vaccines against human respiratory syncytial virus designed by reverse genetics. *Proc Am Thorac Soc* **2**:166-173.
67. **Moore, M. L., M. H. Chi, C. Luongo, N. W. Lukacs, V. V. Polosukhin, M. M. Huckabee, D. C. Newcomb, U. J. Buchholz, J. E. Crowe, Jr., K. Goleniewska, J. V. Williams, P. L. Collins, and R. S. Peebles, Jr.** 2009. A chimeric A2 strain of respiratory syncytial virus (RSV) with the fusion protein of RSV strain line 19 exhibits enhanced viral load, mucus, and airway dysfunction. *J Virol* **83**:4185-4194.
68. **Buchholz, U. J., H. Granzow, K. Schuldt, S. S. Whitehead, B. R. Murphy, and P. L. Collins.** 2000. Chimeric bovine respiratory syncytial virus with glycoprotein gene substitutions from human

- respiratory syncytial virus (HRSV): effects on host range and evaluation as a live-attenuated HRSV vaccine. *J Virol* **74**:1187-1199.
69. **Whitehead, S. S., M. G. Hill, C. Y. Firestone, M. St Claire, W. R. Elkins, B. R. Murphy, and P. L. Collins.** 1999. Replacement of the F and G proteins of respiratory syncytial virus (RSV) subgroup A with those of subgroup B generates chimeric live attenuated RSV subgroup B vaccine candidates. *J Virol* **73**:9773-9780.
70. **Bukreyev, A., I. M. Belyakov, J. A. Berzofsky, B. R. Murphy, and P. L. Collins.** 2001. Granulocyte-macrophage colony-stimulating factor expressed by recombinant respiratory syncytial virus attenuates viral replication and increases the level of pulmonary antigen-presenting cells. *J Virol* **75**:12128-12140.
71. **Jin, H., H. Zhou, X. Cheng, R. Tang, M. Munoz, and N. Nguyen.** 2000. Recombinant respiratory syncytial viruses with deletions in the NS1, NS2, SH, and M2-2 genes are attenuated in vitro and in vivo. *Virology* **273**:210-218.
72. **Biacchesi, S., B. R. Murphy, P. L. Collins, and U. J. Buchholz.** 2007. Frequent frameshift and point mutations in the SH gene of human metapneumovirus passaged in vitro. *J Virol* **81**:6057-6067.
73. **Collins, P. L., and G. W. Wertz.** 1985. Nucleotide sequences of the 1B and 1C nonstructural protein mRNAs of human respiratory syncytial virus. *Virology* **143**:442-451.
74. **Hotard, A. L., F. Y. Shaikh, S. Lee, D. Yan, M. N. Teng, R. K. Plemper, J. E. Crowe, Jr., and M. L. Moore.** 2012. A stabilized

- respiratory syncytial virus reverse genetics system amenable to recombination-mediated mutagenesis. *Virology* **434**:129-136.
75. **Shay, D. K., R. C. Holman, R. D. Newman, L. L. Liu, J. W. Stout, and L. J. Anderson.** 1999. Bronchiolitis-associated hospitalizations among US children, 1980-1996. *JAMA* **282**:1440-1446.
76. **Simoes, E. A.** 1999. Respiratory syncytial virus infection. *Lancet* **354**:847-852.
77. **Simoes, E. A., J. R. Groothuis, D. A. Tristram, K. Alessi, M. V. Lehr, G. R. Siber, and R. C. Welliver.** 1996. Respiratory syncytial virus-enriched globulin for the prevention of acute otitis media in high risk children. *J Pediatr* **129**:214-219.
78. **Hall, C. B.** 2001. Respiratory syncytial virus and parainfluenza virus. *N Engl J Med* **344**:1917-1928.
79. **Pelletier, A. J., J. M. Mansbach, and C. A. Camargo, Jr.** 2006. Direct medical costs of bronchiolitis hospitalizations in the United States. *Pediatrics* **118**:2418-2423.
80. **American Academy of Pediatrics Subcommittee on, D., and B. Management of.** 2006. Diagnosis and management of bronchiolitis. *Pediatrics* **118**:1774-1793.
81. **Garcia, C. G., R. Bhore, A. Soriano-Fallas, M. Trost, R. Chason, O. Ramilo, and A. Mejias.** 2010. Risk factors in children hospitalized with RSV bronchiolitis versus non-RSV bronchiolitis. *Pediatrics* **126**:e1453-1460.

82. **Everard, M. L., A. Swarbrick, M. Wraitham, J. McIntyre, C. Dunkley, P. D. James, H. F. Sewell, and A. D. Milner.** 1994. Analysis of cells obtained by bronchial lavage of infants with respiratory syncytial virus infection. *Arch Dis Child* **71**:428-432.
83. **Kim, E. A., K. S. Lee, S. L. Primack, H. K. Yoon, H. S. Byun, T. S. Kim, G. Y. Suh, O. J. Kwon, and J. Han.** 2002. Viral pneumonias in adults: radiologic and pathologic findings. *Radiographics* **22 Spec No**:S137-149.
84. **Bruder, D., A. Srikiatkachorn, and R. I. Enelow.** 2006. Cellular immunity and lung injury in respiratory virus infection. *Viral Immunol* **19**:147-155.
85. **Johnson, J. E., R. A. Gonzales, S. J. Olson, P. F. Wright, and B. S. Graham.** 2007. The histopathology of fatal untreated human respiratory syncytial virus infection. *Mod Pathol* **20**:108-119.
86. **Welliver, T. P., J. L. Reed, and R. C. Welliver, Sr.** 2008. Respiratory syncytial virus and influenza virus infections: observations from tissues of fatal infant cases. *Pediatr Infect Dis J* **27**:S92-96.
87. **Welliver, T. P., R. P. Garofalo, Y. Hosakote, K. H. Hintz, L. Avendano, K. Sanchez, L. Velozo, H. Jafri, S. Chavez-Bueno, P. L. Ogra, L. McKinney, J. L. Reed, and R. C. Welliver, Sr.** 2007. Severe human lower respiratory tract illness caused by respiratory syncytial virus and influenza virus is characterized by the absence of pulmonary cytotoxic lymphocyte responses. *J Infect Dis* **195**:1126-1136.

88. **Shigeta, S., Y. Hinuma, T. Suto, and N. Ishida.** 1968. The cell to cell infection of respiratory syncytial virus in HEp-2 monolayer cultures. *J Gen Virol* **3**:129-131.
89. **Munday, D. C., E. Emmott, R. Surtees, C. H. Lardeau, W. Wu, W. P. Duprex, B. K. Dove, J. N. Barr, and J. A. Hiscox.** 2010. Quantitative proteomic analysis of A549 cells infected with human respiratory syncytial virus. *Mol Cell Proteomics* **9**:2438-2459.
90. **Fiedler, M. A., K. Wernke-Dollries, and J. M. Stark.** 1996. Inhibition of viral replication reverses respiratory syncytial virus-induced NF-kappaB activation and interleukin-8 gene expression in A549 cells. *J Virol* **70**:9079-9082.
91. **Villenave, R., O. Touzelet, S. Thavagnanam, S. Sarlang, J. Parker, G. Skibinski, L. G. Heaney, J. P. McKaigue, P. V. Coyle, M. D. Shields, and U. F. Power.** 2010. Cytopathogenesis of Sendai virus in well-differentiated primary pediatric bronchial epithelial cells. *J Virol* **84**:11718-11728.
92. **Villenave, R., S. Thavagnanam, S. Sarlang, J. Parker, I. Douglas, G. Skibinski, L. G. Heaney, J. P. McKaigue, P. V. Coyle, M. D. Shields, and U. F. Power.** 2012. In vitro modeling of respiratory syncytial virus infection of pediatric bronchial epithelium, the primary target of infection in vivo. *Proc Natl Acad Sci U S A* **109**:5040-5045.
93. **Parker, J., S. Sarlang, S. Thavagnanam, G. Williamson, D. O'Donoghue, R. Villenave, U. Power, M. Shields, L. Heaney, and G. Skibinski.** 2010. A 3-D well-differentiated model of pediatric



- bronchial epithelium demonstrates unstimulated morphological differences between asthmatic and nonasthmatic cells. *Pediatr Res* **67**:17-22.
94. **Oshansky, C. M., J. P. Barber, J. Crabtree, and R. A. Tripp.** 2010. Respiratory syncytial virus F and G proteins induce interleukin 1alpha, CC, and CXC chemokine responses by normal human bronchoepithelial cells. *J Infect Dis* **201**:1201-1207.
95. **Byrd, L. G., and G. A. Prince.** 1997. Animal models of respiratory syncytial virus infection. *Clin Infect Dis* **25**:1363-1368.
96. **Moore, M. L., and R. S. Peebles, Jr.** 2006. Respiratory syncytial virus disease mechanisms implicated by human, animal model, and in vitro data facilitate vaccine strategies and new therapeutics. *Pharmacol Ther* **112**:405-424.
97. **Collins, P. L., R. H. Purcell, W. T. London, L. A. Lawrence, R. M. Chanock, and B. R. Murphy.** 1990. Evaluation in chimpanzees of vaccinia virus recombinants that express the surface glycoproteins of human respiratory syncytial virus. *Vaccine* **8**:164-168.
98. **Crowe, J. E., Jr., P. L. Collins, W. T. London, R. M. Chanock, and B. R. Murphy.** 1993. A comparison in chimpanzees of the immunogenicity and efficacy of live attenuated respiratory syncytial virus (RSV) temperature-sensitive mutant vaccines and vaccinia virus recombinants that express the surface glycoproteins of RSV. *Vaccine* **11**:1395-1404.

99. **Crowe, J. E., Jr., P. T. Bui, A. R. Davis, R. M. Chanock, and B. R. Murphy.** 1994. A further attenuated derivative of a cold-passaged temperature-sensitive mutant of human respiratory syncytial virus retains immunogenicity and protective efficacy against wild-type challenge in seronegative chimpanzees. *Vaccine* **12**:783-790.
100. **Prince, G. A., A. B. Jenson, R. L. Horswood, E. Camargo, and R. M. Chanock.** 1978. The pathogenesis of respiratory syncytial virus infection in cotton rats. *Am J Pathol* **93**:771-791.
101. **Boukhvalova, M. S., G. A. Prince, and J. C. Blanco.** 2009. The cotton rat model of respiratory viral infections. *Biologicals* **37**:152-159.
102. **Lee, F. E., E. E. Walsh, A. R. Falsey, R. F. Betts, and J. J. Treanor.** 2004. Experimental infection of humans with A2 respiratory syncytial virus. *Antiviral Res* **63**:191-196.
103. **DeVincenzo, J., R. Lambkin-Williams, T. Wilkinson, J. Cehelsky, S. Nochur, E. Walsh, R. Meyers, J. Gollob, and A. Vaishnaw.** 2010. A randomized, double-blind, placebo-controlled study of an RNAi-based therapy directed against respiratory syncytial virus. *Proc Natl Acad Sci U S A* **107**:8800-8805.
104. **Noah, T. L., and S. Becker.** 2000. Chemokines in nasal secretions of normal adults experimentally infected with respiratory syncytial virus. *Clin Immunol* **97**:43-49.
105. **Lukacs, N. W., M. L. Moore, B. D. Rudd, A. A. Berlin, R. D. Collins, S. J. Olson, S. B. Ho, and R. S. Peebles, Jr.** 2006. Differential immune responses and pulmonary pathophysiology are

- induced by two different strains of respiratory syncytial virus. *Am J Pathol* **169**:977-986.
106. **Stokes, K. L., M. H. Chi, K. Sakamoto, D. C. Newcomb, M. G. Currier, M. M. Huckabee, S. Lee, K. Goleniewska, C. Pretto, J. V. Williams, A. Hotard, T. P. Sherrill, R. S. Peebles, Jr., and M. L. Moore.** 2011. Differential pathogenesis of respiratory syncytial virus clinical isolates in BALB/c mice. *J Virol* **85**:5782-5793.
107. **Lewis FA, R. M., Lehman NI, Ferris AA.** 1961. A syncytial virus associated with epidemic disease of the lower respiratory tract in infants and young children. *Medical Journal Australia* **2**:932.
108. **Graham, B. S., L. A. Bunton, P. F. Wright, and D. T. Karzon.** 1991. Role of T lymphocyte subsets in the pathogenesis of primary infection and rechallenge with respiratory syncytial virus in mice. *J Clin Invest* **88**:1026-1033.
109. **Liu, J., T. J. Ruckwardt, M. Chen, J. D. Nicewonger, T. R. Johnson, and B. S. Graham.** 2010. Epitope-specific regulatory CD4 T cells reduce virus-induced illness while preserving CD8 T-cell effector function at the site of infection. *J Virol* **84**:10501-10509.
110. **Chang, J., S. Y. Choi, H. T. Jin, Y. C. Sung, and T. J. Braciale.** 2004. Improved effector activity and memory CD8 T cell development by IL-2 expression during experimental respiratory syncytial virus infection. *J Immunol* **172**:503-508.
111. **Tang, Y. W., and B. S. Graham.** 1995. Interleukin-12 treatment during immunization elicits a T helper cell type 1-like immune response in mice

- challenged with respiratory syncytial virus and improves vaccine immunogenicity. *J Infect Dis* **172**:734-738.
112. **Varga, S. M., E. L. Wissinger, and T. J. Braciale.** 2000. The attachment (G) glycoprotein of respiratory syncytial virus contains a single immunodominant epitope that elicits both Th1 and Th2 CD4+ T cell responses. *J Immunol* **165**:6487-6495.
113. **Herlocher, M. L., M. Ewasyshyn, S. Sambhara, M. Gharaee-Kermani, D. Cho, J. Lai, M. Klein, and H. F. Maassab.** 1999. Immunological properties of plaque purified strains of live attenuated respiratory syncytial virus (RSV) for human vaccine. *Vaccine* **17**:172-181.
114. **Vareille, M., E. Kieninger, M. R. Edwards, and N. Regamey.** 2011. The airway epithelium: soldier in the fight against respiratory viruses. *Clin Microbiol Rev* **24**:210-229.
115. **Mukherjee, A., S. A. Morosky, L. Shen, C. R. Weber, J. R. Turner, K. S. Kim, T. Wang, and C. B. Coyne.** 2009. Retinoic acid-induced gene-1 (RIG-I) associates with the actin cytoskeleton via caspase activation and recruitment domain-dependent interactions. *J Biol Chem* **284**:6486-6494.
116. **Loo, Y. M., J. Fornek, N. Crochet, G. Bajwa, O. Perwitasari, L. Martinez-Sobrido, S. Akira, M. A. Gill, A. Garcia-Sastre, M. G. Katze, and M. Gale, Jr.** 2008. Distinct RIG-I and MDA5 signaling by RNA viruses in innate immunity. *J Virol* **82**:335-345.

117. **Hiemstra, P. S.** 2001. Epithelial antimicrobial peptides and proteins: their role in host defence and inflammation. *Paediatr Respir Rev* **2**:306-310.
118. **McNamara, P. S., B. F. Flanagan, C. A. Hart, and R. L. Smyth.** 2005. Production of chemokines in the lungs of infants with severe respiratory syncytial virus bronchiolitis. *J Infect Dis* **191**:1225-1232.
119. **Uematsu, S., and S. Akira.** 2006. Toll-like receptors and innate immunity. *J Mol Med (Berl)* **84**:712-725.
120. **Groskreutz, D. J., M. M. Monick, L. S. Powers, T. O. Yarovinsky, D. C. Look, and G. W. Hunninghake.** 2006. Respiratory syncytial virus induces TLR3 protein and protein kinase R, leading to increased double-stranded RNA responsiveness in airway epithelial cells. *J Immunol* **176**:1733-1740.
121. **Rudd, B. D., E. Burstein, C. S. Duckett, X. Li, and N. W. Lukacs.** 2005. Differential role for TLR3 in respiratory syncytial virus-induced chemokine expression. *J Virol* **79**:3350-3357.
122. **Haeberle, H. A., R. Takizawa, A. Casola, A. R. Brasier, H. J. Dieterich, N. Van Rooijen, Z. Gatalica, and R. P. Garofalo.** 2002. Respiratory syncytial virus-induced activation of nuclear factor-kappaB in the lung involves alveolar macrophages and toll-like receptor 4-dependent pathways. *J Infect Dis* **186**:1199-1206.
123. **Lukacs, N. W., J. J. Smit, S. Mukherjee, S. B. Morris, G. Nunez, and D. M. Lindell.** 2010. Respiratory virus-induced TLR7 activation

- controls IL-17-associated increased mucus via IL-23 regulation. *J Immunol* **185**:2231-2239.
124. **Singh, D., K. L. McCann, and F. Imani.** 2007. MAPK and heat shock protein 27 activation are associated with respiratory syncytial virus induction of human bronchial epithelial monolayer disruption. *Am J Physiol Lung Cell Mol Physiol* **293**:L436-445.
125. **Dosanjh, A., S. Rednam, and M. Martin.** 2003. Respiratory syncytial virus augments production of fibroblast growth factor basic in vitro: implications for a possible mechanism of prolonged wheezing after infection. *Pediatr Allergy Immunol* **14**:437-440.
126. **Mogensen, T. H., and S. R. Paludan.** 2001. Molecular pathways in virus-induced cytokine production. *Microbiol Mol Biol Rev* **65**:131-150.
127. **Rose, M. C., T. J. Nickola, and J. A. Voynow.** 2001. Airway mucus obstruction: mucin glycoproteins, MUC gene regulation and goblet cell hyperplasia. *Am J Respir Cell Mol Biol* **25**:533-537.
128. **Rose, M. C., and J. A. Voynow.** 2006. Respiratory tract mucin genes and mucin glycoproteins in health and disease. *Physiol Rev* **86**:245-278.
129. **Ordonez, C. L., R. Khashayar, H. H. Wong, R. Ferrando, R. Wu, D. M. Hyde, J. A. Hotchkiss, Y. Zhang, A. Novikov, G. Dolganov, and J. V. Fahy.** 2001. Mild and moderate asthma is associated with airway goblet cell hyperplasia and abnormalities in mucin gene expression. *Am J Respir Crit Care Med* **163**:517-523.
130. **Zuhdi Alimam, M., F. M. Piazza, D. M. Selby, N. Letwin, L. Huang, and M. C. Rose.** 2000. Muc-5/5ac mucin messenger RNA and

protein expression is a marker of goblet cell metaplasia in murine airways. *Am J Respir Cell Mol Biol* **22**:253-260.

131. **Hashimoto, K., B. S. Graham, S. B. Ho, K. B. Adler, R. D. Collins, S. J. Olson, W. Zhou, T. Suzutani, P. W. Jones, K. Goleniewska, J. F. O'Neal, and R. S. Peebles, Jr.** 2004. Respiratory syncytial virus in allergic lung inflammation increases Muc5ac and gob-5. *Am J Respir Crit Care Med* **170**:306-312.
132. **Pack, R. J., L. H. Al-Ugaily, and G. Morris.** 1981. The cells of the tracheobronchial epithelium of the mouse: a quantitative light and electron microscope study. *J Anat* **132**:71-84.
133. **Booth, B. W., K. B. Adler, J. C. Bonner, F. Tournier, and L. D. Martin.** 2001. Interleukin-13 induces proliferation of human airway epithelial cells in vitro via a mechanism mediated by transforming growth factor-alpha. *Am J Respir Cell Mol Biol* **25**:739-743.
134. **Fujisawa, T., K. Ide, M. J. Holtzman, T. Suda, K. Suzuki, S. Kuroishi, K. Chida, and H. Nakamura.** 2008. Involvement of the p38 MAPK pathway in IL-13-induced mucous cell metaplasia in mouse tracheal epithelial cells. *Respirology* **13**:191-202.
135. **Mukherjee, S., D. M. Lindell, A. A. Berlin, S. B. Morris, T. P. Shanley, M. B. Hershenson, and N. W. Lukacs.** 2011. IL-17-induced pulmonary pathogenesis during respiratory viral infection and exacerbation of allergic disease. *Am J Pathol* **179**:248-258.
136. **Borregaard, N., and J. B. Cowland.** 1997. Granules of the human neutrophilic polymorphonuclear leukocyte. *Blood* **89**:3503-3521.

137. **Smith, P. K., S. Z. Wang, K. D. Dowling, and K. D. Forsyth.** 2001. Leucocyte populations in respiratory syncytial virus-induced bronchiolitis. *J Paediatr Child Health* **37**:146-151.
138. 2007. Innate Immunity, p. 65-66. *In* T. Kindt, Goldsby RA, and Osborne BA (ed.), *Kuby Immunology*, Sixth ed. W.H. Freeman and Company, New York.
139. **De Filippo, K., R. B. Henderson, M. Laschinger, and N. Hogg.** 2008. Neutrophil chemokines KC and macrophage-inflammatory protein-2 are newly synthesized by tissue macrophages using distinct TLR signaling pathways. *J Immunol* **180**:4308-4315.
140. **Foley, S. C., and Q. Hamid.** 2007. Images in allergy and immunology: neutrophils in asthma. *J Allergy Clin Immunol* **119**:1282-1286.
141. **Busse, P. J., T. F. Zhang, K. Srivastava, B. P. Lin, B. Schofield, S. C. Sealson, and X. M. Li.** 2005. Chronic exposure to TNF-alpha increases airway mucus gene expression in vivo. *J Allergy Clin Immunol* **116**:1256-1263.
142. **Shao, M. X., and J. A. Nadel.** 2005. Neutrophil elastase induces MUC5AC mucin production in human airway epithelial cells via a cascade involving protein kinase C, reactive oxygen species, and TNF-alpha-converting enzyme. *J Immunol* **175**:4009-4016.
143. **Voynow, J. A., L. R. Young, Y. Wang, T. Horger, M. C. Rose, and B. M. Fischer.** 1999. Neutrophil elastase increases MUC5AC mRNA and protein expression in respiratory epithelial cells. *Am J Physiol* **276**:L835-843.



144. **Abu-Harb, M., F. Bell, A. Finn, W. H. Rao, L. Nixon, D. Shale, and M. L. Everard.** 1999. IL-8 and neutrophil elastase levels in the respiratory tract of infants with RSV bronchiolitis. *Eur Respir J* **14**:139-143.
145. **Stark, J. M., A. W. van Egmond, J. J. Zimmerman, S. K. Carabell, and M. F. Tosi.** 1992. Detection of enhanced neutrophil adhesion to parainfluenza-infected airway epithelial cells using a modified myeloperoxidase assay in a microtiter format. *J Virol Methods* **40**:225-242.
146. **Ratcliffe, D. R., S. L. Nolin, and E. B. Cramer.** 1988. Neutrophil interaction with influenza-infected epithelial cells. *Blood* **72**:142-149.
147. **Stark, J. M., V. Godding, J. B. Sedgwick, and W. W. Busse.** 1996. Respiratory syncytial virus infection enhances neutrophil and eosinophil adhesion to cultured respiratory epithelial cells. Roles of CD18 and intercellular adhesion molecule-1. *J Immunol* **156**:4774-4782.
148. **Wang, S. Z., H. Xu, A. Wraith, J. J. Bowden, J. H. Alpers, and K. D. Forsyth.** 1998. Neutrophils induce damage to respiratory epithelial cells infected with respiratory syncytial virus. *Eur Respir J* **12**:612-618.
149. **Simon, R. H., P. D. DeHart, and R. F. Todd, 3rd.** 1986. Neutrophil-induced injury of rat pulmonary alveolar epithelial cells. *J Clin Invest* **78**:1375-1386.
150. **Wang, S. Z., P. K. Smith, M. Lovejoy, J. J. Bowden, J. H. Alpers, and K. D. Forsyth.** 1998. The apoptosis of neutrophils is accelerated in

- respiratory syncytial virus (RSV)-induced bronchiolitis. *Clin Exp Immunol* **114**:49-54.
151. **Jones, A., J. M. Qui, E. Bataki, H. Elphick, S. Ritson, G. S. Evans, and M. L. Everard.** 2002. Neutrophil survival is prolonged in the airways of healthy infants and infants with RSV bronchiolitis. *Eur Respir J* **20**:651-657.
152. **Jaovisidha, P., M. E. Peeples, A. A. Brees, L. R. Carpenter, and J. N. Moy.** 1999. Respiratory syncytial virus stimulates neutrophil degranulation and chemokine release. *J Immunol* **163**:2816-2820.
153. **Hayashi, F., T. K. Means, and A. D. Luster.** 2003. Toll-like receptors stimulate human neutrophil function. *Blood* **102**:2660-2669.
154. **Wheeler, D. S., M. A. Chase, A. P. Senft, S. E. Poynter, H. R. Wong, and K. Page.** 2009. Extracellular Hsp72, an endogenous DAMP, is released by virally infected airway epithelial cells and activates neutrophils via Toll-like receptor (TLR)-4. *Respir Res* **10**:31.
155. **Halfhide, C. P., S. P. Brearey, B. F. Flanagan, J. A. Hunt, D. Howarth, J. Cummerson, S. Edwards, C. A. Hart, and R. L. Smyth.** 2009. Neutrophil TLR4 expression is reduced in the airways of infants with severe bronchiolitis. *Thorax* **64**:798-805.
156. **Halfhide, C. P., B. F. Flanagan, S. P. Brearey, J. A. Hunt, A. M. Fonceca, P. S. McNamara, D. Howarth, S. Edwards, and R. L. Smyth.** 2011. Respiratory syncytial virus binds and undergoes transcription in neutrophils from the blood and airways of infants with severe bronchiolitis. *J Infect Dis* **204**:451-458.

157. **Kaul, T. N., H. Faden, R. Baker, and P. L. Ogra.** 1984. Virus-induced complement activation and neutrophil-mediated cytotoxicity against respiratory syncytial virus (RSV). *Clin Exp Immunol* **56**:501-508.
158. **Corbeil, S., C. Seguin, and M. Trudel.** 1996. Involvement of the complement system in the protection of mice from challenge with respiratory syncytial virus Long strain following passive immunization with monoclonal antibody 18A2B2. *Vaccine* **14**:521-525.
159. **Edwards, K. M., P. N. Snyder, and P. F. Wright.** 1986. Complement activation by respiratory syncytial virus-infected cells. *Arch Virol* **88**:49-56.
160. **Polack, F. P., M. N. Teng, P. L. Collins, G. A. Prince, M. Exner, H. Regele, D. D. Lirman, R. Rabold, S. J. Hoffman, C. L. Karp, S. R. Kleeberger, M. Wills-Karp, and R. A. Karron.** 2002. A role for immune complexes in enhanced respiratory syncytial virus disease. *J Exp Med* **196**:859-865.
161. **Tate, M. D., Y. M. Deng, J. E. Jones, G. P. Anderson, A. G. Brooks, and P. C. Reading.** 2009. Neutrophils ameliorate lung injury and the development of severe disease during influenza infection. *J Immunol* **183**:7441-7450.
162. **Tate, M. D., L. J. Ioannidis, B. Croker, L. E. Brown, A. G. Brooks, and P. C. Reading.** 2011. The role of neutrophils during mild and severe influenza virus infections of mice. *PLoS One* **6**:e17618.
163. **Sheng, Z. M., D. S. Chertow, X. Ambroggio, S. McCall, R. M. Przygodzki, R. E. Cunningham, O. A. Maximova, J. C. Kash, D.**

- M. Morens, and J. K. Taubenberger.** 2011. Autopsy series of 68 cases dying before and during the 1918 influenza pandemic peak. *Proc Natl Acad Sci U S A* **108**:16416-16421.
164. **McNamara, P. S., P. Ritson, A. Selby, C. A. Hart, and R. L. Smyth.** 2003. Bronchoalveolar lavage cellularity in infants with severe respiratory syncytial virus bronchiolitis. *Arch Dis Child* **88**:922-926.
165. **Chang, J., and T. J. Braciale.** 2002. Respiratory syncytial virus infection suppresses lung CD8+ T-cell effector activity and peripheral CD8+ T-cell memory in the respiratory tract. *Nat Med* **8**:54-60.
166. **Graham, B. S., L. A. Bunton, J. Rowland, P. F. Wright, and D. T. Karzon.** 1991. Respiratory syncytial virus infection in anti-mu-treated mice. *J Virol* **65**:4936-4942.
167. **Fishaut, M., D. Tubergen, and K. McIntosh.** 1980. Cellular response to respiratory viruses with particular reference to children with disorders of cell-mediated immunity. *J Pediatr* **96**:179-186.
168. **Heidema, J., M. V. Lukens, W. W. van Maren, M. E. van Dijk, H. G. Otten, A. J. van Vught, D. B. van der Werff, S. J. van Gestel, M. G. Semple, R. L. Smyth, J. L. Kimpen, and G. M. van Bleek.** 2007. CD8+ T cell responses in bronchoalveolar lavage fluid and peripheral blood mononuclear cells of infants with severe primary respiratory syncytial virus infections. *J Immunol* **179**:8410-8417.
169. **Becker, Y.** 2006. Respiratory syncytial virus (RSV) evades the human adaptive immune system by skewing the Th1/Th2 cytokine balance toward

increased levels of Th2 cytokines and IgE, markers of allergy--a review.

Virus Genes **33**:235-252.

170. **Varga, S. M., X. Wang, R. M. Welsh, and T. J. Braciale.** 2001. Immunopathology in RSV infection is mediated by a discrete oligoclonal subset of antigen-specific CD4(+) T cells. *Immunity* **15**:637-646.
171. **Aberle, J. H., S. W. Aberle, M. N. Dworzak, C. W. Mandl, W. Rebhandl, G. Vollnhofer, M. Kundi, and T. Popow-Kraupp.** 1999. Reduced interferon-gamma expression in peripheral blood mononuclear cells of infants with severe respiratory syncytial virus disease. *Am J Respir Crit Care Med* **160**:1263-1268.
172. **Averbuch, D., A. Chapiro, S. Boisson-Dupuis, J. L. Casanova, and D. Engelhard.** 2011. The clinical spectrum of patients with deficiency of Signal Transducer and Activator of Transcription-1. *Pediatr Infect Dis J* **30**:352-355.
173. **Larranaga, C. L., S. L. Ampuero, V. F. Luchsinger, F. A. Carrion, N. V. Aguilar, P. R. Morales, M. A. Palomino, L. F. Tapia, and L. F. Avendano.** 2009. Impaired immune response in severe human lower tract respiratory infection by respiratory syncytial virus. *Pediatr Infect Dis J* **28**:867-873.
174. **Wilson, R. H., G. S. Whitehead, H. Nakano, M. E. Free, J. K. Kolls, and D. N. Cook.** 2009. Allergic sensitization through the airway primes Th17-dependent neutrophilia and airway hyperresponsiveness. *Am J Respir Crit Care Med* **180**:720-730.

175. **Vargas-Rojas, M. I., A. Ramirez-Venegas, L. Limon-Camacho, L. Ochoa, R. Hernandez-Zenteno, and R. H. Sansores.** 2011. Increase of Th17 cells in peripheral blood of patients with chronic obstructive pulmonary disease. *Respir Med* **105**:1648-1654.
176. **Bera, M. M., B. Lu, T. R. Martin, S. Cui, L. M. Rhein, C. Gerard, and N. P. Gerard.** 2011. Th17 cytokines are critical for respiratory syncytial virus-associated airway hyperresponsiveness through regulation by complement C3a and tachykinins. *J Immunol* **187**:4245-4255.
177. **Hashimoto, K., J. E. Durbin, W. Zhou, R. D. Collins, S. B. Ho, J. K. Kolls, P. J. Dubin, J. R. Sheller, K. Goleniewska, J. F. O'Neal, S. J. Olson, D. Mitchell, B. S. Graham, and R. S. Peebles, Jr.** 2005. Respiratory syncytial virus infection in the absence of STAT 1 results in airway dysfunction, airway mucus, and augmented IL-17 levels. *J Allergy Clin Immunol* **116**:550-557.
178. **Fujisawa, T., M. M. Chang, S. Velichko, P. Thai, L. Y. Hung, F. Huang, N. Phuong, Y. Chen, and R. Wu.** 2011. NF-kappaB mediates IL-1beta- and IL-17A-induced MUC5B expression in airway epithelial cells. *Am J Respir Cell Mol Biol* **45**:246-252.
179. **Faber, T. E., H. Groen, M. Welfing, K. J. Jansen, and L. J. Bont.** 2012. Specific increase in local IL-17 production during recovery from primary RSV bronchiolitis. *J Med Virol* **84**:1084-1088.
180. **Sigurs, N., R. Bjarnason, F. Sigurbergsson, B. Kjellman, and B. Bjorksten.** 1995. Asthma and immunoglobulin E antibodies after

respiratory syncytial virus bronchiolitis: a prospective cohort study with matched controls. *Pediatrics* **95**:500-505.

181. **Sigurs, N., R. Bjarnason, F. Sigurbergsson, and B. Kjellman.** 2000. Respiratory syncytial virus bronchiolitis in infancy is an important risk factor for asthma and allergy at age 7. *Am J Respir Crit Care Med* **161**:1501-1507.
182. **Sigurs, N., P. M. Gustafsson, R. Bjarnason, F. Lundberg, S. Schmidt, F. Sigurbergsson, and B. Kjellman.** 2005. Severe respiratory syncytial virus bronchiolitis in infancy and asthma and allergy at age 13. *Am J Respir Crit Care Med* **171**:137-141.
183. **Sigurs, N., F. Aljassim, B. Kjellman, P. D. Robinson, F. Sigurbergsson, R. Bjarnason, and P. M. Gustafsson.** 2010. Asthma and allergy patterns over 18 years after severe RSV bronchiolitis in the first year of life. *Thorax* **65**:1045-1052.
184. **Pala, P., R. Bjarnason, F. Sigurbergsson, C. Metcalfe, N. Sigurs, and P. J. Openshaw.** 2002. Enhanced IL-4 responses in children with a history of respiratory syncytial virus bronchiolitis in infancy. *Eur Respir J* **20**:376-382.
185. **Johnston, S. L., P. K. Pattemore, G. Sanderson, S. Smith, M. J. Campbell, L. K. Josephs, A. Cunningham, B. S. Robinson, S. H. Myint, M. E. Ward, D. A. Tyrrell, and S. T. Holgate.** 1996. The relationship between upper respiratory infections and hospital admissions for asthma: a time-trend analysis. *Am J Respir Crit Care Med* **154**:654-660.

186. **Burrows, B., R. J. Knudson, and M. D. Lebowitz.** 1977. The relationship of childhood respiratory illness to adult obstructive airway disease. *Am Rev Respir Dis* **115**:751-760.
187. **Kapikian, A. Z., R. H. Mitchell, R. M. Chanock, R. A. Shvedoff, and C. E. Stewart.** 1969. An epidemiologic study of altered clinical reactivity to respiratory syncytial (RS) virus infection in children previously vaccinated with an inactivated RS virus vaccine. *Am J Epidemiol* **89**:405-421.
188. **Kim, H. W., J. G. Canchola, C. D. Brandt, G. Pyles, R. M. Chanock, K. Jensen, and R. H. Parrott.** 1969. Respiratory syncytial virus disease in infants despite prior administration of antigenic inactivated vaccine. *Am J Epidemiol* **89**:422-434.
189. **Welliver, R. C., D. T. Wong, M. Sun, E. Middleton, Jr., R. S. Vaughan, and P. L. Ogra.** 1981. The development of respiratory syncytial virus-specific IgE and the release of histamine in nasopharyngeal secretions after infection. *N Engl J Med* **305**:841-846.
190. **Delgado, M. F., S. Coviello, A. C. Monsalvo, G. A. Melendi, J. Z. Hernandez, J. P. Batalle, L. Diaz, A. Trento, H. Y. Chang, W. Mitzner, J. Ravetch, J. A. Melero, P. M. Irusta, and F. P. Polack.** 2009. Lack of antibody affinity maturation due to poor Toll-like receptor stimulation leads to enhanced respiratory syncytial virus disease. *Nat Med* **15**:34-41.
191. **Anderson, L. J., P. R. Dormitzer, D. J. Nokes, R. Rappuoli, A. Roca, and B. S. Graham.** 2013. Strategic priorities for respiratory



- syncytial virus (RSV) vaccine development. *Vaccine* **31 Suppl 2**:B209-215.
192. **Piedra, P. A., A. M. Jewell, S. G. Cron, R. L. Atmar, and W. P. Glezen.** 2003. Correlates of immunity to respiratory syncytial virus (RSV) associated-hospitalization: establishment of minimum protective threshold levels of serum neutralizing antibodies. *Vaccine* **21**:3479-3482.
193. **Wright, P. F., R. A. Karron, R. B. Belshe, J. Thompson, J. E. Crowe, Jr., T. G. Boyce, L. L. Halburnt, G. W. Reed, S. S. Whitehead, E. L. Anderson, A. E. Wittek, R. Casey, M. Eichelberger, B. Thumar, V. B. Randolph, S. A. Udem, R. M. Chanock, and B. R. Murphy.** 2000. Evaluation of a live, cold-passaged, temperature-sensitive, respiratory syncytial virus vaccine candidate in infancy. *J Infect Dis* **182**:1331-1342.
194. **Karron, R. A., P. F. Wright, R. B. Belshe, B. Thumar, R. Casey, F. Newman, F. P. Polack, V. B. Randolph, A. Deatly, J. Hackell, W. Gruber, B. R. Murphy, and P. L. Collins.** 2005. Identification of a recombinant live attenuated respiratory syncytial virus vaccine candidate that is highly attenuated in infants. *J Infect Dis* **191**:1093-1104.
195. **Karron, R. A., D. A. Buonagurio, A. F. Georgiu, S. S. Whitehead, J. E. Adamus, M. L. Clements-Mann, D. O. Harris, V. B. Randolph, S. A. Udem, B. R. Murphy, and M. S. Sidhu.** 1997. Respiratory syncytial virus (RSV) SH and G proteins are not essential for viral replication in vitro: clinical evaluation and molecular characterization

- of a cold-passaged, attenuated RSV subgroup B mutant. *Proc Natl Acad Sci U S A* **94**:13961-13966.
196. **Tristram, D. A., R. C. Welliver, D. A. Hogerman, S. W. Hildreth, and P. Paradiso.** 1994. Second-year surveillance of recipients of a respiratory syncytial virus (RSV) F protein subunit vaccine, PFP-1: evaluation of antibody persistence and possible disease enhancement. *Vaccine* **12**:551-556.
197. **Hurwitz, J. L.** 2011. Respiratory syncytial virus vaccine development. *Expert Rev Vaccines* **10**:1415-1433.
198. **Langley, J. M., V. Sales, A. McGeer, R. Guasparini, G. Predy, W. Meekison, M. Li, J. Capellan, and E. Wang.** 2009. A dose-ranging study of a subunit Respiratory Syncytial Virus subtype A vaccine with and without aluminum phosphate adjuvantation in adults > or =65 years of age. *Vaccine* **27**:5913-5919.
199. **Bernstein, D. I., E. Malkin, N. Abughali, J. Falloon, T. Yi, F. Dubovsky, and M.-C. Investigators.** 2012. Phase 1 study of the safety and immunogenicity of a live, attenuated respiratory syncytial virus and parainfluenza virus type 3 vaccine in seronegative children. *Pediatr Infect Dis J* **31**:109-114.
200. **Martinello, R. A., M. D. Chen, C. Weibel, and J. S. Kahn.** 2002. Correlation between respiratory syncytial virus genotype and severity of illness. *J Infect Dis* **186**:839-842.
201. **Shim, J. J., K. Dabbagh, I. F. Ueki, T. Dao-Pick, P. R. Burgel, K. Takeyama, D. C. Tam, and J. A. Nadel.** 2001. IL-13 induces mucin

production by stimulating epidermal growth factor receptors and by activating neutrophils. *Am J Physiol Lung Cell Mol Physiol* **280**:L134-140.

## CHAPTER 2

### **Differential Pathogenesis of Respiratory Syncytial Virus (RSV) Clinical Isolates in BALB/c Mice**

The work of this chapter was published in June, 2011 in the *Journal of Virology*

Full article citation:

Stokes KL, Chi MH, Sakomoto K, Newcomb DC, Currier MG, Huckabee MM, Lee S, Goleniewska K, Pretto C, Williams JV, Hotard A, Sherrill, TP, Peebles RS, Moore ML. Differential Pathogenesis of Respiratory Syncytial Virus (RSV) Clinical Isolates in BALB/cJ Mice. *J Virol.* 2011 85: 5782-5793.

**Differential Pathogenesis of Respiratory Syncytial Virus (RSV)  
Clinical Isolates in BALB/c Mice**

**Running Title:** RSV Strain 2-20 Pathogenesis

Kate L. Stokes<sup>1,2</sup>, Michael H. Chi<sup>3</sup>, Kaori Sakamoto<sup>4</sup>, Dawn C. Newcomb<sup>3</sup>, Michael G. Currier<sup>1,2</sup>, Matthew M. Huckabee<sup>3</sup>, Sujin Lee<sup>1,2</sup>, Kasia Goleniewska<sup>3</sup>, Carla Pretto<sup>1</sup>, John V. Williams<sup>5</sup>, Anne Hotard<sup>1,2</sup>, Taylor P. Sherrill<sup>3</sup>, R. Stokes Peebles, Jr.<sup>3\*</sup>, and Martin L. Moore<sup>1,2\*</sup>

Department of Pediatrics, Emory University, Atlanta, GA 30322<sup>1</sup>; Children's Healthcare of Atlanta, Atlanta, GA 30322<sup>2</sup>; Departments of <sup>3</sup>Medicine and <sup>5</sup>Pediatrics, Vanderbilt University School of Medicine, Nashville, Tennessee 37232; Department of Pathology, University of Georgia School of Veterinary Medicine<sup>4</sup>

\* Corresponding author: Mailing address for R. Stokes Peebles, Jr.: T-1218 MCN, Vanderbilt University Medical Center, Nashville, TN 37232-2650. Phone: (615) 322-3412. Fax: (615) 343-7448. Email: [stokes.peebles@vanderbilt.edu](mailto:stokes.peebles@vanderbilt.edu). Mailing address for Martin L Moore: 2015 Uppergate Dr. NE, Emory Children's Center, Room 514, Department of Pediatrics, Emory University, Atlanta, GA 30322. Phone: (404) 727-9162. Fax: (404) 727-9223. E-mail: [martin.moore@emory.edu](mailto:martin.moore@emory.edu).

**ABSTRACT**

Airway mucus is a hallmark of respiratory syncytial virus (RSV) lower respiratory tract illness. Laboratory RSV strains differentially induce airway mucus production in mice. Here, we tested the hypothesis that RSV strains differ in pathogenesis by screening six low passage RSV clinical isolates for mucogenicity and virulence in BALB/cJ mice. The RSV clinical isolates induced variable disease severity, lung interleukin-13 (IL-13) levels, and gob-5 levels in BALB/cJ mice. We chose two of these clinical isolates for further study. Infection of BALB/cJ mice with RSV A2001/2-20 (2-20) resulted in greater disease severity, higher lung IL-13 levels, and higher lung gob-5 levels than infection with RSV strains A2, line 19, Long, and A2001/3-12 (3-12). Like the line 19 RSV strain, the 2-20 clinical isolate induced airway mucin expression in BALB/cJ mice. The 2-20 and 3-12 RSV clinical isolates had higher lung viral loads than laboratory RSV strains 1 day post-infection (p.i.). This increased viral load correlated with higher viral antigen levels in the bronchiolar epithelium and greater histopathologic changes 1 day p.i. The A2 RSV strain had the highest peak viral load at day 4 p.i. RSV 2-20 infection caused epithelial desquamation, bronchiolitis, airway hyperresponsiveness, and increased breathing effort in BALB/cJ mice. We found that RSV clinical isolates induce variable pathogenesis in mice, and we established a mouse model of clinical isolate strain-dependent RSV pathogenesis that recapitulates key features of RSV disease.

## INTRODUCTION

Respiratory syncytial virus (RSV) is the most important cause of bronchiolitis and viral pneumonia in children. Each year in the USA, RSV causes lower respiratory tract illness (LRI) in 20-30% of infants and leads to the hospitalization of approximately 1% of infants at a cost of \$300-400 million (1-3). The incidence and disease severity of RSV can vary from year to year (4). Dominant circulating RSV strains are generally replaced each year, likely by a process involving immune selection (5-8). RSV strain differences may contribute to year-to-year and/or patient-to-patient variations in clinical severity.

In BALB/cJ mice, laboratory RSV strains (A2, Long, and line 19) differ in their ability to cause pulmonary interleukin-13 (IL-13) and mucin expression (9, 10). We are interested in RSV-induced mucin expression in mice because mucus overabundance contributes to airway obstruction in severe RSV disease in children (11-14). IL-13 is a cytokine linked to mucus production (15). The line 19 RSV strain induces lung IL-13 and airway mucin expression in BALB/cJ mice, whereas the A2 and Long RSV strains do not (9, 10). However, the in vitro passage histories of RSV strains A2, Long, and line 19 are not defined and involve many serial passages. Thus, it is possible that mutations in these RSV laboratory strains determine pathogenesis phenotypes in the mouse model. RSV clinical isolates have not been studied extensively in vivo, and the role of RSV strain differences in pathogenesis is not clear.

Here, we tested whether RSV strains exhibit differential pathogenesis phenotypes in BALB/cJ mice using low-passage RSV clinical isolates. We derived six antigenic subgroup A RSV clinical isolates and generated low-passage stocks of these strains. Infection of BALB/cJ mice with these strains resulted in variable weight loss and airway mucin expression phenotypes. We found that RSV clinical isolate A2001/2-20 (2-20) induced higher lung IL-13 levels, airway mucin expression, and airway dysfunction than a related isolate RSV A2001/3-12 (3-12). As RSV 2-20 and 3-12 are genotypically similar and isolated in the same year (2001), their divergent pathogenesis phenotypes suggest a role for RSV strain variation in differential disease severity observed during RSV epidemics.

## **MATERIALS AND METHODS**

### **Viruses**

The A2, line 19, and Long strains of RSV were propagated as described (10, 16). First-passage (P1) HEp-2 supernatants of RSV antigenic subgroup A clinical isolates were obtained from the Vanderbilt Vaccine Clinic (Nashville, TN) (17). Ten-fold serial dilutions of the P1 supernatants were used to infect HEp-2 cells in 6-well plates. For each isolate, supernatant from the most dilute inoculum exhibiting >50% CPE was harvested for sequential passage in HEp-2 cells. The isolates were passaged by limiting dilution 9 times in HEp-2 cells. HEp-2 cells in flasks were infected with the supernatants from the 9<sup>th</sup> limiting dilution passage (P10 overall). Master stocks (P11) and working stocks (P12) were generated as described (16). Six antigenic subgroup A clinical isolates strains were propagated: 2-20, 3-12, A1997/12-35 (12-35), A1998/3-2 (3-2), A1998/12-21 (12-21), and



A2000/3-4 (3-4). Isolates are named with their subtype letter (A or B), followed by the year and month they were collected and their isolate number. Viral stocks were propagated and titrated by plaque assay in HEp-2 cells. A2001/2-20 was placed in a Petri dish approximately 4 inches from a 40-watt UV light on ice for 4 hours. UV-inactivated virus was titrated on HEp-2 cells to ensure inactivation.

### **Cells and Mice**

HEp-2 cells were cultured in minimal essential media (MEM) supplemented with L-glutamine, Earle's salts, 10% fetal bovine serum (Hyclone, ThermoFisher), and a penicillin G/streptomycin sulfate/amphotericin B solution (Invitrogen).

BEAS-2B human bronchial epithelial cells were a gift from Dr. Pierre Massion (Vanderbilt University, Nashville, TN) and cultured in Roswell Park Memorial Institute medium supplemented with 10% fetal bovine serum and penicillin G/streptomycin sulfate/amphotericin B solution. Female, 6 to 8 wk old BALB/cJ mice were obtained from Jackson Laboratories. IL-13<sup>-/-</sup> mice were obtained from Dr. Gurjit K. Hershey at Cincinnati Children's Hospital Medical Center (18). All mice were maintained under specific pathogen-free conditions. Six to eight week old female mice were lightly anaesthetized and infected intranasally (i.n.) with RSV or with mock-infected cell culture supernatant as described (16).

### **Sequencing RSV glycoprotein (G) and fusion (F) genes**

As described above, RSV clinical isolates A2001/2-20 (2-20) and A2001/3-12 (3-12) were passaged by limiting dilution in HEp-2 cells. Total RNA was isolated from passage 2 (P2) and working stock (P12) supernatants using Trizol

(Invitrogen). In order to sequence the F genes, cDNA was reverse transcribed using primer F-r, and F genes were PCR-amplified using primers FStuI and FSphI, as described (10). In order to sequence the G genes, cDNA was reverse transcribed using primer G-r (CCATTGTTATTTGCCCCAGA). PCR was performed using primer SHfEcoRI (AGGAATTCGGAAGCACACAGCTACACG) and primer GrStuI (GGTCAAGGCCTTTTGTGATAATATG), and generated approximately 1.6 kb amplicons containing the SH and the G genes. The EcoRI and StuI sites (underlined) facilitated cDNA cloning for future studies. RSV F and G PCR amplicons from P2 and P12 supernatants were gel-purified and sequenced using primers complementary to these regions of the published RSV A2 and line 19 genomes. Sequences were analyzed using VectorNTI software (Invitrogen Corp.). Multisequence alignments were performed using AlignX software (neighbor-joining method) within VectorNTI.

### **Multi-step virus growth curves**

Subconfluent HEp-2 or BEAS-2B cells in 6-well dishes were infected in triplicate with RSV strains A2, 2-20, or 3-12 at an MOI of 0.5 in 750  $\mu$ l. After 1 hr adsorption at room temperature on a rocking platform, the cells were washed with medium, and fresh medium was added. Supernatants were harvested 24 hr, 48 hr, 72 hr, and 96 hr from each well, clarified by centrifugation, and RSV was titrated in duplicate by plaque assay on HEp-2 cells as described (16).

### **Quantification of lung viral load**

Lungs were harvested from BALB/cJ mice infected with  $10^5$  PFU of RSV. We used a Beadbeater (Biospec Products, Bartlesville, OK) to homogenize the lungs. 2-ml deep 96-well plates (Axygen Scientific, Union City, CA) were loaded with 1 ml of zirconium beads (Biospec Products), sealed with rubber lid (Axiomat, Axigen Scientific), and autoclaved. Sterile MEM (500  $\mu$ l) was added to each well, and the plate was briefly centrifuged then kept in deep ice. For each mouse, the left lung lobe was harvested, weighed, cut into 4-5 pieces, and placed into a well of the 2-ml deep 96-well plate on ice. An additional 400  $\mu$ l MEM was added to each well, and the plate was sealed with the Axiomat lid. The plate was shaken in the Beadbeater for one min followed by one minute plunge in ice/water slurry. This was repeated 9 times for a total of 10-one minute homogenizations. The plate was centrifuged at 2000 RPM for 5 min at 4° C. Lung homogenates were immediately serially diluted and used to inoculate subconfluent HEP-2 cells in 24-well dishes. After 1 hr adsorption at room temperature on a rocking platform, the cells were overlaid with MEM/10% FBS/penicillin G/streptomycin sulfate/amphotericin B solution/0.75% methylcellulose. After five days, the overlay media was removed and the cells fixed with methanol. Plaques were visualized by immunodetection as described (19).

### **IL-13 ELISA and gob-5 Western blot**

Lungs were removed and snap-frozen in liquid nitrogen. IL-13 and gob-5 Western blots were performed as described (10). Briefly, lungs were homogenized in 1 ml of modified radioimmunoprecipitation assay buffer [120 mM NaCl, 50

mM Tris-HCl pH 8.0, 1% TritonX-100, 0.1% SDS, 1% deoxycholate, 10 mM DTT, 1mM EDTA, 0.2mM PMSF, 1% protease inhibitor cocktail (P8340, Sigma)].

Homogenates were clarified by centrifugation at 2000 x *g*. IL-13 was quantified by enzyme-linked immunosorbent assay (ELISA) (Quantikine, R&D Systems, Minneapolis, MN). Gob-5 and actin were detected by Western blotting (10).

### **Histopathology**

Heart and lung samples were fixed in 10% formalin overnight. Lungs were transferred to 70% ethanol then embedded in paraffin blocks. Tissue sections (5  $\mu$ m) were stained with hematoxylin and eosin stains (H&E) to assess histologic changes. A pathologist blinded to the groups scored lymphocytes, neutrophils, macrophages, and eosinophils on a 0-4 scale for peribronchiolar, perivascular, interstitial, and alveolar spaces. Perivascular edema was scored on a 0-4 scale such that if a vessel had edema equal to its thickness, it was given a score of 1. If a vessel had edema twice as thick as the vessel, the score was 2, etc. All vessels were analyzed, and lungs were assigned the score of the vessel with the most edema. Slides were also scored for the presence or absence of bronchiolar exudates containing necrotic cell debris. Additional sections were stained with periodic acid-Schiff (PAS) stain to assess goblet cell hyperplasia as a measure of mucin expression. PAS-stained slides were digitally scanned using a MIRAX MIDI microscope with a 20X objective having a 0.85 numerical aperture (Carl Zeiss Microimaging Inc., Thornwood, NY) (20). Areas of airway epithelium were annotated using Histoquant software (3D Histech, Budapest, Hungary). All

airways involved in the tissue sections were analyzed. PAS-positive areas within the airway epithelium were identified by Histoquant software.

### **Immunofluorescence in lung tissue**

Three  $\mu\text{m}$  thick sections of paraffin-embedded lung tissues were incubated at 37 °C overnight as described (21). The sections were deparaffinized in Clear Rite-3 (ThermoFisher) then rehydrated in a series of graded alcohols. Slides were placed in a plastic coplin jar with Antigen Unmasking Solution (Vector Labs, Burlingame, CA), and the jar was placed in a pressure chamber (Pascal, Dako USA, Carpinteria, CA). The slides were heated at 125 °C for 30 sec, passively cooled to 90 °C, heated at 90 °C 10 seconds, then removed from the pressure chamber and cooled 20 minutes on the bench. Slides were then washed in PBS, treated with PBS/0.2% Tween-20 for 30 min, washed three times with PBS, and blocked 1 hr with PBS/10% normal rabbit serum. Slides were washed three times with PBS then treated for 15 min with an avidin-blocking reagent and 15 min with a biotin-blocking reagent (Avidin/Biotin Blocking Kit, Vector Labs). The tissues were probed one hour at room temperature in a humidified chamber with a goat polyclonal Ab to RSV (AB1128, Millipore) diluted 1:400 in PBS/5% rabbit serum. After washing three times with PBS, the slides were treated 30 min with 5  $\mu\text{g}/\text{ml}$  biotinylated anti-goat IgG in PBS/5% rabbit serum. The slides were washed three times in PBS then 20  $\mu\text{g}/\text{ml}$  fluorescein-avidin (Vector Labs) in PBS was applied for 10 min. The tissues were washed three times in PBS and mounted with Prolong Gold antifade with DAPI according to the manufacturer's

instructions (Invitrogen). The slides were digitally scanned using a MIRAX MIDI fluorescence microscope (Carl Zeiss Microimaging).

### **Flow cytometric analysis of lung mononuclear cells**

Mice were euthanized intraperitoneally (i.p.) with sodium pentobarbital (8.5 mg/kg body weight) and lungs were harvested 8 d p.i. Cells were isolated using ficoll gradients and counted with a hemocytometer. Cells were stimulated for 6 hours with PMA/ionomycin and stained with the following antibodies: anti-CD8, anti-CD3, and anti-IFN- $\gamma$ .  $1 \times 10^6$  cells were analyzed using a LSR II flow cytometer (BD Biosciences). The total numbers of IFN- $\gamma$ -expressing CD8<sup>+</sup> T cells in lungs were determined by multiplying the percentage of lymphocytes (defined by forward and side scatter properties in flow cytometry) that were CD3<sup>+</sup>CD8<sup>+</sup>IFN- $\gamma$ <sup>+</sup> by the total number of mononuclear cells isolated. Data were analyzed using FlowJo software (Tree Star).

### **Methacholine Challenge**

We measured airway hyperresponsiveness (AHR) 9 days p.i. (9, 10). The mice to be tested were anesthetized with i.p. pentobarbital. The trachea was cannulated with a 20 gauge metal stub adapter. The animal was placed on a small animal ventilator, flexiVent (SCIREQ, Montreal, Canada), with 150 breaths/min and a tidal volume of 10 ml/kg body weight. Airway responsiveness was assessed by administering incremental concentrations of aerosolized methacholine (0, 30, 60, 100 mg/ml in saline) via an in-line ultranebulizer (Aeroneb, SCIREQ,

Montreal, Canada). The SCIREQ software calculates the resistance by dividing the change in pressure by the change in flow (units = cm H<sub>2</sub>O/ml/sec).

### **Pulse Oximetry**

For breath distension measurements, mice were anesthetized using an isoflurane (2.5%)/oxygen (2L/min) mixture provided by an anesthesia machine (VetEquip, Pleasanton, CA). Mice were anesthetized at a time in a plexiglass box connected to the anesthesia machine. One mouse at a time was removed from the plexiglass box and placed on its back on a pad with its nose in an isoflurane/oxygen nosecone connected to the anesthesia machine. The anesthetized mouse's feet were restrained to a pad with tape. A rodent pulse oximeter (MouseOx, Starr Life Sciences Corp., Oakmont, PA) was used. The MouseOx sensor was applied to the mouse's thigh, and the mouse was covered with a cloth to reduce ambient light. The machine measured arterial O<sub>2</sub> saturation, heart rate, pulse rate, pulse distension, and breath distension approximately every 0.1 sec (MouseOx Software Version 4.0). Each mouse was analyzed for 1 to 5 minutes. Only time points in which all of these physiological parameters were successfully measured were included in analyses, approximately 30 sec to 2 min per mouse. Data were exported to Microsoft Excel for analysis. Breath distension for each group (mock or RSV strain) was calculated by averaging measurements for each mouse then averaging these values per group (8 to 10 mice).

### **Statistical analyses**

Unless otherwise indicated, groups were compared by one-way ANOVA and Tukey multiple comparison tests.  $P < 0.05$  was considered significant. Data values below limits of detection were assigned a value of half the limit of detection. Data are representative of at least three replicate experiments having consistent results.

### **Nucleotide sequence accession numbers**

The 2-20 F and G sequences were submitted to GenBank under the accession numbers JF279544 and JF279545. The sequence data for 3-12 F and G was submitted under the accession numbers JF279546 and JF279543.

## **RESULTS**

**RSV clinical isolates caused differential disease severity.** Weight loss is a quantitative measure of RSV illness severity in the BALB/cJ mouse model, and the A2 strain of RSV causes weight loss one week p.i. (16, 22, 23). We compared weight loss in BALB/cJ mice that were mock-infected or infected with RSV laboratory strains A2, line 19, Long, or RSV clinical isolates 2-20, 3-12, 12-35, 3-4, 3-2, or 12-21. The clinical isolates 2-20 and 3-12 caused significant weight loss 2 d p.i. (Fig. 1A and 1B). The 2-20 RSV strain uniquely exhibited a bimodal weight loss pattern in which the second peak of weight loss occurred slightly earlier than A2-induced weight loss (Fig. 1). Like the 2-20 strain, RSV clinical isolate strain 12-35 caused weight loss 6 d p.i. (Fig. 1B). Compared to mock-infection, RSV clinical isolate strains 3-4, 3-2 and 12-21 caused no weight loss in



BALB/cJ mice (data not shown). RSV laboratory strains line 19 and Long caused no weight loss with a virus dose of  $10^5$  PFU (Fig. 1B). Thus, three of the six clinical isolates caused weight loss in BALB/cJ mice, and the weight loss pattern of those three strains was different: 3-12 (early weight loss), 2-20 (early and late bimodal weight loss), and 12-35 (late weight loss). Across multiple experiments, there was no consistent difference in the degree of early weight loss at d 2 p.i. caused by 2-20 and 3-12 (compare Fig. 1A to Fig. 1B).

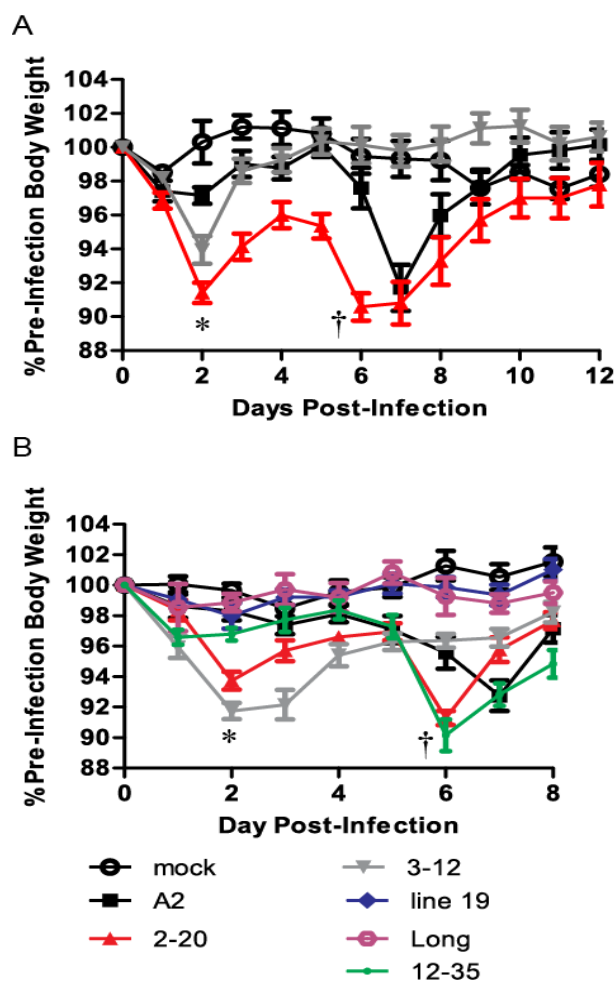


**Figure 1.** Differential weight loss patterns with RSV clinical isolates. (A) BALB/cJ mice were mock-infected (n=4) or infected with  $5 \times 10^5$  PFU of A2, 2-20, or 3-12 (n=8/group). (B) BALB/cJ mice were mock-infected (n=6) or

infected with  $10^5$  PFU of A2 (n=8), 2-20 (n=10), 12-35 (n=10), 3-12 (n=10), line 19 (n=8), or Long (n=6). Weight loss  $\pm$  SEM is shown. \*, at day 2, RSV 2-20 and 3-12 were significantly lower ( $P < 0.05$ , ANOVA) than other RSV strains. †, at day 6, RSV 2-20 and 12-35 were significantly lower ( $P < 0.05$ , ANOVA) than other RSV strains.

Infection with UV-inactivated 2-20 does not cause weight loss (Fig. 2). Therefore, 2-20 weight loss required replication-competent virus. Over the time course, RSV 2-20 caused greater illness severity in BALB/cJ mice than the other RSV strains tested.

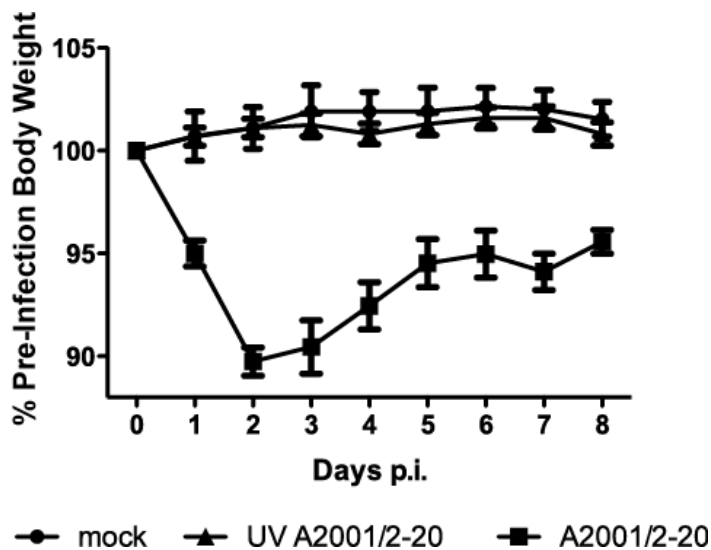


**Figure 2.** Weight loss after infection with UV-inactivated RSV 2-20. BALB/cJ mice were mock-infected (n=8), infected with  $1.2 \times 10^6$  PFU of 2-20 (n=8), or infected with UV-inactivated 2-20 (n=8). Weight loss  $\pm$  SEM is shown.

### Lung IL-13 and gob-5 levels in mice infected with RSV laboratory and clinical isolate strains

In contrast to the A2 and Long RSV strains, the RSV strain line 19 induces lung IL-13 expression on day 8 p.i. and IL-13-dependent airway mucus expression (9, 10, 24). We quantified IL-13 levels in BALB/cJ mice that were mock-infected or infected with RSV strains A2, line 19, Long, 2-20, 3-12, 12-35, 3-2, 12-21, or 3-4. RSV line 19, 2-20, 12-35, and 3-4 infections resulted in significantly elevated lung IL-13 expression (Fig. 3). RSV 2-20 and 12-35 infections resulted in higher levels of lung IL-13 than RSV line 19 infection (Fig. 3).

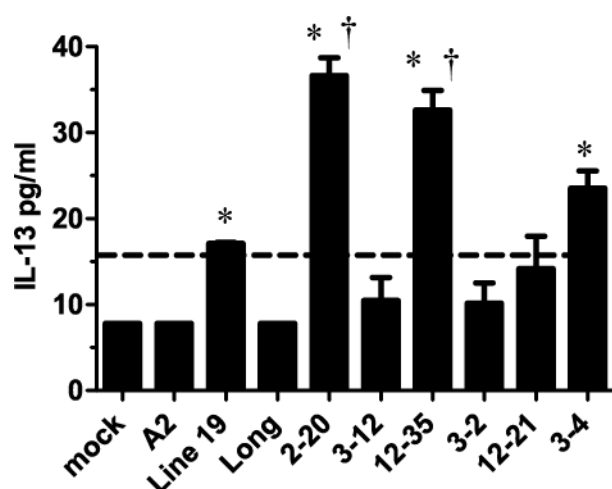


**Figure 3.** BALB/cJ mice were mock-infected (n=3) or infected with  $10^5$  PFU of the indicated RSV strain (n=4/group). IL-13 protein levels were quantified by ELISA in left lung lobe homogenates. The dashed line represents the limit of detection. \*,  $P < 0.05$  compared to mock. †, significantly higher ( $P < 0.05$ , ANOVA) than line 19.

Gob-5 protein levels are a marker of pulmonary mucus expression. Gob-5 has been identified as a key molecule in the induction of murine allergic airway inflammation and is selectively expressed in the setting of AHR (25). RSV strain line 19 infection increases lung gob-5 levels (9, 10, 26, 27). We determined gob-5 levels at 8 d p.i. in lung homogenates of BALB/cJ mice mock-infected or infected with  $10^5$  PFU of A2, line 19, Long, 2-20, 3-12, 12-35, 3-2, 12-21, or 3-4 RSV strains. Of the clinical isolate strains, 12-35, 12-21, 3-4, and 2-20 induced relatively high levels of lung gob-5 (Fig. 4). Gob-5 and IL-13 levels correlated well with each other in these experiments (Fig. 3 and 4). Taken together, RSV clinical isolate strains 2-20, 12-35, and 3-4 induced relatively high levels of gob-5 and IL-13 in BALB/cJ mice at 8 d p.i.

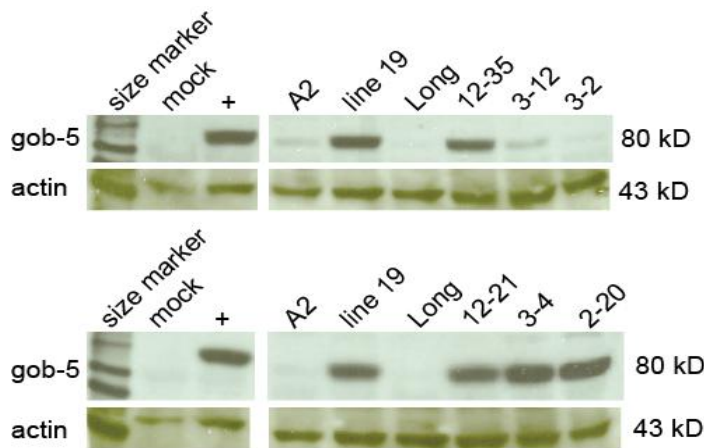


**Figure 4.** Gob-5 Western blotting. BALB/cJ mice were mock-infected with  $10^5$  PFU of RSV strains A2, line 19, Long, or clinical isolate strains (n=5/group). Lungs were harvested 8 d p.i. Each lane contains 100  $\mu$ g total lung homogenate protein pooled from five mice. The membrane was probed with anti-gob-5 then stripped and re-probed with anti-actin as a loading control.

### **RSV strain 2-20 and 3-12 G and F gene sequences**

Of the six RSV clinical isolates we screened for weight loss, IL-13 levels, and gob-5 levels, we chose 2-20 and 3-12 for further study because these two strains, both from the 2000-2001 RSV season, exhibited differential phenotypes. RSV 2-20 and 3-12, both antigenic subgroup A isolates, were obtained from the Vanderbilt Vaccine Clinic during the 2001 RSV season. In order to determine the effect of limiting dilution culture on G and F sequence, we sequenced 2-20 and 3-12 G and F genes from P2 and final working stocks (P12). The G genes of RSV 2-20 and 3-12 were identical between passages 2 and 12. There was one nt difference between P2 and P12 F genes of RSV 2-20, resulting in a predicted amino acid change at position 76 (V in P2, G in P20). There was one nt difference between P2 and P12 F genes of RSV 3-12, resulting in a predicted amino acid change at position 101 (P in P2, Q in P12). Mutations may have occurred in additional regions of these viruses, but they were not sequenced. Passage in HEp-2 did not alter partial (C-terminal) SH gene sequences of RSV 2-20 and 3-12 (data not shown). Thus, 10 passages (P2 to P12) had no effect on the G genes of 2-20 and 3-12 and altered one residue of the F genes for each virus.

We defined the genetic relatedness of 2-20 and 3-12 to each other and to other RSV isolates. Phylogenetic analysis of a hypervariable 270 nt region of the G gene divides subgroup A RSV isolates into clades (GA1-GA7) that have remained distinct clusters of circulating RSV in several studies (5-8, 28-31). We performed multisequence alignments of the 270 nt C-terminal region of the G genes of 2-20, 3-12, and published C-terminal RSV G sequences (7, 8, 29, 32-40). Both RSV 2-20 and 3-12 are GA2 clade viruses. In this analysis, the virus most closely

related to RSV 2-20 was RSV MON/1/94 (Uruguay, 1994) (33). The RSV most closely related to RSV 3-12 was RSV A2.20 (Germany, 2000-2001) (37).

Comparing the predicted full-length G proteins, RSV 2-20 and 3-12 G differ in sequence by 16 amino acids. The predicted 2-20 and 3-12 F protein sequences differ by six amino acids. RSV 2-20 and 3-12 are distinct antigenic subgroup A, GA2 clade strains that were circulating in Nashville, Tennessee in 2001.

### **In vitro replication of RSV 2-20 and 3-12 strains**

We compared the in vitro growth of RSV strains A2, 2-20, and 3-12. In HEp-2 cells commonly used for RSV propagation, RSV 3-12 grew to lower titers at 24 and 48 hr p.i. in HEp-2 cells than RSV A2 and 2-20 (Fig. 5A), as did the five other clinical isolates (see materials and methods). Only the yield of RSV 2-20 was similar to RSV A2 (Fig. 5A). RSV primarily infects epithelial cells of the proximal airways. The human bronchial epithelial cell line BEAS-2B has been used to study host responses to RSV (41-44). In BEAS-2B cells, RSV strains A2, 2-20 and 3-12 had equivalent growth kinetics (Fig. 5B).

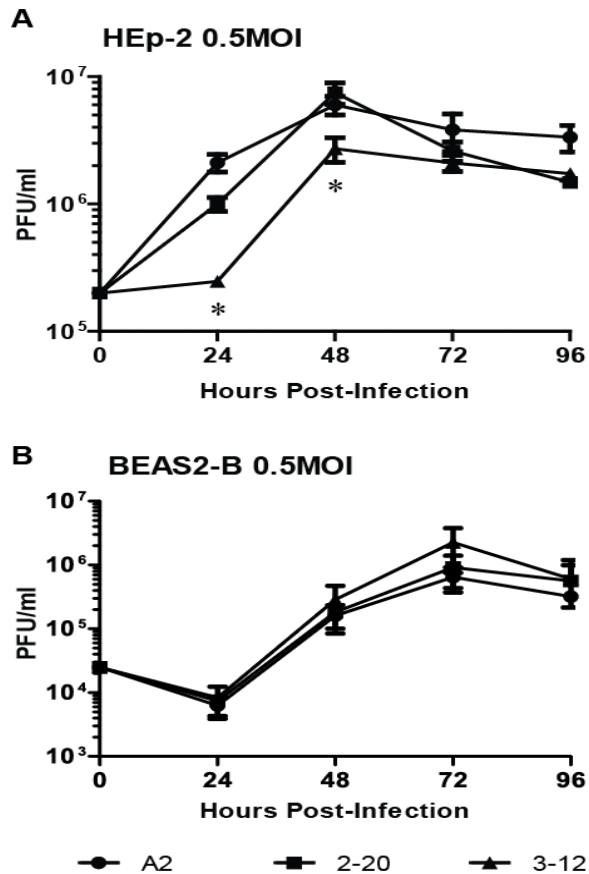


**Figure 5.** In vitro growth of RSV strains A2, 2-20, and 3-12. Infectious yield in supernatants of (A) HEp-2 cells and (B) BEAS-2B cells infected at MOI 0.5 with RSV A2, 2-20, or 3-12. Error bars represent SEM of three separate infections. \*, titers from cells infected with RSV 3-12 are significantly less than titers from cells infected with A2 or 2-20 ( $P < 0.05$  ANOVA).

### Viral load of RSV 2-20 and 3-12 in BALB/cJ mice

BALB/cJ mice are semi-permissive for RSV replication. It was previously shown that the non-mucogenic A2 RSV strain has a higher viral load than the mucogenic line 19 RSV strain in BALB/cJ mice at 4 and 6 d p.i. (9). We compared viral loads of RSV strains A2, line 19, 2-20, and 3-12. We infected BALB/cJ mice with  $5 \times 10^5$

PFU of these RSV strains and performed lung viral load, time course experiments. The clinical isolate strains 2-20 and 3-12 had significantly higher viral loads than the A2 and line 19 strains at 1 d p.i. (Fig. 6). Like the line 19 strain, the 2-20 and 3-12 strains had lower viral loads than A2 at days 4 and 6 p.i. (Fig. 6). Although there was a trend that the 3-12 peak viral load was lower than 2-20 by approximately one half log in replicate experiments these differences did not reach statistical significance (Fig. 6). RSV 2-20 and 3-12 had high viral loads 1 d p.i. and exhibited peak viral loads and clearance similar to the line 19 strain.

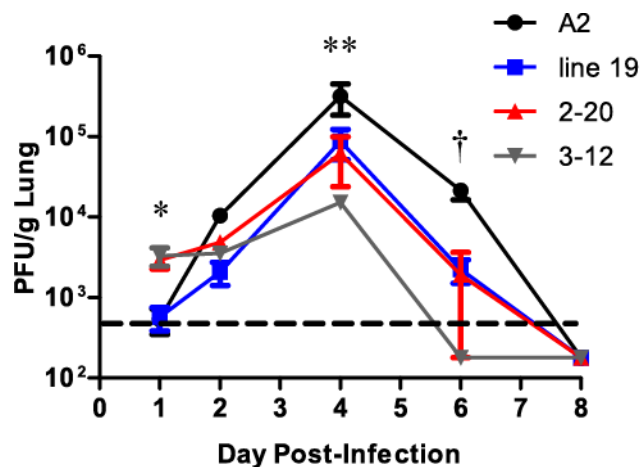


**Figure 6.** Viral load of RSV strains A2, 2-20, and 3-12. BALB/cJ mice were infected with  $5 \times 10^5$  PFU of A2, 2-20, or 3-12 ( $n=5$ /group). Lungs were harvested at the indicated days p.i. and infectious RSV was titrated by an immunodetection plaque assay. Data are means  $\pm$  SEM. \*, at day 1 p.i. 2-20 and 3-12 were significantly higher than A2 and line 19 ( $P < 0.05$ , ANOVA). \*\*, at day 4 p.i. A2 was significantly higher than 2-20, 3-12, and line 19 ( $P < 0.05$ , ANOVA). †, at day 6, A2 was significantly higher than 2-20, 3-12, and line 19 ( $P < 0.05$ , ANOVA). The dotted line represents the limit of detection.



### **Localization of virus antigen**

It has been shown that at the peak of viral load, RSV A2 strain antigen is detected exclusively in alveolar parenchyma of BALB/cJ mice (45). Using immunofluorescence, we analyzed the distribution of RSV antigen in lungs of BALB/cJ mice infected with RSV A2, 2-20, 3-12, and line 19. In agreement with published data, we found that RSV antigen was detected exclusively in alveolar regions at 4 d p.i., and this was the case with each RSV strain (data not shown). Because RSV 2-20 and 3-12 had higher viral loads than A2 and line 19 one d p.i. (Fig. 6), we also performed immunofluorescence for RSV antigens in lung tissues 1 d p.i. At this time point, RSV antigen was detected in the bronchiolar epithelium (Fig. 6) and not in the alveolar regions (data not shown). Consistent with the viral load data, RSV strains 2-20 and 3-12 exhibited greater viral antigen than the A2 strain (Fig. 7). The RSV-positive cells are located in the bronchiolar epithelium as the airways are clearly evident in adjacent sections stained with H&E (Fig. 7). In these H&E stains (1 d p.i.), the airways shown in 2-20- and 3-12-infected mice exhibited intraluminal necrotic cell debris whereas the airways in mock- and A2-infected mice lacked this cell debris (Fig. 7).

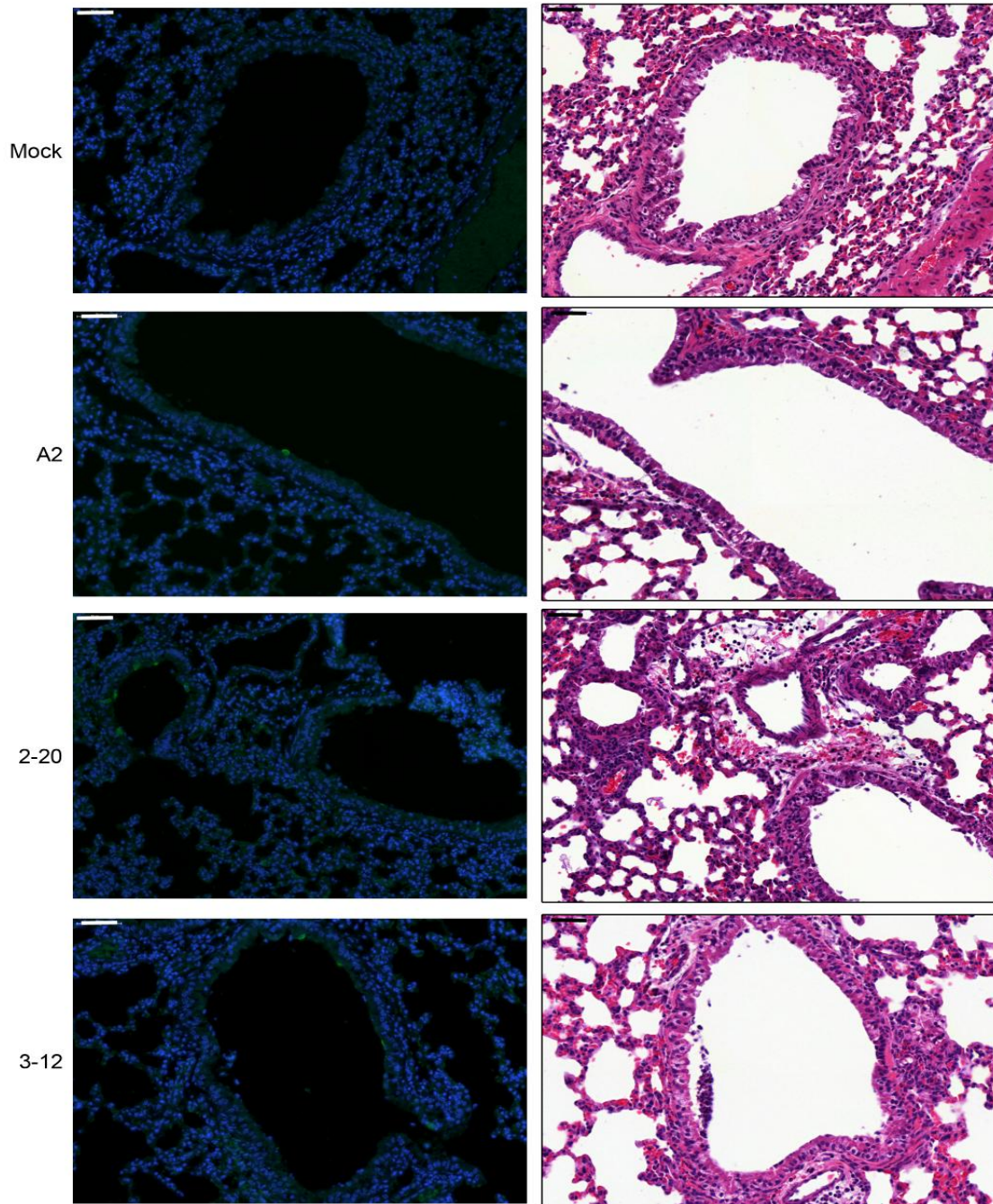


**Figure 7.** RSV antigen in bronchiolar epithelium. BALB/cJ mice were infected with  $5 \times 10^5$  PFU of A2, 2-20, or 3-12 (n=5/group). Lungs harvested day 1 p.i. were probed for RSV by immunofluorescence as described in the Materials and Methods. The left column shows RSV-positive cells (FITC green) in RSV A2-, 2-20-, and 3-12-infected mice and nuclei (DAPI blue counterstain). White

arrowheads indicate FITC-positive cells. The right column (H&E) depicts lung sections adjacent to those in the left column, showing airways corresponding to those in the immunofluorescence images. Black arrowheads indicate necrotic cell debris. Scale bar in upper left corners represents 50  $\mu\text{m}$

### **Histologic features of RSV 2-20 infection**

We analyzed lungs of BALB/cJ mice that were mock-infected or infected with  $5 \times 10^5$  PFU of RSV A2, 2-20, or 3-12 over a time course. Lungs were harvested days 1, 2, 4, 6, and 8 d p.i. There were no differences in lung histologic features between mice infected with A2, 2-20, and 3-12 RSV strains on days 2, 4, 6, and 8 p.i. (data not shown). Mice infected with these RSV strains had indistinguishable inflammation consisting of lymphocytes, neutrophils, and macrophages in perivascular and interstitial spaces on these days (data not shown). At 1 d p.i., however, mice infected with RSV 2-20 or 3-12 had greater perivascular edema than mice that were mock-infected or infected with RSV A2 (Fig. 7, yellow bars). The perivascular edema scores of two experiments combined were the following: mock =  $0.75 \pm 0.25$  (n=4), A2 =  $2.1 \pm 0.15$  (n=9), 2-20 =  $2.9 \pm 0.11$  (n=9), and 3-12 =  $3.0 \pm 0.0$  (n=9). Using ANOVA, the perivascular edema scores of 2-20- and 3-12-infected mice were significantly higher than A2- and mock-infected mice, and A2-infected mice had greater perivascular edema than mock-infected mice. BALB/cJ mice infected with RSV 2-20 or 3-12 also exhibited greater necrotic cellular debris in the airway epithelium at 1 d p.i. than mock-infected or A2-infected mice (Fig. 8, arrows). Increased bronchiolar luminal debris 1 d p.i. in

2-20- and 3-12-infected mice (Fig. 8) correlates with increased viral load (Fig. 6) and antigen load in the bronchiolar epithelium (Fig. 7).

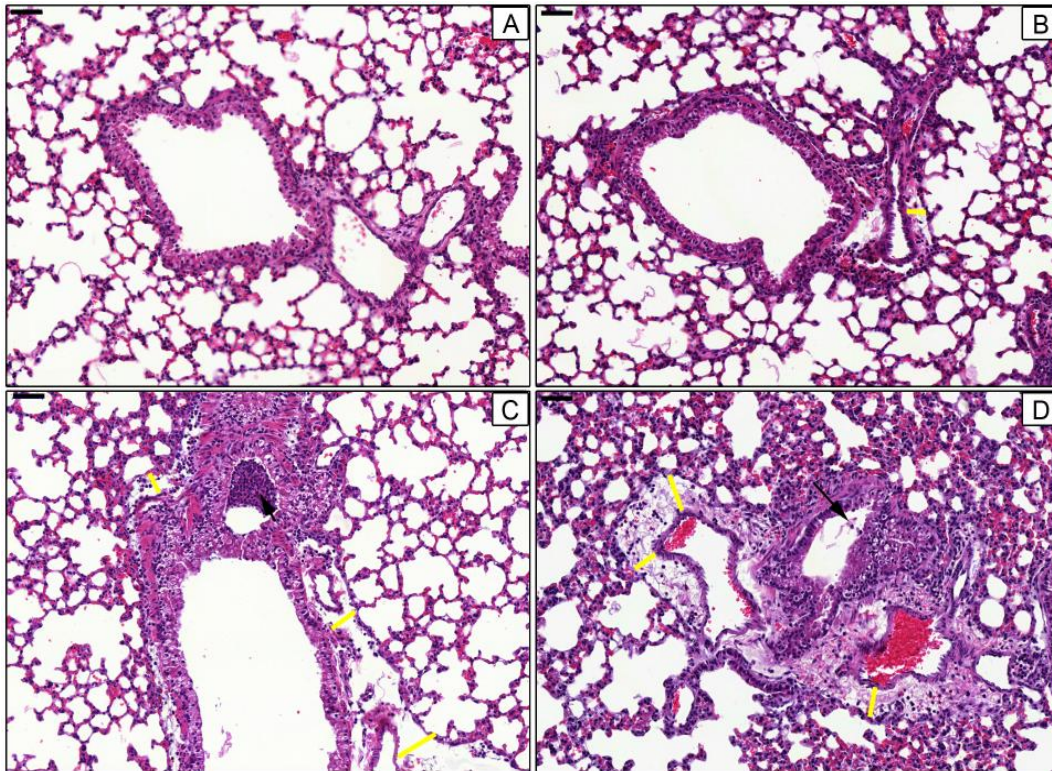


**Figure 8.** Early histopathologic lesions of RSV 2-20 and 3-12 infection. BALB/cJ mice were mock-infected (A) or infected with  $5 \times 10^5$  PFU of A2 (B), 2-20 (C), or 3-12 (D),  $n=4-5$ /group. Lungs harvested 1 d p.i., stained with H&E, and analyzed for histologic changes as described in the Materials and Methods. Representative airways are shown. Yellow bars indicate distance between vascular wall and adjacent tissue, as a measure of perivascular edema. Arrows indicate intrabronchiolar exudates of necrotic cell debris. Scale bar in upper left represents 50  $\mu\text{m}$ .

## **RSV strain 2-20 infection results in increased airway mucin expression**

Overabundance of airway mucus is a key feature of severe RSV disease resulting in hospitalization. In contrast to the A2 and Long strains, the line 19 RSV strain induces airway mucin expression in BALB/cJ mice (10). We used Periodic Acid-Schiff (PAS) staining to measure mucin expression in the airway epithelium of BALB/cJ mice that were mock-infected or infected with  $10^5$  PFU of RSV strains A2, line 19, 2-20, or 3-12. We previously utilized a semi-quantitative scoring system to measure PAS positivity in RSV-infected mice (10). Here, we used morphometric software (see Materials and Methods) to quantify PAS staining. RSV strains line 19 and 2-20 caused significantly increased airway mucin expression over mock-infected controls, whereas RSV strains A2 and 3-12 did not (Fig. 9B). There was no difference in the quantity of PAS staining between mice infected with line 19 and 2-20 (Fig. 9B). In these experiments, approximately 10% of the individual airways in line 19- and 2-20-infected mice had  $\geq 10\%$  PAS positivity (Fig. 9B). Thus, the majority of airways in line 19- and 2-20-infected mice were unaffected. Many of the PAS<sup>+</sup> airways in line 19- and 2-20-infected mice were smaller airways (Fig. 9A and 9C).

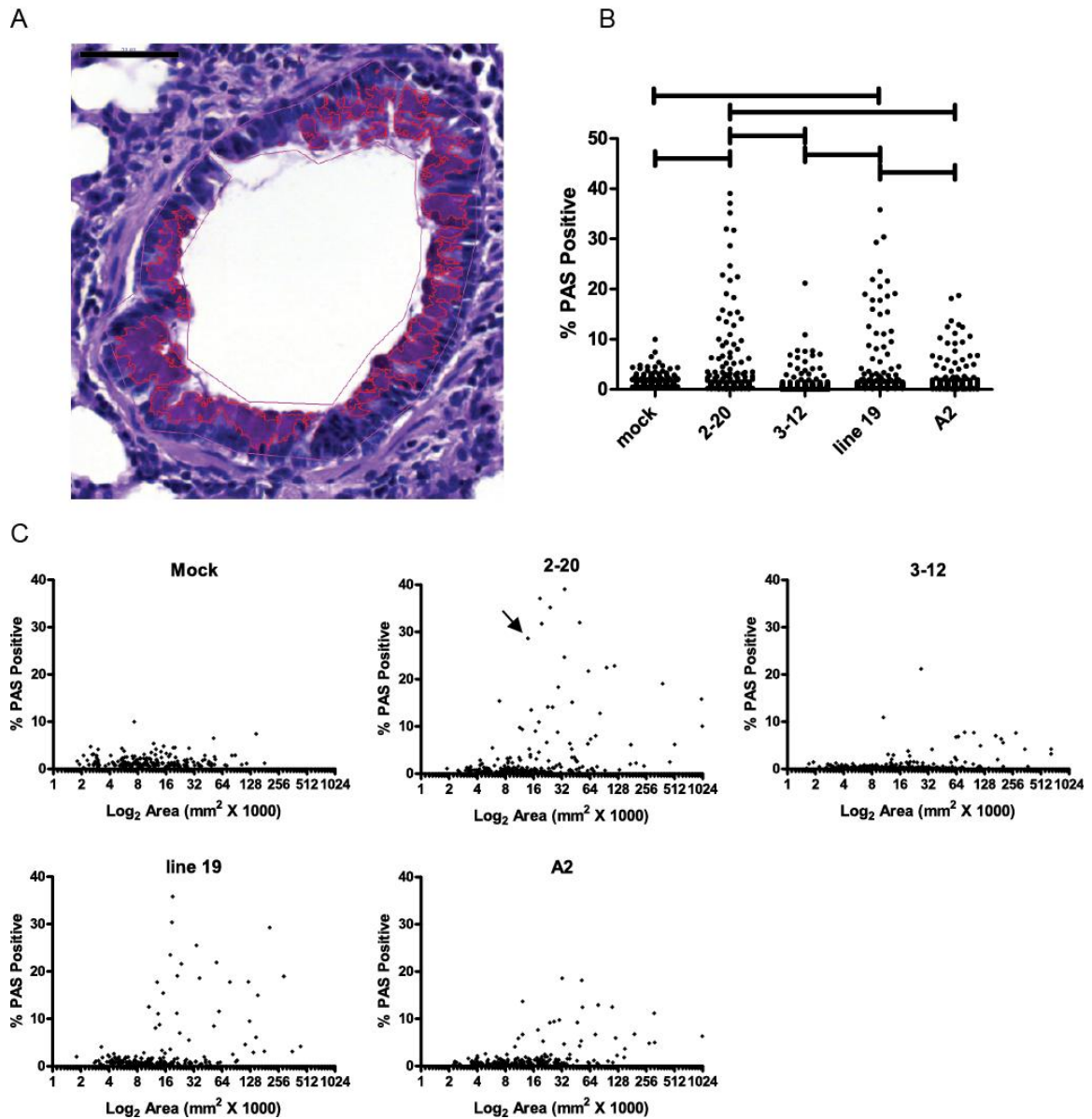


**Figure 9.** RSV A2001/2-20 induced high levels of pulmonary mucin expression. BALB/cJ mice were mock-infected ( $n = 3$  per group) or infected with  $10^5$  PFU of A2 ( $n=4$ ), line 19 ( $n=4$ ), 2-20 ( $n=5$ ), or 3-12 ( $n = 5$ ). Lungs were harvested 8 d p.i. and processed for PAS staining. The lung tissues were digitized, and each area of airway epithelium was annotated by hand as described in the Materials and Methods. (A) Example of airway epithelium (annotated by thin red line) in 2-20 infected mouse. The software detects PAS positivity based on color (thin red lines

outlining PAS stain). (B) The percentage of area that was PAS-positive for each airway was determined, > 200 individual airways shown per group. Each round symbol represents one airway. Capped lines indicate significant differences between groups,  $P < 0.05$  (ANOVA). (C) Same % PAS data as in (B) plotted with size of all airways. Airway depicted in (A) is indicated by an arrow.

Airways from infected IL-13<sup>-/-</sup> mice were also analyzed. 2-20 infection of wildtype BALB/cJ mice induced significantly more mucus than 2-20 infection of IL-13 knockout mice (Fig. 10). Thus, RSV line 19 and 2-20 infection resulted in significantly increased airway mucin expression in the small airways that was IL-13-dependent.

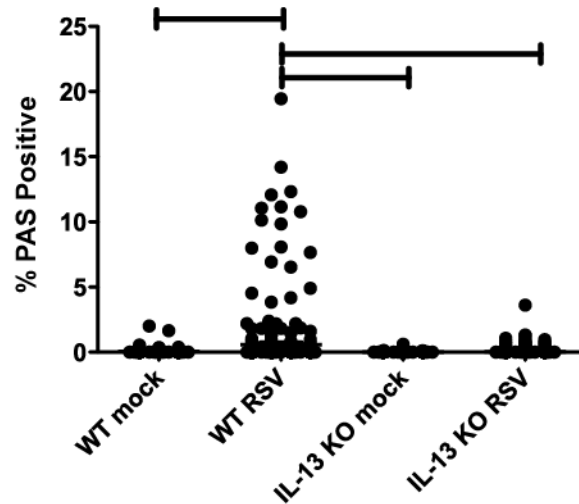


**Figure 10.** RSV 2-20 induced mucin expression is IL-13-dependent. BALB/cJ mice or IL-13 KO mice were mock-infected or infected with  $10^5$  PFU of 2-20 ( $n = 5$  per group). Lungs were harvested 8 d p.i. and processed for PAS staining. The lung tissues were digitized, and each area of airway epithelium was annotated by

hand as described in the Materials and Methods. % PAS positivity is plotted per group. Capped lines indicated significant differences between groups,  $P < 0.001$  (ANOVA).

### **RSV 2-20 infection caused lung dysfunction in BALB/cJ mice**

Airway dysfunction is the key feature of severe RSV bronchiolitis. A common radiologic finding in infants with severe RSV disease is pulmonary air trapping (46). A correlate of pulmonary obstruction and air trapping in humans is pulsus paradoxus, an exaggeration of normal variation in the pulse volume with respiration that can be caused by labored breathing (47-49). We observed labored breathing in RSV 2-20-infected mice (data not shown). We used a rodent pulse oximeter to quantify pulsus paradoxus as a measure of breathing effort in mock-infected and RSV-infected mice. The 2-20 strain of RSV caused increased breathing effort, whereas the A2 and 3-12 RSV strains did not (Fig. 11A). As the 2-20 strain infection caused increased breathing effort, we also measured AHR in mice infected with 2-20 using methacholine challenge in mechanically ventilated mice. In these experiments, we used mock infection as the negative control and RSV line 19 infection as the positive control; the A2 strain has repeatedly been shown to not cause AHR in BALB/cJ mice (9, 22, 24, 50). We found that, similar to the line 19 RSV strain, the 2-20 RSV strain caused AHR in BALB/cJ mice (Fig. 11B). Taken together, the data show that RSV strain 2-20 caused significant airway dysfunction in BALB/cJ mice.



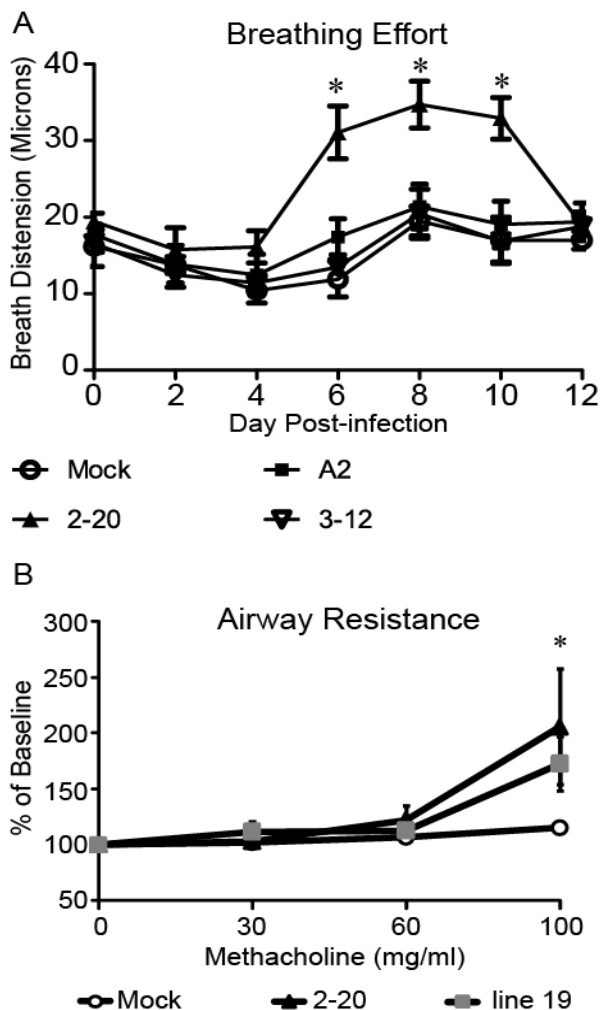


**Figure 11.** Lung dysfunction caused by RSV 2-20. (A) BALB/cJ mice were mock-infected (n=4) or infected with  $10^5$  PFU of A2, 2-20, or 3-12 RSV. Breath distension of peripheral arteries, a measure of pulsus paradoxus and pulmonary obstruction, was quantified at the indicated days non-invasively by pulse oximetry as described in the Materials and Methods. (B) BALB/cJ mice were mock-infected or infected with  $10^5$  PFU of 2-20 or line 19 (n=10/group). AHR was measured 9 d p.i. Means and SEM are shown. \*  $P < 0.05$  comparing 2-20 or line 19 to mock at 100 mg/ml methacholine dose. \*  $P < 0.05$  comparing 2-20 to mock, A2, and 3-12 groups.

### Lung CD8<sup>+</sup> T cell responses to RSV strains A2, 2-20, and 3-12

CD8<sup>+</sup> T cells play a role in RSV clearance as well as mediating illness by enhancing Th1 and inhibiting Th2 responses (51, 52). We used flow cytometry and intracellular staining to quantify IFN- $\gamma$ -producing CD8<sup>+</sup> T cells after infection with 10<sup>5</sup> PFU of RSV strains A2, 2-20, 3-12, and line 19. We found that A2 infection resulted in significantly more lung IFN- $\gamma$ -producing CD8<sup>+</sup> T cells in the lung than RSV strains 2-20 and line 19 at 8 d p.i. ( $P < 0.05$ ) (Fig. 12).

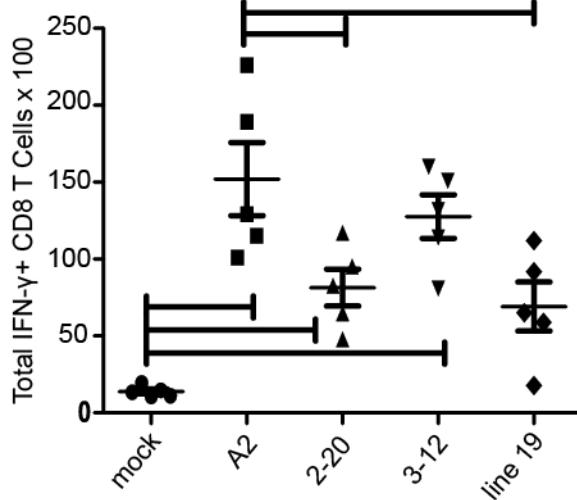


**Figure 12.** RSV A2 and 3-12 induced higher levels of IFN- $\gamma$  producing CD8<sup>+</sup> T cells than 2-20 and line 19. BALB/cJ mice ( $n = 5$  per group) were mock-infected or infected with 10<sup>5</sup> PFU of A2, line 19, 2-20, or 3-12. Lungs were harvested 8 d p.i. and cells were isolated using a Ficoll gradient.  $1 \times 10^6$  cells were stained with fluorescently-conjugated anti-CD3, anti-CD8, and anti-IFN- $\gamma$  antibodies and then analyzed by flow cytometry. Total cells were calculated as described in the Materials and Methods. Each symbol represents one mouse. Means and SEM are

shown for each group. Brackets indicate significant differences between groups ( $P < 0.05$ , ANOVA)

We also infected IL-13<sup>-/-</sup> mice with RSV 2-20 and used flow cytometry and intracellular staining to quantify IFN- $\gamma$ -producing CD8<sup>+</sup>T cells. There was no difference in number of IFN- $\gamma$ -producing CD8<sup>+</sup>T cells in the lung between wt and IL-13<sup>-/-</sup> mice (Fig. 13). Taken together, the IL-13 and mucus-inducing RSV strains 2-20 and line 19 had lower numbers of IFN- $\gamma$ -expressing CD8<sup>+</sup> T cells than nonmucogenic RSV strains A2, consistent with a hypothesis that T<sub>h</sub>1 and T<sub>h</sub>2 responses play a role in modulating RSV pathogenesis (Fig. 12).

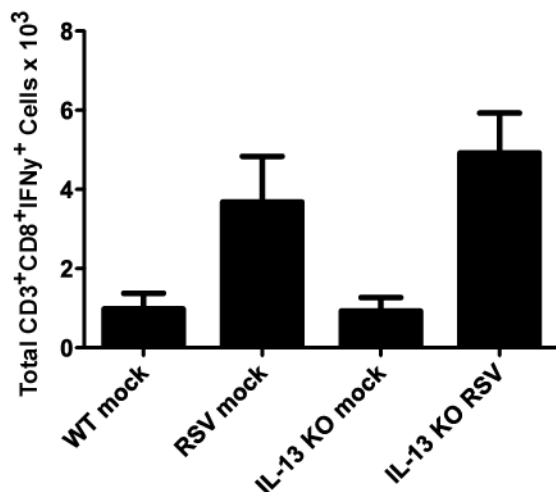


**Figure 13.** IFN- $\gamma$ -producing CD8<sup>+</sup>T cells in 2-20 infected BALB/cJ and IL-13 KO mice. IL-13 KO mice (n=4 for mock, n=5 per group for RSV infection) or wt BALB/cJ mice (n=2 per group) were mock-infected or infected with 10<sup>5</sup> PFU of 2-20. Lungs were harvested d 8 p.i. and cells were isolated using a ficoll gradient. Cells were stained with fluorescently-conjugated anti-CD3, anti-CD8, and anti IFN- $\gamma$  antibodies and then analyzed by flow cytometry. Total cells were calculated

as described in the Materials and Methods. Means and SEM are shown for each group.

## **DISCUSSION**

The laboratory RSV strains A2 and Long are widely used in animal models of RSV pathogenesis. It was previously shown that in contrast to A2 and Long, RSV strain, line 19, induces airway mucus expression in BALB/cJ mice (9, 10).

However, the passage histories of these RSV strains are not recorded. We have shown that the RSV clinical isolate strain 2-20 is more pathogenic in BALB/cJ mice than commonly used laboratory RSV strains and a closely related clinical isolate 3-12. In contrast to RSV A2 and 3-12 infection in BALB/cJ mice, strain 2-20 caused lung dysfunction, as measured by increased breathing effort, airway resistance, and mucin expression. We cannot rule out the possibility that differences in pathogenesis phenotypes between RSV 2-20 and 3-12 strains are due to mutations in these viruses that arose during their low number of passages in vitro. Nevertheless, our findings support the hypothesis that RSV strain differences are a determinant of disease phenotypes and severity. Future studies with strain-chimeric RSVs may shed light on mechanisms of RSV 2-20-induced phenotypes (10).

It is well-established that minor genetic differences in viral genomes can have a large impact on pathogenesis. For example, the molecular basis for the highly pathogenic H5N1 influenza virus was found to be a single amino acid substitution (53). An attenuated A2 RSV strain (*cp*-RSV) was found to differ from its parental

strain (HEK-7) by five amino acids (54-56). Circulating RSV strains exhibit considerable genomic variation, especially in the viral glycoprotein. RSV has one serotype, within which there are two antigenic subgroups, A and B (57). RSV subgroup A is associated with greater illness than RSV subgroup B (1, 58). Within antigenic subgroups, RSV strains can be further classified into clades based on sequence of a hypervariable region of the G gene (6-8). Generally, annual RSV epidemics consist of a dominant clade that is replaced the following season (6-8, 59). RSV clade differences have been associated with disease severity (60, 61). We found that two antigenic subgroup A strains within the same clade (GA2) exhibited differential virulence in a mouse model, suggesting that minor sequence variations affect pathogenicity.

Both RSV clinical isolates 2-20 and 3-12 had higher viral loads, higher antigen load in the airway epithelium, and caused more perivascular edema and damage to the airway epithelium at 1 d p.i. than laboratory RSV strains. One possibility for increased clinical isolate viral load at 1 d p.i. is that RSV clinical isolates have greater in vivo stability than RSV A2. However, RSV 2-20 and 3-12 do not exhibit greater in vitro stability than A2 (data not shown). We speculate that RSV clinical isolates enter mouse airway epithelial cells more efficiently than laboratory RSV strains that have been adapted to cell culture lines. Future studies will be required to determine if this is the case. For example, differences in the F protein may lead to enhanced entry and fusion, resulting in greater epithelial damage. Bronchiolar cytopathology is an important feature of RSV bronchiolitis and is thought to contribute to airway obstruction (11). Airway epithelial damage in

calves infected with bovine RSV (BRSV) contributes significantly to pathogenesis (62, 63). Many groups have focused on the later, adaptive immune response to RSV. It is likely that both early virus-induced epithelial damage and the ensuing cascade of innate and adaptive immune responses contribute to lung dysfunction. RSV clinical isolates described in this study provide a mouse model for investigating consequences of early airway histopathology.

Although both RSV strains 2-20 and 3-12 caused early epithelial cytopathology in mice and had similar viral loads over the time course, different cytokine responses that can be characterized as  $T_h1$  or  $T_h2$  were observed. RSV 2-20 strain infection resulted in dramatically higher lung IL-13 and mucin expression compared to 3-12 infection. RSV 2-20 infection also resulted in lower numbers of IFN- $\gamma$ -expressing CD8<sup>+</sup> T cells in the lung compared to A2 and 3-12 at 8 d p.i. The  $T_h1$  and  $T_h2$  responses to RSV are important because  $T_h2$ -type responses are associated with RSV immunopathology (13). Mixed  $T_h1/T_h2$  responses are observed in RSV-infected children, with some groups reporting a skew towards  $T_h2$  inflammation in severe RSV disease and other groups reporting a lack of association between  $T_h2$  cytokine levels and RSV disease (64-66). If RSV strain differences contribute to differential immune responses, this may confound comparison of these reports because different RSV strains may have been circulating in the studies. The role of  $T_h2$ -type responses in primary RSV infection is not completely defined. It is established in RSV vaccine-enhanced disease that  $T_h2$  cells mediate immunopathology (67). In primary A2 strain RSV infection in mice, IL-4 suppresses IFN- $\gamma$  expression, promotes RSV-specific Ab

production, and contributes to pulmonary mononuclear cell inflammation; but IL-4 deficiency has no effect on viral load, viral clearance, or disease severity (20, 68). In primary A2 strain infection, IL-13 was shown to play a protective role in limiting viral load and disease severity (69). Additionally, mucin expression during 2-20 infection was shown to be IL-13-dependent (Fig. 10). In line19 infection, mucus and AHR were also shown to be IL-13-dependent (70). Th2 responses to RSV infection may be a double-edged sword in promoting viral clearance and Ab responses but contributing to pulmonary obstruction.

The mechanisms by which RSV strain 2-20 induces IL-13 and mucus production are currently unknown. IL-13 has been shown to downregulate Th1 type cytokines (71). Conversely, IFN- $\gamma$  antagonizes IL-13 and IL-4 production and inhibits mucus production (72, 73). In allergic inflammation, IFN- $\gamma$  inhibits Th2 responses by activating the epithelium (73). In our model, however, 2-20-infected IL-13<sup>-/-</sup> mice did not show a decrease in IFN- $\gamma$ . Therefore, the decrease in IFN- $\gamma$ -producing CD8<sup>+</sup>T cells in 2-20 infected mice is not due to IL-13 production. In addition to T cells, other immune cells have been shown to be involved in a Th2-type response. RSV A2 infection of BALB/cJ and STAT1-deficient mice results in basophil IL-4 expression (20). Recently, RSV was shown to induce alternatively activated macrophages to produce IL-13 and IL-4 (74). Additional studies will be required to determine the contribution of innate immune cells to RSV 2-20 pathogenesis.

RSV 3-12-infected mice had approximately as many IFN- $\gamma$ -expressing T cells in the lungs as RSV A2-infected mice (Fig. 12). This was surprising because CD8<sup>+</sup> T

cells contribute to weight loss in A2-infected mice (75), but RSV 3-12 did not cause weight loss (Fig. 1) (76). There were no differences between total CD8<sup>+</sup> T cells in the lung and total RSV-specific (M2<sub>82-90</sub> tetramer) CD8<sup>+</sup> T cells in the lung between A2- and 3-12-infected mice (data not shown). Comparing 2-20 to 3-12 pathogenesis, mice infected with 3-12 had equivalent numbers (or slightly more in some experiments) of IFN- $\gamma$ -expressing T cells to 2-20-infected mice (Fig. 12). As 2-20 was more pathogenic than 3-12 as measured by weight loss, airway mucus, and lung dysfunction, T cells may play a protective role in RSV clinical isolate strain pathogenesis. Although T cells clearly cause immunopathology in RSV A2-infected mice, the role of T cells in human RSV disease is not known. Peak levels of activated T cells correlate with recovery from RSV disease, whereas neutrophil influx to the lung correlates with immunopathology (77, 78). Investigating the pathogenesis of RSV clinical isolates in mice may enable further insights into the role of neutrophils and T cells in RSV disease.

## **ACKNOWLEDGMENTS**

We thank Pierre Massion for the BEAS-2B cells. This work was supported by NIH HL090664 (Peebles), NIH AI070672 (Peebles), 1I01BX000624 (Peebles), NIH GM07569 (Morrow), NIH AI077507 (Moore), and AI087798 (Moore).



## REFERENCES

1. **Hall, C. B.** 2001. Respiratory syncytial virus and parainfluenza virus. *N.Engl.J.Med.* **344**:1917-1928.
2. **Hall, C. B., G. A. Weinberg, M. K. Iwane, A. K. Blumkin, K. M. Edwards, M. A. Staat, P. Auinger, M. R. Griffin, K. A. Poehling, D. Erdman, C. G. Grijalva, Y. Zhu, and P. Szilagyi.** 2009. The burden of respiratory syncytial virus infection in young children. *N Engl J Med* **360**:588-598.
3. **Howard, T. S., L. H. Hoffman, P. E. Stang, and E. A. Simoes.** 2000. Respiratory syncytial virus pneumonia in the hospital setting: length of stay, charges, and mortality. *J Pediatr* **137**:227-232.
4. **Nair, H., D. J. Nokes, B. D. Gessner, M. Dherani, S. A. Madhi, R. J. Singleton, K. L. O'Brien, A. Roca, P. F. Wright, N. Bruce, A. Chandran, E. Theodoratou, A. Sutanto, E. R. Sedyaningsih, M. Ngama, P. K. Munywoki, C. Kartasasmita, E. A. Simoes, I. Rudan, M. W. Weber, and H. Campbell.** 2010. Global burden of acute lower respiratory infections due to respiratory syncytial virus in young children: a systematic review and meta-analysis. *Lancet* **375**:1545-1555.
5. **Botosso, V. F., P. M. Zanotto, M. Ueda, E. Arruda, A. E. Gilio, S. E. Vieira, K. E. Stewien, T. C. Peret, L. F. Jamal, M. I. Pardini, J. R. Pinho, E. Massad, O. A. Sant'anna, E. C. Holmes, and E. L. Durigon.** 2009. Positive selection results in frequent reversible amino

- acid replacements in the G protein gene of human respiratory syncytial virus. *PLoS Pathog* **5**:e1000254.
6. **Cane, P. A.** 2001. Molecular epidemiology of respiratory syncytial virus. *Rev.Med.Virol.* **11**:103-116.
  7. **Peret, T. C., C. B. Hall, G. W. Hammond, P. A. Piedra, G. A. Storch, W. M. Sullender, C. Tsou, and L. J. Anderson.** 2000. Circulation patterns of group A and B human respiratory syncytial virus genotypes in 5 communities in North America. *J.Infect.Dis.* **181**:1891-1896.
  8. **Peret, T. C., C. B. Hall, K. C. Schnabel, J. A. Golub, and L. J. Anderson.** 1998. Circulation patterns of genetically distinct group A and B strains of human respiratory syncytial virus in a community. *J.Gen.Virol.* **79 ( Pt 9)**:2221-2229.
  9. **Lukacs, N. W., M. L. Moore, B. D. Rudd, A. A. Berlin, R. D. Collins, S. J. Olson, S. B. Ho, and R. S. Peebles, Jr.** 2006. Differential immune responses and pulmonary pathophysiology are induced by two different strains of respiratory syncytial virus. *Am.J.Pathol.* **169**:977-986.
  10. **Moore, M. L., M. H. Chi, C. Luongo, N. W. Lukacs, V. V. Polosukhin, M. M. Huckabee, D. C. Newcomb, U. J. Buchholz, J. E. Crowe, Jr., K. Goleniewska, J. V. Williams, P. L. Collins, and R. S. Peebles, Jr.** 2009. A chimeric A2 strain of respiratory syncytial virus (RSV) with the fusion protein of RSV strain line 19 exhibits enhanced viral load, mucus, and airway dysfunction. *J Virol* **83**:4185-4194.

11. **Aherne, W., T. Bird, S. D. Court, P. S. Gardner, and J. McQuillin.** 1970. Pathological changes in virus infections of the lower respiratory tract in children. *J.Clin.Pathol.* **23**:7-18.
12. **Lugo, R. A., and M. C. Nahata.** 1993. Pathogenesis and treatment of bronchiolitis. *Clin.Pharm.* **12**:95-116.
13. **Moore, M. L., and R. S. Peebles, Jr.** 2006. Respiratory syncytial virus disease mechanisms implicated by human, animal model, and in vitro data facilitate vaccine strategies and new therapeutics. *Pharmacol.Ther.*
14. **Quinn, S. F., S. Erickson, D. Oshman, and F. Hayden.** 1985. Lobar collapse with respiratory syncytial virus pneumonitis. *Pediatr.Radiol.* **15**:229-230.
15. **Walter, D. M., J. J. McIntire, G. Berry, A. N. McKenzie, D. D. Donaldson, R. H. DeKruyff, and D. T. Umetsu.** 2001. Critical role for IL-13 in the development of allergen-induced airway hyperreactivity. *J Immunol* **167**:4668-4675.
16. **Graham, B. S., M. D. Perkins, P. F. Wright, and D. T. Karzon.** 1988. Primary respiratory syncytial virus infection in mice. *J.Med.Virol.* **26**:153-162.
17. **Williams, J. V., P. A. Harris, S. J. Tollefson, L. L. Halburnt-Rush, J. M. Pingsterhaus, K. M. Edwards, P. F. Wright, and J. E. Crowe, Jr.** 2004. Human metapneumovirus and lower respiratory tract disease in otherwise healthy infants and children. *N.Engl.J.Med.* **350**:443-450.

18. **Muller, U., W. Stenzel, G. Kohler, C. Werner, T. Polte, G. Hansen, N. Schutze, R. K. Straubinger, M. Blessing, A. N. McKenzie, F. Brombacher, and G. Alber.** 2007. IL-13 induces disease-promoting type 2 cytokines, alternatively activated macrophages and allergic inflammation during pulmonary infection of mice with *Cryptococcus neoformans*. *Journal of immunology* **179**:5367-5377.
19. **Miller, A. L., T. L. Bowlin, and N. W. Lukacs.** 2004. Respiratory syncytial virus-induced chemokine production: linking viral replication to chemokine production in vitro and in vivo. *J.Infect.Dis.* **189**:1419-1430.
20. **Moore, M. L., D. C. Newcomb, V. V. Parekh, L. Van Kaer, R. D. Collins, W. Zhou, K. Goleniewska, M. H. Chi, D. Mitchell, J. A. Boyce, J. E. Durbin, C. Sturkie, and R. S. Peebles, Jr.** 2009. STAT1 negatively regulates lung basophil IL-4 expression induced by respiratory syncytial virus infection. *J Immunol* **183**:2016-2026.
21. **Piedimonte, G., M. M. Rodriguez, K. A. King, S. McLean, and X. Jiang.** 1999. Respiratory syncytial virus upregulates expression of the substance P receptor in rat lungs. *Am J Physiol* **277**:L831-840.
22. **Peebles, R. S., Jr., K. Hashimoto, R. D. Collins, K. Jarzecka, J. Furlong, D. B. Mitchell, J. R. Sheller, and B. S. Graham.** 2001. Immune interaction between respiratory syncytial virus infection and allergen sensitization critically depends on timing of challenges. *J.Infect.Dis.* **184**:1374-1379.
23. **Moore, M. L., M. H. Chi, W. Zhou, K. Goleniewska, J. F. O'Neal, J. N. Higginbotham, and R. S. Peebles, Jr.** 2007. Cutting Edge:

- Osetamivir decreases T cell GM1 expression and inhibits clearance of respiratory syncytial virus: potential role of endogenous sialidase in antiviral immunity. *J.Immunol.* **178**:2651-2654.
24. **Tekkanat, K. K., H. F. Maassab, D. S. Cho, J. J. Lai, A. John, A. Berlin, M. H. Kaplan, and N. W. Lukacs.** 2001. IL-13-induced airway hyperreactivity during respiratory syncytial virus infection is STAT6 dependent. *J.Immunol.* **166**:3542-3548.
25. **Nakanishi, A., S. Morita, H. Iwashita, Y. Sagiya, Y. Ashida, H. Shirafuji, Y. Fujisawa, O. Nishimura, and M. Fujino.** 2001. Role of gob-5 in mucus overproduction and airway hyperresponsiveness in asthma. *Proc Natl Acad Sci U S A* **98**:5175-5180.
26. **Hashimoto, K., J. E. Durbin, W. Zhou, R. D. Collins, S. B. Ho, J. K. Kolls, P. J. Dubin, J. R. Sheller, K. Goleniewska, J. F. O'Neal, S. J. Olson, D. Mitchell, B. S. Graham, and R. S. Peebles, Jr.** 2005. Respiratory syncytial virus infection in the absence of STAT 1 results in airway dysfunction, airway mucus, and augmented IL-17 levels. *J.Allergy Clin.Immunol.* **116**:550-557.
27. **Hashimoto, K., B. S. Graham, S. B. Ho, K. B. Adler, R. D. Collins, S. J. Olson, W. Zhou, T. Suzutani, P. W. Jones, K. Goleniewska, J. F. O'Neal, and R. S. Peebles, Jr.** 2004. Respiratory syncytial virus in allergic lung inflammation increases Muc5ac and gob-5. *Am.J.Respir.Crit Care Med.* **170**:306-312.
28. **Agenbach, E., C. T. Tiemessen, and M. Venter.** 2005. Amino acid variation within the fusion protein of respiratory syncytial virus subtype A

- and B strains during annual epidemics in South Africa. *Virus Genes* **30**:267-278.
29. **Matheson, J. W., F. J. Rich, C. Cohet, K. Grimwood, Q. S. Huang, D. Penny, M. D. Hendy, and J. R. Kirman.** 2006. Distinct patterns of evolution between respiratory syncytial virus subgroups A and B from New Zealand isolates collected over thirty-seven years. *J. Med. Virol.* **78**:1354-1364.
30. **Parveen, S., S. Broor, S. K. Kapoor, K. Fowler, and W. M. Sullender.** 2006. Genetic diversity among respiratory syncytial viruses that have caused repeated infections in children from rural India. *J. Med. Virol.* **78**:659-665.
31. **Scott, P. D., R. Ochola, M. Ngama, E. A. Okiro, N. D. James, G. F. Medley, and P. A. Cane.** 2006. Molecular analysis of respiratory syncytial virus reinfections in infants from coastal Kenya. *J. Infect. Dis.* **193**:59-67.
32. **Cane, P. A., D. A. Matthews, and C. R. Pringle.** 1991. Identification of variable domains of the attachment (G) protein of subgroup A respiratory syncytial viruses. *J Gen Virol* **72 ( Pt 9)**:2091-2096.
33. **Garcia, O., M. Martin, J. Dopazo, J. Arbiza, S. Frabasile, J. Russi, M. Hortal, P. Perez-Brena, I. Martinez, and B. Garcia-Barreno.** 1994. Evolutionary pattern of human respiratory syncytial virus (subgroup A): cocirculating lineages and correlation of genetic and antigenic changes in the G glycoprotein. *The Journal of Virology* **68**:5448-5459.

34. **Lim, C. S., G. Kumarasinghe, and V. T. Chow.** 2003. Sequence and phylogenetic analysis of SH, G, and F genes and proteins of Human respiratory syncytial virus isolates from Singapore. *Acta Virol* **47**:97-104.
35. **Madhi, S. A., M. Venter, R. Alexandra, H. Lewis, Y. Kara, W. F. Karshagen, M. Greef, and C. Lassen.** 2003. Respiratory syncytial virus associated illness in high-risk children and national characterisation of the circulating virus genotype in South Africa. *J Clin Virol* **27**:180-189.
36. **Moura, F. E., A. Blanc, S. Frabasile, A. Delfraro, M. J. de Sierra, L. Tome, E. A. Ramos, M. M. Siqueira, and J. Arbiza.** 2004. Genetic diversity of respiratory syncytial virus isolated during an epidemic period from children of northeastern Brazil. *J Med Virol* **74**:156-160.
37. **Reiche, J., and B. Schweiger.** 2009. Genetic variability of group A human respiratory syncytial virus strains circulating in Germany from 1998 to 2007. *J Clin Microbiol* **47**:1800-1810.
38. **Sullender, W. M., M. A. Mufson, G. A. Prince, L. J. Anderson, and G. W. Wertz.** 1998. Antigenic and genetic diversity among the attachment proteins of group A respiratory syncytial viruses that have caused repeat infections in children. *J.Infect.Dis.* **178**:925-932.
39. **Venter, M., S. A. Madhi, C. T. Tiemessen, and B. D. Schoub.** 2001. Genetic diversity and molecular epidemiology of respiratory syncytial virus over four consecutive seasons in South Africa: identification of new subgroup A and B genotypes. *J Gen Virol* **82**:2117-2124.
40. **Wertz, G. W., P. L. Collins, H. A. Yung, C. Gruber, S. Levine, and L. A. Ball.** 1985. Nucleotide-Sequence of the G-Protein Gene of Human

Respiratory Syncytial Virus Reveals an Unusual Type of Viral Membrane-Protein. *Proceedings of the National Academy of Sciences of the United States of America* **82**:4075-4079.

41. **Behera, A. K., M. Kumar, H. Matsuse, R. F. Lockey, and S. S. Mohapatra.** 1998. Respiratory syncytial virus induces the expression of 5-lipoxygenase and endothelin-1 in bronchial epithelial cells. *Biochem Biophys Res Commun* **251**:704-709.
42. **Huang, Y. C., Z. Li, X. Hyseni, M. Schmitt, R. B. Devlin, E. D. Karoly, and J. M. Soukup.** 2009. Identification of gene biomarkers for respiratory syncytial virus infection in a bronchial epithelial cell line. *Genomic Med.*
43. **Stanciu, L. A., C. M. Bellettato, V. Laza-Stanca, A. J. Coyle, A. Papi, and S. L. Johnston.** 2006. Expression of programmed death-1 ligand (PD-L) 1, PD-L2, B7-H3, and inducible costimulator ligand on human respiratory tract epithelial cells and regulation by respiratory syncytial virus and type 1 and 2 cytokines. *J Infect Dis* **193**:404-412.
44. **Thomas, L. H., J. S. Friedland, M. Sharland, and S. Becker.** 1998. Respiratory syncytial virus-induced RANTES production from human bronchial epithelial cells is dependent on nuclear factor-kappa B nuclear binding and is inhibited by adenovirus-mediated expression of inhibitor of kappa B alpha. *J Immunol* **161**:1007-1016.
45. **Anderson, J. J., J. Norden, D. Saunders, G. L. Toms, and R. Scott.** 1990. Analysis of the local and systemic immune responses induced



- in BALB/c mice by experimental respiratory syncytial virus infection. *J.Gen.Virol.* **71 ( Pt 7)**:1561-1570.
46. **Osborne, D.** 1978. Radiologic appearance of viral disease of the lower respiratory tract in infants and children. *AJR Am J Roentgenol* **130**:29-33.
  47. **Hartert, T. V., A. P. Wheeler, and J. R. Sheller.** 1999. Use of pulse oximetry to recognize severity of airflow obstruction in obstructive airway disease: correlation with pulsus paradoxus. *Chest* **115**:475-481.
  48. **Knowles, G. K., and T. J. Clark.** 1973. Pulsus paradoxus as a valuable sign indicating severity of asthma. *Lancet* **2**:1356-1359.
  49. **Rebuck, A. S., and L. D. Pengelly.** 1973. Development of pulsus paradoxus in the presence of airways obstruction. *N Engl J Med* **288**:66-69.
  50. **Peebles, R. S., Jr., J. R. Sheller, R. D. Collins, K. Jarzecka, D. B. Mitchell, and B. S. Graham.** 2000. Respiratory syncytial virus (RSV)-induced airway hyperresponsiveness in allergically sensitized mice is inhibited by live RSV and exacerbated by formalin-inactivated RSV. *J.Infect.Dis.* **182**:671-677.
  51. **Srikiatkachorn, A., and T. J. Braciale.** 1997. Virus-specific CD8+ T lymphocytes downregulate T helper cell type 2 cytokine secretion and pulmonary eosinophilia during experimental murine respiratory syncytial virus infection. *J Exp Med* **186**:421-432.
  52. **Hussell, T., and P. J. Openshaw.** 1998. Intracellular IFN-gamma expression in natural killer cells precedes lung CD8+ T cell recruitment

- during respiratory syncytial virus infection. *J Gen Virol* **79 ( Pt 11)**:2593-2601.
53. **Hatta, M., P. Gao, P. Halfmann, and Y. Kawaoka.** 2001. Molecular basis for high virulence of Hong Kong H5N1 influenza A viruses. *Science* **293**:1840-1842.
54. **Connors, M., J. E. Crowe, Jr., C. Y. Firestone, B. R. Murphy, and P. L. Collins.** 1995. A cold-passaged, attenuated strain of human respiratory syncytial virus contains mutations in the F and L genes. *Virology* **208**:478-484.
55. **Crowe, J. E., Jr., C. Y. Firestone, S. S. Whitehead, P. L. Collins, and B. R. Murphy.** 1996. Acquisition of the ts phenotype by a chemically mutagenized cold-passaged human respiratory syncytial virus vaccine candidate results from the acquisition of a single mutation in the polymerase (L) gene. *Virus Genes* **13**:269-273.
56. **Whitehead, S. S., K. Juhasz, C. Y. Firestone, P. L. Collins, and B. R. Murphy.** 1998. Recombinant respiratory syncytial virus (RSV) bearing a set of mutations from cold-passaged RSV is attenuated in chimpanzees. *J Virol* **72**:4467-4471.
57. **Collins, P. L. a. C., J. E., Jr.** 2007. Respiratory Syncytial Virus and Metapneumovirus p. 1601-1646. *In* D. M. a. H. Knipe, P. M. (ed.), *Fields Virology*, Fifth ed. Lippincott Williams & Wilkins Philadelphia, PA.
58. **Hall, C. B., E. E. Walsh, K. C. Schnabel, C. E. Long, K. M. McConnochie, S. W. Hildreth, and L. J. Anderson.** 1990. Occurrence of groups A and B of respiratory syncytial virus over 15 years:

- associated epidemiologic and clinical characteristics in hospitalized and ambulatory children. *J.Infect.Dis.* **162**:1283-1290.
59. **Sullender, W. M.** 2000. Respiratory syncytial virus genetic and antigenic diversity. *Clin.Microbiol.Rev.* **13**:1-15, table.
60. **Gilca, R., G. De Serres, M. Tremblay, M. L. Vachon, E. Leblanc, M. G. Bergeron, P. Dery, and G. Boivin.** 2006. Distribution and clinical impact of human respiratory syncytial virus genotypes in hospitalized children over 2 winter seasons. *J.Infect.Dis.* **193**:54-58.
61. **Martinello, R. A., M. D. Chen, C. Weibel, and J. S. Kahn.** 2002. Correlation between respiratory syncytial virus genotype and severity of illness. *J.Infect.Dis.* **186**:839-842.
62. **Viuff, B., K. Tjernehoj, L. E. Larsen, C. M. Rontved, A. Uttenthal, L. Ronsholt, and S. Alexandersen.** 2002. Replication and clearance of respiratory syncytial virus: apoptosis is an important pathway of virus clearance after experimental infection with bovine respiratory syncytial virus. *Am.J.Pathol.* **161**:2195-2207.
63. **Woolums, A. R., M. L. Anderson, R. A. Gunther, E. S. Schelegle, D. R. LaRochelle, R. S. Singer, G. A. Boyle, K. E. Friebertshauser, and L. J. Gershwin.** 1999. Evaluation of severe disease induced by aerosol inoculation of calves with bovine respiratory syncytial virus. *Am.J.Vet.Res.* **60**:473-480.
64. **de Waal, L., L. P. Koopman, I. J. van Bente, A. H. Brandenburg, P. G. Mulder, R. L. de Swart, W. J. Fokkens, H. J. Neijens, and A. D. Osterhaus.** 2003. Moderate local and systemic

- respiratory syncytial virus-specific T-cell responses upon mild or subclinical RSV infection. *J Med Virol* **70**:309-318.
65. **Mobbs, K. J., R. L. Smyth, U. O'Hea, D. Ashby, P. Ritson, and C. A. Hart.** 2002. Cytokines in severe respiratory syncytial virus bronchiolitis. *Pediatr Pulmonol* **33**:449-452.
66. **Tripp, R. A., D. Moore, A. t. Barskey, L. Jones, C. Moscatiello, H. Keyserling, and L. J. Anderson.** 2002. Peripheral blood mononuclear cells from infants hospitalized because of respiratory syncytial virus infection express T helper-1 and T helper-2 cytokines and CC chemokine messenger RNA. *J Infect Dis* **185**:1388-1394.
67. **Varga, S. M., and T. J. Braciale.** 2002. RSV-induced immunopathology: dynamic interplay between the virus and host immune response. *Virology* **295**:203-207.
68. **Fischer, J. E., J. E. Johnson, R. K. Kuli-Zade, T. R. Johnson, S. Aung, R. A. Parker, and B. S. Graham.** 1997. Overexpression of interleukin-4 delays virus clearance in mice infected with respiratory syncytial virus. *The Journal of Virology* **71**:8672-8677.
69. **Zhou, W., K. Hashimoto, M. L. Moore, J. A. Elias, Z. Zhu, J. Durbin, G. Colasurdo, J. A. Rutigliano, C. L. Chiappetta, K. Goleniewska, J. F. O'Neal, B. S. Graham, and R. S. Peebles, Jr.** 2006. IL-13 is associated with reduced illness and replication in primary respiratory syncytial virus infection in the mouse. *Microbes Infect* **8**:2880-2889.

70. **Lukacs, N. W., M. L. Moore, B. D. Rudd, A. A. Berlin, R. D. Collins, S. J. Olson, S. B. Ho, and R. S. Peebles, Jr.** 2006. Differential immune responses and pulmonary pathophysiology are induced by two different strains of respiratory syncytial virus. *Am J Pathol* **169**:977-986.
71. **Li, H., T. C. Sim, and R. Alam.** 1996. IL-13 released by and localized in human basophils. *J Immunol* **156**:4833-4838.
72. **Dickensheets, H. L., and R. P. Donnelly.** 1997. IFN-gamma and IL-10 inhibit induction of IL-1 receptor type I and type II gene expression by IL-4 and IL-13 in human monocytes. *J Immunol* **159**:6226-6233.
73. **Cohn, L., L. Whittaker, N. Q. Niu, and R. J. Homer.** 2002. Cytokine regulation of mucus production in a model of allergic asthma. *Mucus Hypersecretion in Respiratory Disease* **248**:201-220.
74. **Shirey, K. A., L. M. Pletneva, A. C. Puche, A. D. Keegan, G. A. Prince, J. C. Blanco, and S. N. Vogel.** Control of RSV-induced lung injury by alternatively activated macrophages is IL-4R alpha-, TLR4-, and IFN-beta-dependent. *Mucosal Immunol* **3**:291-300.
75. **Graham, B. S., L. A. Bunton, P. F. Wright, and D. T. Karzon.** 1991. Role of T lymphocyte subsets in the pathogenesis of primary infection and rechallenge with respiratory syncytial virus in mice. *J Clin Invest* **88**:1026-1033.
76. **Graham, B. S., L. A. Bunton, P. F. Wright, and D. T. Karzon.** 1991. Role of T lymphocyte subsets in the pathogenesis of primary

infection and rechallenge with respiratory syncytial virus in mice.

J.Clin.Invest **88**:1026-1033.

77. **Heidema, J., M. V. Lukens, W. W. van Maren, M. E. van Dijk, H. G. Otten, A. J. van Vught, D. B. van der Werff, S. J. van Gestel, M. G. Semple, R. L. Smyth, J. L. Kimpen, and G. M. van Bleek.**  
2007. CD8+ T cell responses in bronchoalveolar lavage fluid and peripheral blood mononuclear cells of infants with severe primary respiratory syncytial virus infections. J Immunol **179**:8410-8417.
78. **Lukens, M. V., A. C. van de Pol, F. E. Coenjaerts, N. J. Jansen, V. M. Kamp, J. L. Kimpen, J. W. Rossen, L. H. Ulfman, C. E. Tacke, M. C. Viveen, L. Koenderman, T. F. Wolfs, and G. M. van Bleek.**  
2010. A systemic neutrophil response precedes robust CD8(+) T-cell activation during natural respiratory syncytial virus infection in infants. J Virol **84**:2374-2383.

## CHAPTER 3

### **The Respiratory Syncytial Virus Fusion Protein and Neutrophils Mediate the Airway Mucin Response to Pathogenic RSV infection**

The work of this chapter was published in September, 2013 in the *Journal of Virology*

Full article citation:

Stokes KL, Currier MG, Sakamoto K, Lee S, Collins PL, Plemper RK, Moore ML. The Respiratory Syncytial Virus Fusion Protein and Neutrophils Mediate the Airway Mucin Response to Pathogenic RSV infection. *J Virol.* 2013 87: 10070-10082.

**The Respiratory Syncytial Virus Fusion Protein and Neutrophils  
Mediate the Airway Mucin Response to Pathogenic RSV infection**

**Running title:** Neutrophils Mediate RSV-Induced Mucin Response

Kate L. Stokes<sup>1,2</sup>, Michael G. Currier<sup>1,2</sup>, Kaori Sakamoto<sup>3</sup>, Sujin Lee<sup>1,2</sup>, Peter L. Collins<sup>4</sup>, Richard K. Plemper<sup>1,2</sup>, and Martin L. Moore<sup>1,2#</sup>

<sup>1</sup>Department of Pediatrics, Emory University, Atlanta, Georgia 30322

<sup>2</sup>Children's Healthcare of Atlanta, Atlanta, Georgia 30322

<sup>3</sup>Department of Pathology, College of Veterinary Medicine, University of Georgia, Athens, Georgia

<sup>4</sup>Laboratory of Infectious Diseases, National Institute of Allergy and Infectious Diseases, Bethesda, Maryland, USA

#Corresponding author: Mailing address for Martin L Moore: 2015 Uppergate Dr. NE, Emory Children's Center, Room 514, Department of Pediatrics, Emory University, Atlanta, GA 30322. Phone: (404) 727-9162. Fax: (404) 727-9223. E-mail: [martin.moore@emory.edu](mailto:martin.moore@emory.edu).



**ABSTRACT**

Respiratory syncytial virus (RSV) is the leading cause of death due to a viral etiology in infants. RSV disease is characterized by epithelial desquamation, neutrophilic bronchiolitis and pneumonia, and obstructive pulmonary mucus. It has been shown that infection of BALB/cJ mice with RSV clinical isolate A2001/2-20 (2-20) results in a higher early viral load, greater airway necrosis, and higher levels of interleukin-13 (IL-13) and airway mucin expression than infection with RSV laboratory strain A2. We hypothesized that the fusion (F) protein of RSV 2-20 is a mucus-inducing viral factor. *In vitro*, the fusion activity of 2-20 F but not that of A2 F was enhanced by expression of RSV G. We generated a recombinant F-chimeric RSV by replacing the F gene of A2 with the F gene of 2-20, generating A2-2-20F. Similar to the results obtained with the parent 2-20 strain, infection of BALB/cJ mice with A2-2-20F resulted in a higher early viral load and higher levels of subsequent pulmonary mucin expression than infection with the A2 strain. A2-2-20F infection induced greater necrotic airway damage and neutrophil infiltration than A2 infection. We hypothesized that the neutrophil response to A2-2-20F infection is involved in mucin expression. Antibody-mediated depletion of neutrophils in RSV-infected mice resulted in lower tumor necrosis factor alpha levels, fewer IL-13-expressing CD4 T cells, and less airway mucin production in the lung. Our data are consistent with a model in which the F and attachment (G) glycoprotein functional interaction leads to enhanced fusion and F is a key factor in airway epithelium infection, pathogenesis, and subsequent airway mucin expression.

## INTRODUCTION

Respiratory syncytial virus (RSV) is the most important cause of bronchiolitis and viral pneumonia in infants and the most common cause of hospitalization in infants younger than 1 year of age (1). RSV infects practically all children by the age of 2 causing approximately 400 infant deaths and up to 125,000 hospitalizations per year in the US (2, 3). Worldwide, RSV is the leading cause of death due to viral etiology in children younger than 1 year of age (3). RSV infection results in airway obstruction and lung inflammation, which lead to hyperresponsiveness involving leukocyte infiltration, mucus production, and epithelial damage (4). The virus targets the epithelial cells of the nasopharynx, trachea, and bronchi resulting in the formation of thick mucus plugs mixed with cell debris, fibrin, and lymphocytes (5). An understanding of how RSV causes epithelial damage and mucus production that leads to lung dysfunction may aid the development of approaches to prevent severe respiratory illness.

Excess neutrophils are found in the airways of infants with acute RSV bronchiolitis as well as in the bronchoalveolar lavage (BAL) fluid of RSV-infected children (6-9). However, the precise role of neutrophils in RSV pathogenesis is unknown. Neutrophils recruited to airways cause epithelial damage through mechanisms such as the release of free oxygen radicals, neutrophil elastase, and proteolytic enzymes (10). *In vitro*, neutrophils can enhance RSV-induced epithelial damage and detachment of cells (11). It is not known whether this occurs *in vivo*. Furthermore, neutrophils are a major source of tumor necrosis factor alpha (TNF- $\alpha$ ). Intratracheal administration of TNF- $\alpha$  in BALB/cJ mice

induces mucus associated proteins such as gob5, Muc5ac, leading to mucus expression in the airways (12).

We previously reported that infection of BALB/cJ mice with clinical strain RSV A2001/2-20 (2-20) results in greater disease severity and higher lung interleukin-13 (IL-13) levels compared to infection with laboratory strain A2 (13). Another laboratory RSV strain, line 19, also induces airway mucin expression in an IL-13-dependent manner similar to RSV 2-20 (14, 15). RSV 2-20 is useful because it is a clinical isolate of known passage history (13). A chimeric virus containing the line 19 F protein in the A2 genetic background indicated that the fusion protein of RSV plays a role in pulmonary mucus expression in the mouse model (16). Interestingly, the unique residues of the line 19 F protein do not occur in RSV clinical isolates, suggesting that line 19 may have acquired mutations during passage (A.L. Hotard and M.L. Moore, unpublished).

We hypothesized that the F protein of 2-20 also plays a role in RSV-induced mucus production. In order to test this, we generated a chimeric virus strain containing the RSV 2-20 F gene in an RSV A2 backbone (referred to as A2-2-20F) and employed antibody-depletion to further probe the role of neutrophils in RSV pathogenesis. Infection of BALB/cJ mice with chimeric virus strain A2-2-20F caused greater early airway epithelium necrosis and neutrophil infiltration as well as pulmonary mucus expression compared to RSV A2. Neutrophil depletion caused diminished airway mucin expression and TNF- $\alpha$  production during 2-20 infection. Our results elucidate a novel pathway of RSV pathogenesis whereby the

F protein results in airway cell debris, and the ensuing robust neutrophil response mediates  $T_{h2}$  cell IL-13 expression and airway mucin expression. Mechanistic characterization identified a unique functional interaction between the RSV attachment (G) glycoprotein and F protein that may be important for RSV fusion and pathogenesis.

## **MATERIALS AND METHODS**

### **Cells, viruses, and mice**

HEp-2 cells were obtained from the ATCC and propagated in MEM supplemented with 10% FBS, penicillin G-streptomycin sulfate-amphotericin B solution (Mediatech, Manassas, VA). 293T cells were obtained from the ATCC and propagated in MEM supplemented with 10% FBS, penicillin G-streptomycin sulfate-amphotericin B solution. The A2 strain of RSV was provided by Stokes Peebles (Vanderbilt, Nashville, TN) and maintained by passage in HEp-2 cells. The 2-20 RSV strain was maintained by passage in HEp-2 cells (13). Viral stocks were propagated and titrated by plaque assay in HEp-2 cells as described previously (13). Female, 6-week-old BALB/cJ mice were obtained from Jackson Laboratories (Bar Harbor, ME). All mice were maintained under specific-pathogen-free conditions. Mice were anesthetized by intramuscular injection of a ketamine-xylazine solution and infected intranasally (i.n.) with RSV virus stock or with mock-infected HEp-2 cell culture supernatant, as described (17). All animal procedures were conducted according to the guidelines of the Emory University Institutional Animal Care and Use Committee.

### **Generation and recovery of chimeric A2-2-20F RSV**

Total RNA was isolated from HEp-2 cells infected with RSV strain 2-20. cDNA was reverse transcribed as described using primer F-r (16). PCR amplicons were gel-purified and sequenced. The 2-20 F cDNA sequence from three separate infections was compared to the published 2-20 F sequence and confirmed (13). The F cDNA was then PCR-amplified using forward primer FStuI and reverse primer FSphI, which incorporated StuI and SphI restriction sites into the G-F intergenic region and F-M2 intergenic region, respectively, and added flanking EcoRI sites, as described previously (16). The 2-20 F cDNA was cloned into the EcoRI site of pGEM-9Zf (Promega, Madison WI) then moved using StuI and SphI into a low copy number subclone (pLG4) harboring a XhoI/BamHI fragment of RSV antigenomic cDNA clone D46/6120 containing the RSV A2 G gene and the F gene flanked by StuI and SphI and partial M2 sequence of RSV, thereby replacing the A2 F gene (16). The XhoI/BamHI fragment containing 2-20 F was then cloned into RSV antigenomic cDNA plasmid D46/6120, yielding the full-length A2-2-20F plasmid, in which the sequence of the F gene was confirmed.

BSRT7/5 cells, which constitutively express T7 polymerase (provided by Ursula J. Buchholz and Karl-Klaus Conzelmann), were transfected with A2-A2-2-20F and four support plasmids which express RSV N, P, M2-1, and L proteins under the control of the T7 promoter (18, 19). Transfected cells were passaged until syncytia were observed, at which point they were scraped into the medium, snap-frozen, thawed, and used to infect HEp-2 cells (16). When maximal cytopathic effect was observed in HEp-2 cells, serial dilutions of clarified supernatants were used to

infect fresh HEp-2 cells, which were overlaid with agarose-medium. Single plaques were picked and amplified in HEp-2 cells to generate viral stocks. The F cDNA was PCR amplified as described above from the recovered working A2-2-20F virus stock, and the F cDNA sequence was confirmed. The stock was confirmed mycoplasma-free based on PCR-based testing (Venor GeM Mycoplasma Detection Kit, PCR-based, Sigma-Aldrich, St. Louis, Missouri).

### **Multistep virus growth curves**

Subconfluent HEp-2 cells in six-well dishes were infected in triplicate with RSV strains A2, 2-20, or A2-2-20F at a multiplicity of infection (MOI) of 1.0 in 250  $\mu$ l. After 1 hour adsorption at room temperature on a rocking platform, the cells were washed with PBS, and fresh medium was added. Supernatants were harvested at 12 hours, 24 hours, 48 hours, and 72 hours from each well, and RSV was titrated in duplicate by plaque assay on HEp-2 cells as described previously (13).

### **Quantification of lung viral load**

BALB/cJ mice were infected with  $10^5$  plaque-forming units (PFU) of RSV and lungs were harvested at indicated time points. A BeadBeater apparatus (Biospec Products, Bartlesville, OK) was used to homogenize the lungs as previously described (13). Lung homogenates were serially diluted and used to inoculate subconfluent HEp-2 cells in 24-well dishes as described and overlaid with MEM supplemented with 10% FBS, penicillin G-streptomycin sulfate-amphotericin B solution, and 0.75% methylcellulose (13). After 6 days, plaques were visualized by immunodetection as described previously (13).

## **Histopathology**

Lungs were fixed in 10% neutral-buffered formalin for 24 hours and then transferred to 70% ethanol. Lungs were then embedded in paraffin blocks and 5  $\mu\text{m}$  thick tissue sections were cut and then stained with hematoxylin and eosin (H&E) stains to examine histologic changes. A pathologist blinded to the groups scored the samples for severity of infiltrates of lymphocytes, neutrophils, macrophages, and eosinophils on a scale of 0 to 4 for peribronchiolar, perivascular, interstitial, and alveolar spaces. Slides were scored for the presence or absence of bronchiolar exudates containing necrotic cell debris. Additional sections were also stained with periodic acid-Schiff (PAS) stain to quantify the amount of mucin expression in airways. PAS-stained slides were digitally scanned using a Mirax Midi microscope and slides were analyzed for PAS-positive airways using HistoQuant software (3D Histotech, Budapest, Hungary) as we previously described (13). Each airway was outlined individually, and all airways in the section were included in the data.

## **Dual-functional split-reporter (DSP) fusion assay**

An assay using fused split reporter proteins *Renilla* luciferase (RL) and green fluorescent protein (GFP), which recover activity when they reassociate due to cell fusion allow for quantification of viral protein-induced cell-cell fusion (20). The GFP reporter protein is made up of a small fragment of GFP fragment harboring a  $\beta$ -sheet (21). Transfected cells expressing DSP<sub>1-7</sub> or DSP<sub>8-12</sub> were used (22). Plasmids expressing cDNAs codon-optimized for mammalian expression (GeneArt; Invitrogen, Carlsbad, CA) of RSV A2 F, A2 G, 2-20 F, and 2-20 G were

cloned into pcDNA3.1(+) (Invitrogen) and sequence confirmed. 293T (90% confluent) cells were transfected with plasmids expressing A2 F, 2-20 F, A2 F and A2 G, 2-20 F and 2-20 G, or 2-20 F and A2 G as well as DSP<sub>1-7</sub>. Additional wells were transfected with plasmids expressing DSP<sub>8-11</sub>. 293T cells were transfected with Lipofectamine 2000 (Invitrogen) and incubated in MEM with 10% FBS and 1% pen/strep/amphotericin B containing 250 nM RSV fusion inhibitor BMS-433771 (Alios Biopharma, San Francisco, CA) for 24 hours at 37°C, 5% CO<sub>2</sub>. Twenty-four hours post-transfection, cells were washed with 1 ml PBS and resuspended in 1 ml medium containing 1:1,000 EnduRen Live Cell Substrate (Promega, Madison, WI). Cells expressing DSP<sub>1-7</sub> as well as A2 F, 2-20 F, A2 F and A2 G, 2-20 F and 2-20 G or 2-20 F and A2 G were mixed in equal volume with cells expressing DSP<sub>8-11</sub>. 100 µl of each cell mixture were plated in a white 96-well plate and RL activity was measured with a Top Count Luminometer (PerkinElmer, Waltham, MA) at indicated time points.

### **Western blotting analysis of F and G levels in transfected 293T cells**

For immunoblotting, proteins were separated by SDS-PAGE followed by transfer to a PVDF membrane. After electroblotting, the membranes were probed using the SNAP i.d. system (Millipore, Billerica, MA). Briefly, the blot was saturated in 0.5% non-fat dry milk in Tris-buffered saline-Tween 20 (TBS-T). After blocking, the membrane was washed three times with TBS-T followed by incubation with primary antibody against RSV F (Palivizumab antibody: 1:10000, a gift from James Crowe, Vanderbilt, Nashville, TN) or RSV G (131-2G: 1:5000 Millipore, Billerica, MA) for 10 minutes. Membranes were washed three times and



incubated with HRP-conjugated secondary antibodies (anti-mouse: 1:10000; anti-human: 1:10000; Sigma-Aldrich, St. Louis, MS) for 10 minutes. Signals were detected by chemiluminescence detection using ECL Western Blotting Substrate reagent (Pierce Biology Protein Products Rockford, IL).

### **Flow cytometry analysis of F and G surface levels in transfected 293T cells**

293T (90% confluent) cells were transfected with plasmids expressing A2 F, A2 G, 2-20 F, or 2-20 G in a pcDNA 3.1 vector and DSP<sub>1-7</sub> as in the dual split protein fusion assay. Cells were incubated for 36 hours at 32°C to limit syncytia formation. Cells were harvested and washed in PBS containing 2% FBS and 0.1% NaN<sub>3</sub>. Cells were stained with Palivizumab or anti-RSV G (131-2G, Millipore) at a concentration of 1:100. Samples were incubated at 4°C in the dark for 2 hours. Cells were then washed in 2 ml PBS containing 2% FBS and 0.1% NaN<sub>3</sub> and centrifuged for 5 minutes at 456 × g. F Samples were stained with anti-human phycoerythrin (PE) (SouthernBiotech, Birmingham, AL) or human IgG1, K isotype control (SouthernBiotech). G samples were stained with anti-mouse APC (G) (RMG1-1, Biolegend, San Diego, CA) or mouse IgG2a, K isotype control (eBM2a, ebioscience, San Diego, CA). Cells were analyzed using an LSR II flow cytometer (BD Biosciences, San Jose, CA). Data were analyzed using Flowjo software (Tree Star Inc., Ashland, OR).

**Neutrophil depletion in BALB/cJ mice**

7- to 8-week-old BALB/cJ mice were depleted with 1 mg anti-Ly6G (1A8, Bio X cell, West Lebanon, NH) intraperitoneally (i.p.) 2 days prior to infection. 0.5 mg anti-Ly6G antibody was given to mice on days 0, 2, 4, and 6 post-infection.

Control mice were treated with rat IgG2a isotype control (2A3, Bio X cell) on days -2, 0, 2, 4, and 6 post-infection.

**Flow cytometric analysis of blood cells**

Blood was collected by submandibular bleed on days 1 and 7 post-infection

Peripheral blood mononuclear cells (PBMC) were isolated using RBC Lysis buffer (0.15 M  $\text{NH}_4\text{Cl}$ , 10 mM  $\text{KHCO}_3$ , and 0.1 mM EDTA) and counted with a

hemocytometer. Cells were stained with anti-CD11b (M1/70, ebioscience) and

anti-Gr-1(RB6-8C5, BD Biosciences). A total of  $5 \times 10^5$  cells were analyzed using

an LSR II flow cytometer (BD Biosciences). The total numbers of neutrophils was

calculated by multiplying the percentage of  $\text{CD11b}^+\text{Gr-1}^+$  by the total cells

isolated. Data were analyzed using FlowJo software (Tree Star Inc).

**Flow cytometric analysis of lung mononuclear cells**

Mice were euthanized with sodium pentobarbital (8.5 mg/kg body weight) i.p.,

and lungs were harvested at 1 and 8 days post-infection Cells were isolated using

Ficoll and counted with a hemocytometer. Cells were stained with the following

antibodies: anti-CD11b and anti-Gr-1 or anti-MHC-II (M5/114.15.2, ebioscience),

anti-CD11b (M1/70, ebioscience), and anti-Gr-1(RB6-8C5, BD). A total of  $5 \times 10^5$

cells were analyzed using a LSR II flow cytometer (BD Biosciences). The total

numbers of neutrophils was calculated by multiplying the percentage of CD11b<sup>+</sup>Gr-1<sup>+</sup> cells or the percentage of MHC-II-CD11b<sup>+</sup>Ly6G<sup>+</sup> cells by the total cells isolated. The total numbers of macrophages was calculated by multiplying the percentage of MHC-II<sup>+</sup>CD11b<sup>+</sup>Ly6G<sup>-</sup> cells by the total cells isolated. Cells were stained using intracellular staining (ICS) for IL-13 and IFN- $\gamma$ . Isolated cells were stimulated with phorbol myristate acetate (PMA)-ionomycin for 5 hours and stained with antibodies to CD3 (145-2C11, BD Biosciences), CD4 (RM4-5, BD Biosciences), CD8 (53-6.7, BD Biosciences), IL-13 (ebio13A, ebioscience), and IFN- $\gamma$  (XMG1.2, ebioscience). The total numbers of IFN- $\gamma$ -expressing CD8<sup>+</sup> T cells and IL-13-expressing CD4<sup>+</sup>T cells in the lungs were determined by multiplying the percentage of lymphocytes (defined by forward and side scatter properties in flow cytometry) that were CD3<sup>+</sup> CD8<sup>+</sup> IFN- $\gamma$ <sup>+</sup> and CD3<sup>+</sup> CD4<sup>+</sup> IL-13<sup>+</sup> by the total number of mononuclear cells isolated. Data were analyzed using FlowJo software (Tree Star Inc).

### **Cytokine quantification**

Cytokines in lung homogenates were analyzed by Luminex bead analysis (Invitrogen) according to the manufacture's protocol. Samples were centrifuged in a tabletop centrifuge at room temperature for 5 seconds, and 50  $\mu$ l of sample were incubated with antibody-coated capture beads for 2 hours at room temperature. After washing the beads three times, protein-specific biotinylated detector antibodies were added and incubated with the beads for 1 hour. After removal of excess biotinylated antibodies, streptavidin conjugated to a fluorescent protein: R-Phycoerythrin (Streptavidin-RPE) was added and

incubated for 30 minutes. After washing of unbound Streptavidin-RPE, the beads were analyzed with the Luminex 200 machine (Austin, TX).

### **Generation of prefusion RSV fusion protein model**

Structural models are based on the recently reported coordinates of the RSV F protein in its prefusion conformation (PDB 4JHW) (23). UCSF chimera (24) and MacPyMol were used for structure analysis and presentation.

### **Statistical analyses**

Unless otherwise indicated, groups were compared by one-way analysis of variance (ANOVA) and Tukey multiple comparison tests ( $P < 0.05$ ). Values below the limit of detection were assigned a value of half the limit of detection, as shown in the figures.

## **RESULTS**

### **RSV A2-2-20F replication in human cells and viral load in BALB/cJ mice**

RSV strain 2-20 infection causes airway mucin expression in BALB/cJ mice (13). The fusion (F) protein of the mucus-inducing RSV strain line 19 was shown to be a factor in airway mucin expression induced by RSV infection in BALB/cJ mice (16). We hypothesized that the 2-20 F protein may similarly be a mucin-inducing factor in RSV infection. We generated a chimeric RSV strain that contains the 2-20 gene in an RSV A2 genetic background. We first compared the *in vitro* growth of RSV A2-2-20F to RSV A2 and RSV 2-20. In HEp-2 cells, RSV A2-2-20F grew

to lower titers ( $P < 0.05$ , ANOVA) compared to its parent strains at 48 hours post-infection, and there were no significant differences between strains at any other time points (Fig. 1A). BALB/cJ mice are semi-permissive for RSV replication. We previously showed that RSV 2-20 exhibits a higher viral load on day 1 post-infection and lower peak viral load than RSV A2 (13). The viral loads of RSV strains A2, 2-20, and A2-2-20F were compared over a time course. BALB/cJ mice were infected with  $10^5$  PFU of each strain. RSV A2-2-20F and 2-20 had significantly higher viral loads compared to A2 on day 1 post-infection, although these titers were near the limit of detection of the plaque assay. RSV A2 had a significantly higher viral load on day 4 and 6 post-infection (Fig. 1B) and A2 grows to higher peak titer *in vivo*. However, early viral load differences may play a role in RSV pathogenesis in BALB/cJ mice. The similar viral loads of 2-20 and A2-2-20F show that the 2-20 F gene is a determinant of the viral load.

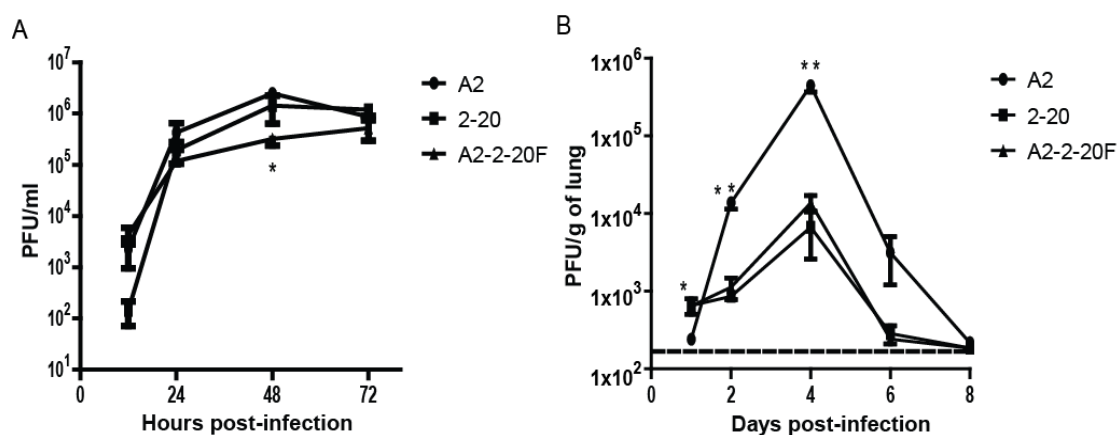


**Figure 1.** *In vitro* growth and *in vivo* viral load of RSV strains A2, 2-20, and A2-2-20F. (A) Infectious yield in supernatants of HEp-2 cells infected at an MOI of 1.0 with RSV A2, 2-20, or A2-2-20F. Error bars represent SEM of two replicates.

Data are means  $\pm$  SEMs. \*, the infectious yield of A2 was significantly higher than A2-2-20F at 48 hours post-infection ( $P < 0.05$ , ANOVA). Results shown represent 3 experiments with similar data. (B) BALB/cJ mice were infected with  $5 \times 10^5$  PFU of A2, 2-20, or A2-2-20F ( $n = 5$ /group). Lungs were harvested at the indicated days post-infection, and infectious RSV was titrated by plaque assay. Data are means  $\pm$  SEMs. \*, at day 1 post-infection values for 2-20 and A2-2-20F were significantly higher than A2 ( $P < 0.05$ , ANOVA); \*\*, at day 4 post-infection the value for A2 was significantly higher than values for 2-20 and A2-2-20F ( $P < 0.05$ , ANOVA); The dashed line represents the limit of detection. The results shown represent those for three experiments with similar data.

### **RSV A2-2-20F causes early lung lesions in BALB/cJ mice**

Lung injury is common in severe RSV infection, shown by loss of lung epithelial cells, edema, hemorrhage, and alveolar inflammation (25). Lung damage is thought to be mediated by both direct effects of the virus as well as the immune response (26). We previously reported that RSV 2-20 infects the airway epithelium at 1 day post-infection in mice (13). We sought to determine if early viral load correlates with early lung lesion development in RSV A2-2-20F infected mice. At day 1 post-infection, mice infected with RSV A2-2-20F exhibited increased interstitial pneumonia involving increased thickening of alveolar walls associated with inflammatory cell infiltrates, compared to mock-infected and RSV A2-infected mice (Fig. 2A, 2B). RSV 2-20-infected mice also had significantly more interstitial pneumonia than mock-infected mice (Fig. 2A, 2B). There was no difference in the interstitial pneumonia scores between groups

on d 4, 6, or 8 post-infection (data not shown). The airways of RSV 2-20 and A2-2-20F-infected mice contained more necrotic cell debris than mock- and A2-infected mice on d 1 post-infection (Fig. 2C). One of ten mock-infected and 1 of 10 A2-infected mice exhibited airway necrotic cell debris. In contrast, necrotic cell debris was observed in 6 of 10 mice infected with RSV 2-20 and 8 of 10 mice infected with RSV A2-2-20F. Epithelial cell debris and bronchoalveolar lavage cells in the airways of infected mice reportedly contribute to the pathogenesis of RSV [23]. Our data show that A2-2-20F infected mice exhibit lung epithelial damage and inflammation on day 1 post-infection.

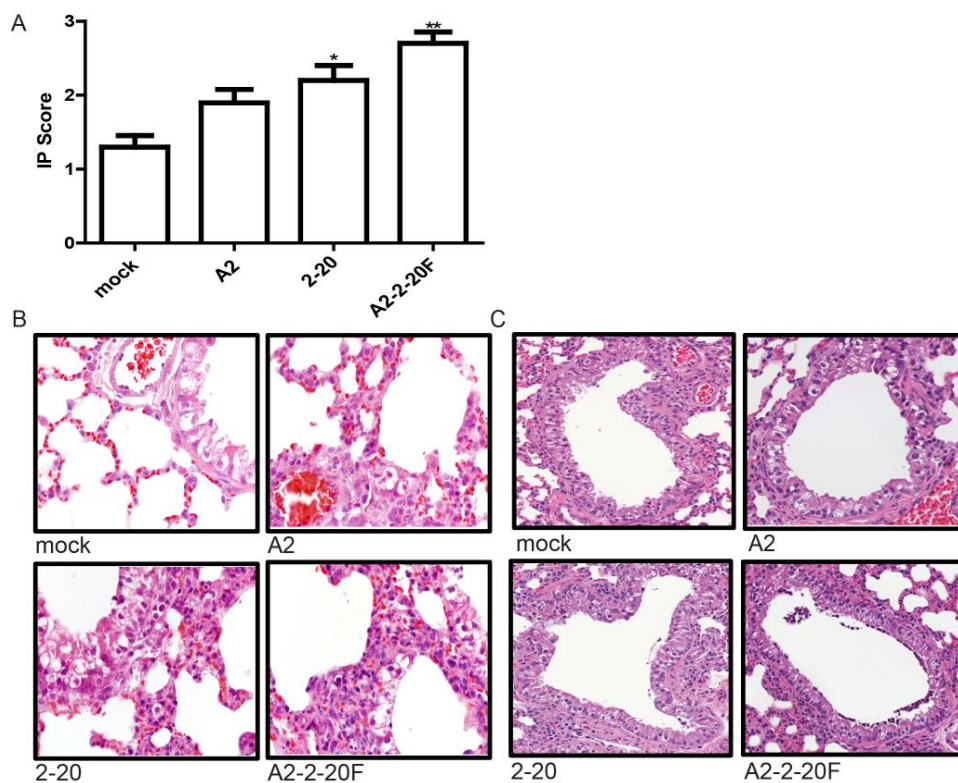


**Figure 2.** RSV A2-2-20F infection resulted in early lung lesions in BALB/cJ mice. BALB/cJ mice were mock infected or infected with  $10^5$  PFU of the indicated strain. Lungs were harvested day 1 post-infection, stained with H&E, and

analyzed for histologic changes. (A) Interstitial pneumonia (IP) score for each group. \* represents significant difference from mock ( $P < 0.01$ , ANOVA), \*\* indicates significant difference from mock and A2 ( $P < 0.05$ , ANOVA) (B) Representative airways indicating IP in mock-, A2-, 2-20-, and A2-2-20F-infected mice. (C) Representative airways containing cell debris in mock-, A2-, 2-20-, and A2-2-20F-infected mice. The results shown represent those from two experiments with similar data.

### **RSV A2-2-20F infection causes airway mucin expression**

Pulmonary mucus expression is a hallmark of severe RSV disease in infants (27). RSV 2-20 infection of BALB/cJ mice triggers higher airway mucin expression than infection with RSV A2 (13). We used the chimeric virus RSV A2-2-20F to determine whether the 2-20 F protein is responsible for this phenotype. Periodic acid-Schiff (PAS) staining was used to examine mucin distribution in the airways of RSV-infected mice. Mice were infected with  $10^5$  PFU of RSV and lungs were harvested day 8 post-infection. Both 2-20 and A2-2-20F-infected mice exhibited significantly greater PAS positivity than mock and A2-infected mice (Fig. 3). Greater than 5% of the airways in 2-20 and A2-2-20F-infected mice had approximately 10% mucin positivity compared to approximately 1% of airways in A2-infected mice (Fig. 3). These results show that 2-20 and A2-2-20F infection both result in more airway mucin expression in the airways of BALB/cJ mice than A2 infection, suggesting the 2-20 F protein as a mucus-inducing factor in RSV infection.



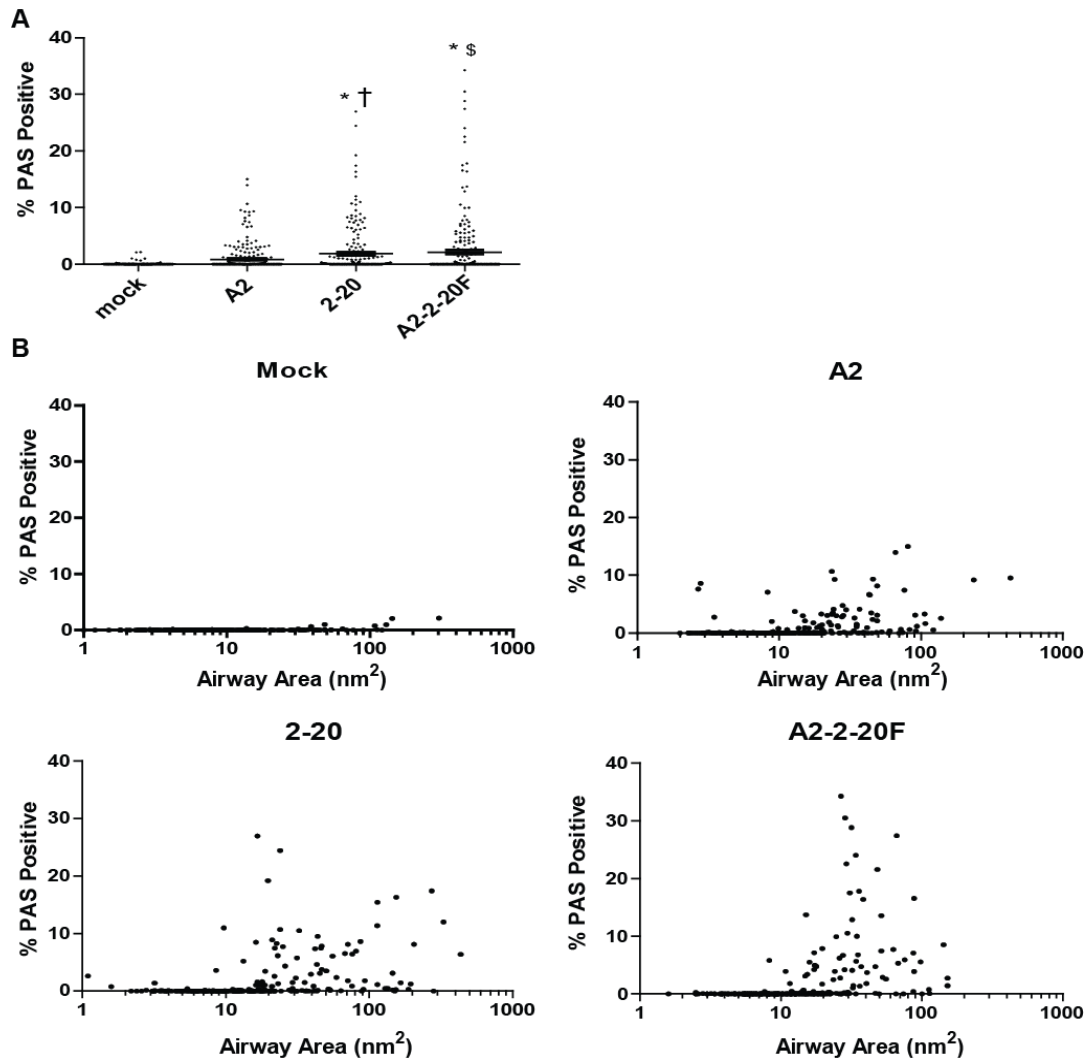


**Figure 3.** 2-20 F is a mucogenic factor in RSV infection. BALB/cJ mice were mock infected ( $n = 3$ ) or infected with  $10^5$  PFU of A2 ( $n = 5$ ), 2-20 ( $n = 5$ ), or A2-2-20F ( $n = 5$ ), and lungs were harvested day 8 post-infection. The PAS positive area was determined for each airway. (A)  $>200$  individual airways are shown per group. Each symbol represents one airway. †, significant difference compared to mock and ( $P < 0.001$ ) \*, significant difference compared to A2 ( $P < 0.05$ , ANOVA). \$, significant difference compared to A2 ( $P < 0.001$ , ANOVA). (B) The same percent PAS data as in panel A plotted against the size of all airways. The results are representative of those from two experiments with similar results.

### **Fusion activity**

We sought to determine the underlying mechanisms of 2-20 F protein-mediated pathogenesis. We hypothesized that 2-20 F protein has greater fusion activity than A2 F protein. To quantify cell-to-cell fusion, we used a bioluminescence reporter-based content mixing assay (20). 293T cells were transfected with A2 F, 2-20 F, A2 F+A2 G, 2-20 F+2-20 G, or 2-20 F+ A2 G and DSP<sub>1-7</sub> and mixed with 293T cells transfected with DSP<sub>8-11</sub>. An RSV fusion inhibitor, BMS-433771 was used during transfection to eliminate effector-to-effector cell fusion. This inhibitor was removed prior to cell mixing to allow for effector-to-target cell fusion. Transfected cells expressed total cell (Fig. 4A and 4B) and surface (Fig. 4C and 4D) levels of F and G proteins equivalently. Contrary to our hypothesis, A2 F and 2-20 F had equal fusion activity (Fig. 4E and 4F). It has been shown that coexpression of the RSV attachment (G) glycoprotein promotes fusion (28). We therefore also tested whether RSV A2 G and/or 2-20 G can enhance fusion. Both G proteins increased the fusion activity of 2-20 F, but not that of A2 F. RSV F and G glycoproteins interact to form a complex on the surface of infected cells, suggesting that G plays a role in RSV fusion (29). We identified a specific, functional interaction between 2-20 F and RSV G.

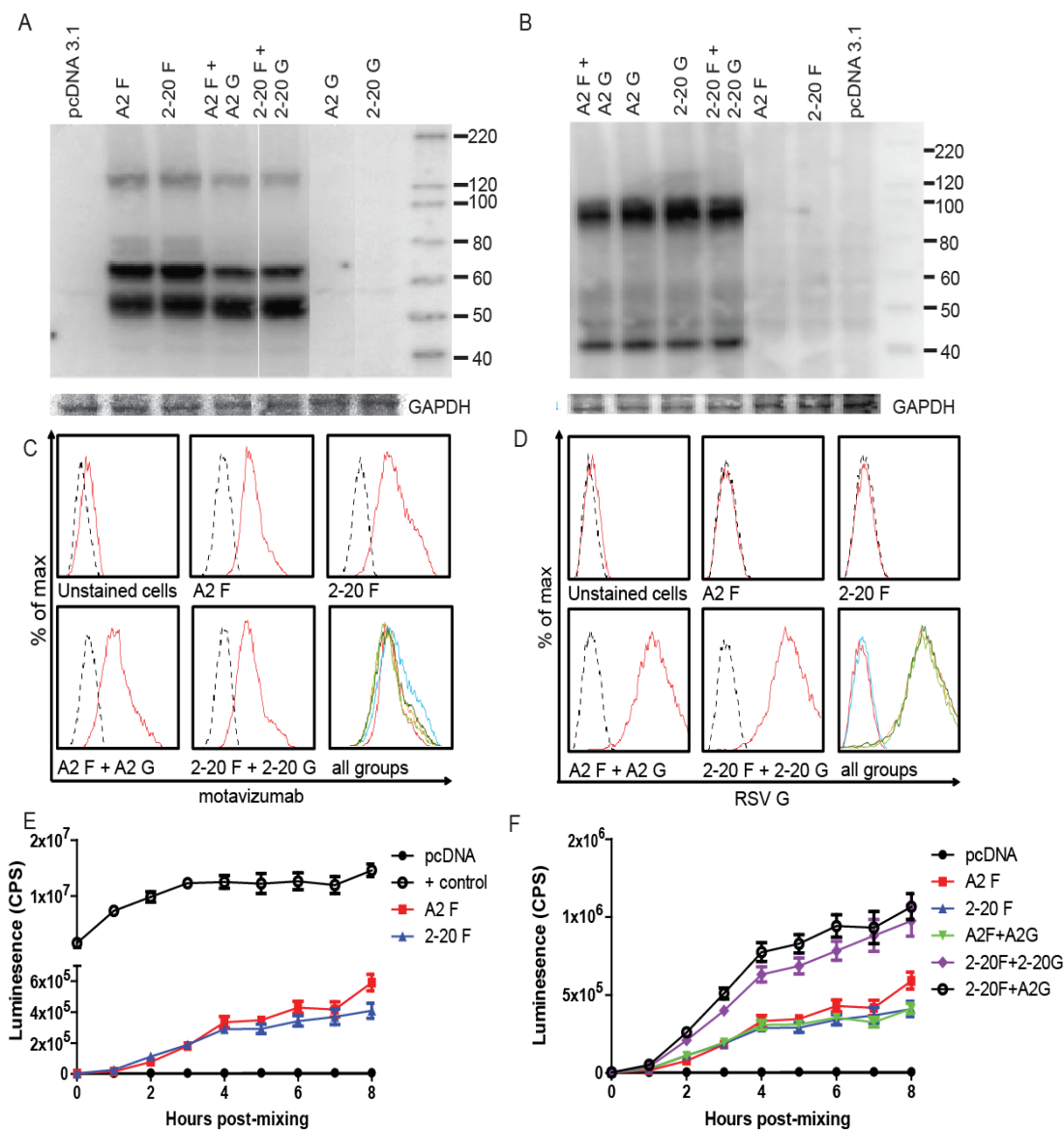


**Figure 4.** 2-20 F is more fusogenic than A2 F when co-expressed with RSV G protein. (A and B) Total cell steady state levels of RSV F (A) and RSV G (B) proteins expressed in 293T cells after transfection. Blots were probed with Palivizumab and HRP-conjugated anti-human secondary or anti-RSV G and HRP-conjugated anti-mouse secondary. Representative of 3 experiments. (C and D) Transfected cells were stained with Palivizumab and anti-human PE or anti-RSV G and anti-mouse APC to quantify F (C) and G (D) surface levels. Dashed lines,

isotype control-stained samples. Representative of 3 experiments. (E) and (F) DSP-expressing cells transfected with A2 F, 2-20 F, A2 F+A2 G, 2-20 F+2-20 G or 2-20 F+A2 G were mixed in equal amounts. Luciferase activity was measured at indicated time points. The results are representative of those from three experiments (4 to 5 wells per group) with similar results.

### **RSV A2-2-20F infection results in lung neutrophil recruitment in BALB/cJ mice**

Neutrophils are present in the lungs of children infected with severe RSV (9, 30). Additionally, neutrophils are among the first cells to be recruited to the site of infection and have been shown to contribute to cell damage (11, 31). H&E staining revealed neutrophil infiltration in the lungs of A2-2-20F-infected mice (data not shown). We used flow cytometry to determine neutrophil levels in the lungs of infected BALB/cJ mice on d 1 post-infection and found significantly higher levels in the lungs of A2-2-20F-infected BALB/cJ mice than in mock and A2-infected mice (Fig. 5). Thus, the 2-20 F protein contributes to pulmonary neutrophil recruitment. 2-20-infected mice show an intermediate phenotype higher than A2-infected mice but slightly less than A2-2-20F-infected mice (Fig. 5). There are many sequence differences between the 2-20 and A2 genomes (GenBank accession numbers M74568 and JX069798, respectively), but the A2-2-20F recombinant narrows the candidate pool to residues within the F protein. A2-2-20F permits the analysis of the 2-20 F protein specifically.

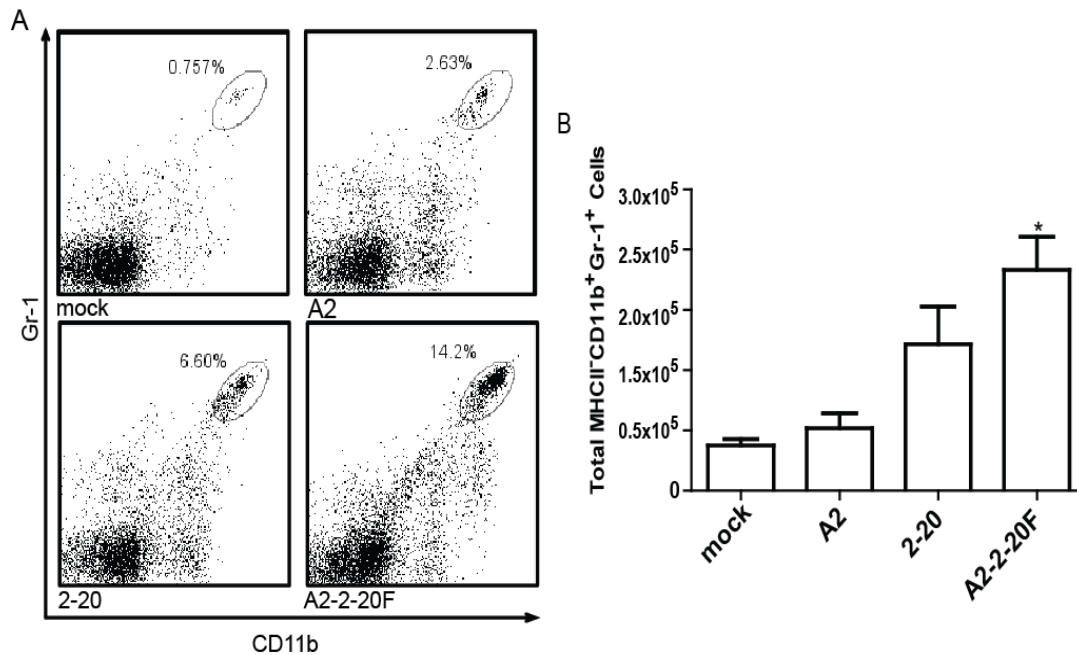


**Figure 5.** A2-2-20F causes neutrophil infiltration in the lungs of BALB/cJ mice. Mice were mock-infected or infected with the indicated RSV strain. Lungs were harvested d 1 post-infection and cells were isolated and stained for CD11b and Gr-1. (A) Representative flow plots from the indicated group. (B) Quantification from three replicates. \*, significant differences from mock and A2 ( $P < 0.05$ , ANOVA).

### Neutrophil depletion in RSV-infected BALB/cJ mice

Monoclonal antibody anti-Ly6G clone 1A8 has been shown to be specific for neutrophils (32). BALB/cJ mice were treated with anti-Ly6G in order to investigate the role of neutrophils in the context of RSV-induced airway mucin expression. Lung and peripheral blood mononuclear cells were isolated from mock and RSV-infected mice that were treated with anti-Ly6G or IgG2a isotype control antibody. Administration of this anti-Ly6G the context of RSV infection resulted in depletion of neutrophils for the duration of infection in both the blood

and lungs of BALB/cJ mice (Fig. 6). Mock-infected mice had greater numbers of neutrophils in the lung on day 1 than day 7 post-infection, indicating that the mock preparation does induce an early neutrophil response in the lung (Fig. 6G and 6H). The macrophage population in anti-Ly6G-treated mice was also investigated. Levels of MHCII<sup>+</sup>Gr-1<sup>+</sup>CD11b<sup>+</sup> cells were not significantly affected by antibody treatment (Fig. 7). Eosinophils do not express Ly6G and therefore are not affected by 1A8 antibody treatment (32).

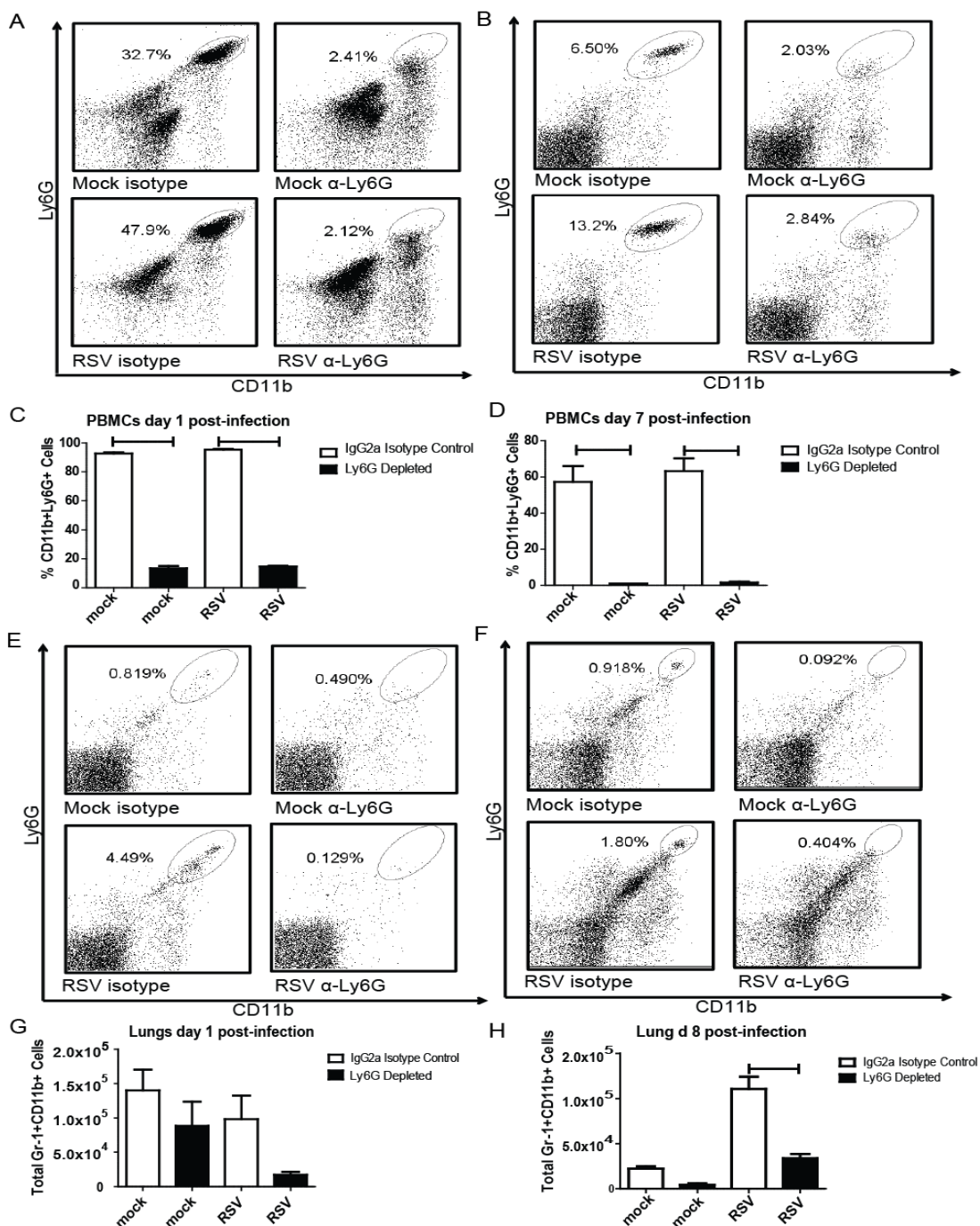


**Figure 6.** Anti-Ly6G treatment results in depletion of neutrophils in the blood and lungs of RSV-infected mice. BALB/cJ mice were treated with Ig2a control antibody or anti-Ly6G antibody. These mice were mock infected or infected with  $1 \times 10^6$  PFU RSV 2-20. Blood was taken at days 1 and 7 post-infection Lungs were

harvested on days 1 and 8 post-infection. Cells were isolated via ficol gradient and stained for CD11b and Gr-1. (A) Representative flow plots of PBMCs indicated group on day 1 post-infection (B) Representative flow plots of PBMCs from indicated groups on day 7 post-infection (C) Quantification of PBMCs on day 1. Results are representative of those from three replicate experiments. (D) Quantification of PBMCs on day 7. Results are representative of those from three replicate experiments. (E) Representative flow plots of lung cells from indicated group on day 1 post-infection. (F) Representative flow plots of lung cells from indicated group on day 8 post-infection (G) Quantification of lung cells on day 1. Results are representative of those from three replicate experiments. (H) Quantification of lung cells on day 8. Results are representative of those from three replicate experiments. Bars, significant differences ( $P < 0.05$ , ANOVA).

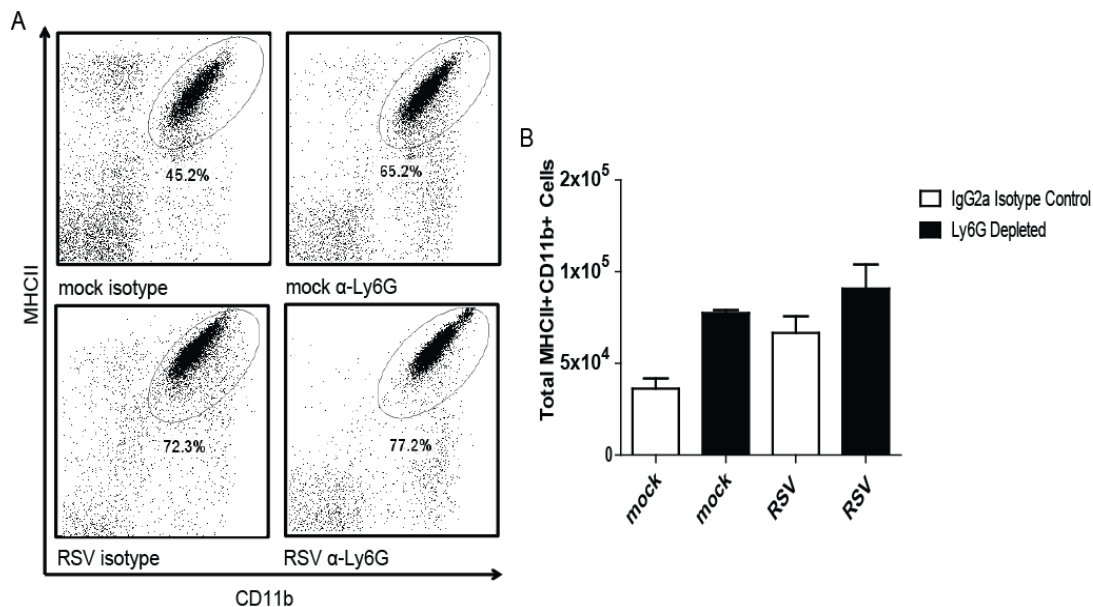


**Figure 7.** 1A8 administration does not affect macrophage numbers in mock- or RSV-infected mice. BALB/cJ mice were treated with IgG2a isotype control



antibody or anti-Ly6G antibody. These mice were mock infected ( $n = 3$  or  $5$  per group) or infected with  $1 \times 10^6$  PFU of 2-20 ( $n = 3$  or  $5$ ). Lungs were harvested at day 6 post-infection. Cells were isolated via ficol gradient and stained for MHC-II and CD11b. Data were analyzed using Flowjo software. (A) Representative flow plots gated for MHC-II+CD11b+ cells; (B) quantification of three replicates.

To assess the contribution of neutrophils to RSV clearance, we examined viral load in neutrophil-depleted and isotype-control treated BALB/cJ mice. Though neutrophil-depleted mice had a slightly higher viral load on days 4, 6, and 8 post-infection, this difference never reached significance (Fig. 8). These results show that neutrophils do not contribute to viral clearance in this RSV infection model.

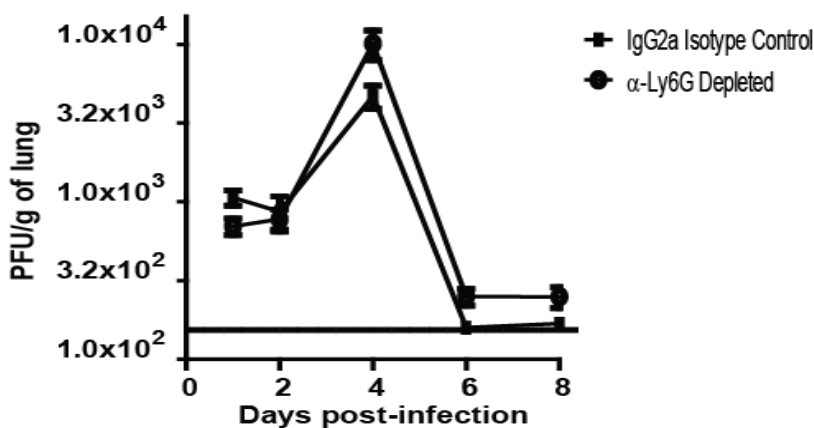


**Figure 8.** Viral load after neutrophil depletion. BALB/cJ mice were treated with IgG2a isotype control antibody or anti-Ly6G antibody. BALB/cJ mice were mock infected ( $n = 5$ ) or infected with  $1 \times 10^6$  PFU of 2-20 ( $n = 5$ ). Lungs were harvested at the indicated days and infectious RSV was titrated by an immunodetection plaque assay. The solid line represents the limit of detection. Data represent the results of three replicate experiments.

## Neutrophil depletion during RSV infection modulates airway mucin expression

Neutrophils have been shown to be associated with lung mucus in models such as COPD and asthma (23, 24). We hypothesized that neutrophils also modulate mucin expression in the lungs of RSV-infected mice. To examine this, lungs were harvested on d 8 post-infection from mock- or RSV-infected mice treated with anti-Ly6G or isotype-control, and stained with PAS. Neutrophil depletion in RSV-infected mice resulted in significantly more PAS-positive airways compared to RSV-infected isotype-control treated mice (Fig. 9). These data indicate that neutrophils play a role in airway mucin expression during pathogenic RSV 2-20 infection.

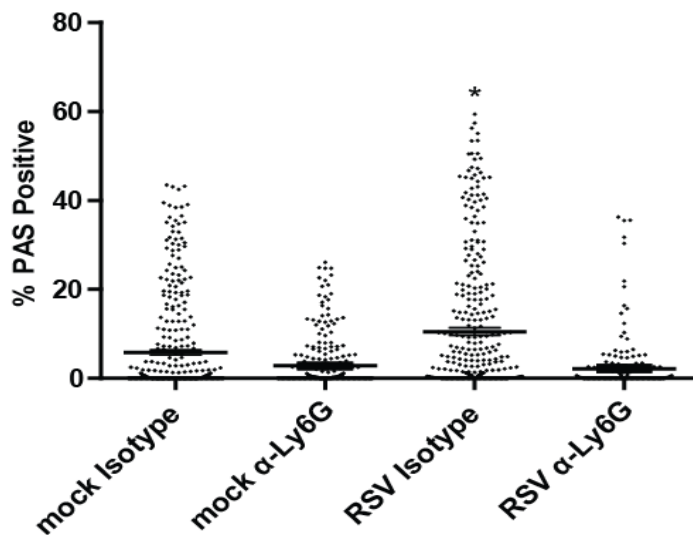


**Figure 9.** Neutrophil depletion decreased mucin production. BALB/c mice were treated with IgG2a isotype control antibody or anti-Ly6G antibody. These mice were mock infected ( $n = 5$  per group) or infected with  $1 \times 10^6$  PFU of 2-20 ( $n = 5$ ). Lungs were harvested at 8 days post-infection and processed for PAS staining. Data show the percentage of area that was PAS positive for each airway was

determined; >200 individual airways are shown per group. Each symbol represents one airway. \*, significant differences other groups ( $P < 0.05$ , ANOVA). Data represent those from two replicate experiments.

### Neutrophil depletion in the setting of RSV infection decreases lung TNF- $\alpha$ levels

TNF- $\alpha$  is a cytokine that has been linked to mucus production. Intratracheal administration of TNF- $\alpha$  to BALB/cJ mice was shown to induce mucus production (12). Because activated neutrophils release TNF- $\alpha$ , we postulated that depletion of neutrophils would result in less TNF- $\alpha$  in the lungs (33). Indeed, RSV-infected mice treated with anti-Ly6G antibody had significantly decreased TNF- $\alpha$  levels in the lungs on day 1 post-infection (Fig. 10). This decrease coincides with a decrease in neutrophil levels in the lungs due to antibody depletion.

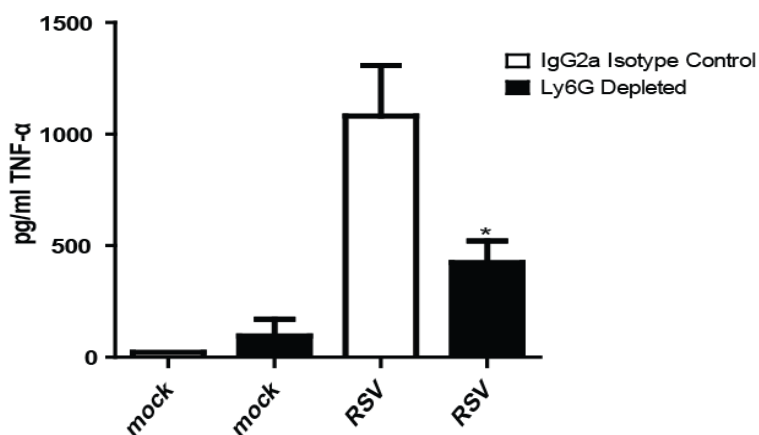


**Figure 10.** Neutrophil depletion results in decreased TNF- $\alpha$  levels during RSV infection. BALB/c mice were treated with IgG2a isotype control antibody or anti-Ly6G antibody. These mice were mock-infected ( $n = 5$ ) or infected with  $1 \times 10^6$

PFU of 2-20 (n = 5). Lungs were harvested day 1 post-infection to measure TNF- $\alpha$  levels. \*, significant differences compared to RSV-infected isotype-control antibody-treated mice ( $P < 0.001$ , ANOVA). Data represent those from four replicate experiments.

### **Neutrophil depletion during RSV infection results in less pulmonary IL-13<sup>+</sup> CD4 T cells compared to control mice**

IL-13 is a key factor that mediates mucus production in the lungs (15, 34, 35). This cytokine is necessary for both RSV line 19- and 2-20-induced PAS-positivity (13, 16). We previously showed that RSV 2-20 results in greater IL-13 production compared to RSV A2 (13). Here, we sought to determine a cell source of IL-13 in the RSV infection model and define the effect of neutrophil depletion on IL-13 production. IL-13 producing CD4 T cells were quantified on day 6 post-infection. Neutrophil depletion did not affect the number of lung CD4<sup>+</sup> T cells or CD8<sup>+</sup> T cells (data not shown) but resulted in fewer IL-13<sup>+</sup> CD4 T cells compared to isotype-treated mice (Fig. 11). These CD4<sup>+</sup> T cells are likely an important source of IL-13 that causes mucin expression during RSV infection. Our data show that neutrophils modulate CD4 T cell IL-13 expression in RSV infection.

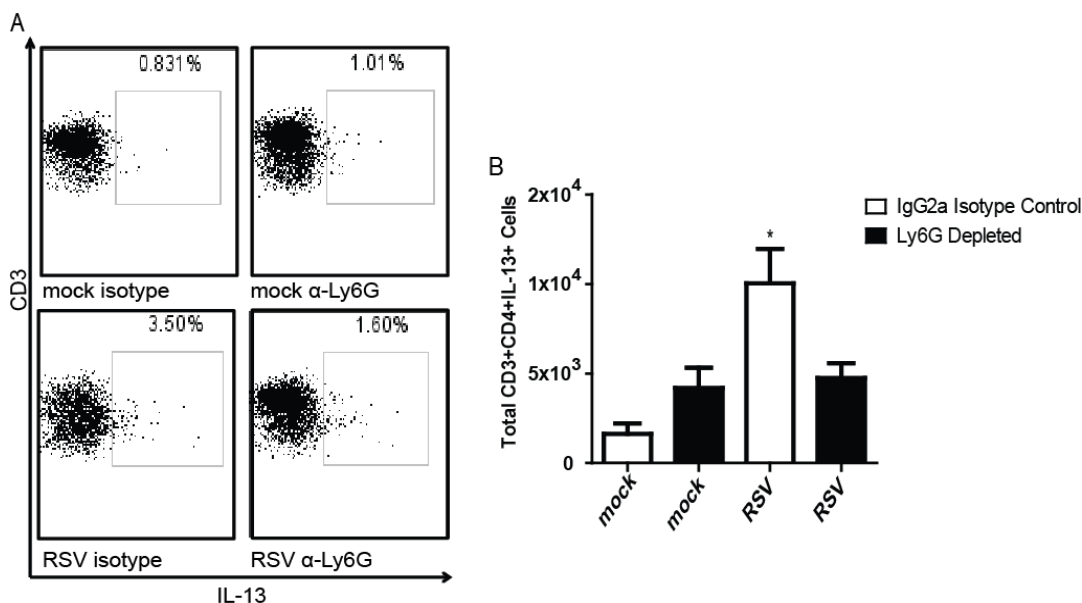


**Figure 11.** Neutrophil depletion reduces IL-13 producing CD4<sup>+</sup> T cells in lungs of RSV-infected BALB/cJ mice. BALB/cJ mice were injected i.p. with anti-Ly6G antibody or an IgG2a isotype control. These mice were mock infected (n = 3) or infected with  $1 \times 10^6$  PFU RSV 2-20 (n = 3). Lungs were harvested on day 6 post-infection and cells were isolated and stained for CD3, CD4, and IL-13. (A) Representative flow plots gated for CD3<sup>+</sup>CD4<sup>+</sup>IL-13<sup>+</sup> cells; (B) results for three experiments are combined.

## DISCUSSION

Using a genetically-controlled chimeric virus approach, we have shown that the F protein of RSV 2-20 increases pathogenicity of the laboratory strain A2, as evidenced by greater interstitial pneumonia, increased mucin levels, and more necrotic cell debris in the airways. Increased early viral load correlated with airway necrotic cell debris. Additionally, infection with RSV A2-2-20F resulted in greater neutrophil infiltration into the lungs of BALB/cJ mice compared to mock

and A2 infection. Our data show that neutrophils play an important immunomodulatory role in RSV infection. Depletion of neutrophils had no effect on viral load but resulted in less airway mucin expression, lung TNF- $\alpha$  and fewer IL-13-producing CD4<sup>+</sup> T cells compared to isotype-control antibody treated animals during RSV infection. Therefore, neutrophils contribute to pulmonary mucus expression and RSV pathogenesis, potentially through modulation of TNF- $\alpha$  expression and IL-13-expressing CD4<sup>+</sup> T cells.

It was previously shown that the fusion protein of RSV strain line 19 is a factor that plays a role in pulmonary mucin expression in the setting of RSV infection (16). BALB/cJ mouse infection with chimeric A2-line19F resulted in a higher peak viral load than the parent viruses A2 and line 19 (16). The unique amino acids in RSV line 19 F, however, are not found in any clinical isolates of RSV (A.L. Hotard and M.L. Moore, unpublished). The passage history of the Line 19 strain is unclear and included many passages through human embryonic diploid lung (MRC-5) cells (36). On the other hand, 2-20 is a clinical isolate with a defined low number of passages (13). Unlike A2-line19F, A2-2-20F had a viral load pattern similar to that of parent virus 2-20. This suggests that although infection of BALB/cJ mice with line 19 and 2-20 both induces pulmonary mucin expression, the underlying mechanisms leading to its phenotype are distinct. Our data show that both 2-20 and A2-2-20F infection results in early (day 1) lung debris in the airway epithelium of BALB/cJ mice. We hypothesize that this early damage affects the subsequent immune response and results in mucus production. We previously showed that RSV 2-20 viral antigen is detectable in the airway

epithelium on d 1 post-infection (13) while viral antigen at 4 days post-infection is localized to the alveoli region (37). Our data are consistent with a model in which 2-20 F renders the mouse airway epithelium susceptible to infection. Infection of the airway epithelium results in necrosis, neutrophil recruitment, and subsequent mucin expression.

Although RSV F can trigger fusion without G, its cognate attachment protein, our data suggest that G and F interaction promotes fusion. Activation of most *Paramyxovirinae* subfamily F proteins involves interaction with the attachment protein (38). In an *in vitro* fusion assay, 2-20 F was more fusogenic than A2 F when it was co-expressed with either A2 G or homotypic 2-20 G protein. These data suggest that RSV G boosts 2-20 F fusion activity, but the precise mechanism is unknown. The F and G proteins likely interact to form a complex on the surface of infected cells (29). Hydrophobic residues located in the lower half of the head of the measles (MeV) F protein were shown to be important for fusion and interactions with the MeV attachment protein (39). We hypothesize that this increased fusion activity due to 2-20 F affects subsequent RSV pathogenesis. In previous studies, infection of both primary and immortalized human airway epithelial cells did not result in obvious syncytia formation (40, 41). Cell-to-cell fusion, however, was observed in recent studies performed in well-differentiated pediatric bronchial epithelial cells (WD-PECs) cultured at an air-liquid interface (42). Interestingly, more syncytia were observed in WD-PECs infected with a RSV clinical isolate than with RSV A2 strain (42). Cell-to-cell fusion was also seen in WD-PECs after infection with Sendai virus (SeV) (43). It has been shown that

specific residues in the fusion protein of SeV modulate its virulence by influencing both the spread of the virus and severity of inflammation (44).

There are 15 amino acid differences between the structures of RSV A2 and 2-20 fusion proteins (Fig. 12). Residues 4, 8, 16, 20, and 25 are not present in the protein because they are part of the signal peptide that directs the FO precursor to the ER. Residue 124 is present in the short 26 residue peptide between furin cleavage sites. Of the remaining residues, mutations at positions 519 and 524 are in immediate proximity to the membrane and may influence interaction with lipids, which reportedly affects bioactivity of viral fusion proteins (45). For instance, a membrane proximal glycine residue of the influenza HA2 fusion protein is required for viral fusion and infectivity (46). Residue 384 (Fig. 12) lies in a region where the head and stalk domains come together, which was previously shown to be a determinant for prefusion MeV F protein stability and fusion activity (47). When all other residues were highlighted in a structural model of the RSV F protein in its prefusion conformation, we noted a concentration of changes in a microdomain mapping closely to the top of the prefusion F trimer (residues 63, 66, and 76). These residues may contribute to metastability (48). In future studies, we will explore whether residues contribute to controlling the thermodynamic stability of the prefusion RSV F trimer and/or affect its interaction with the RSV G protein.



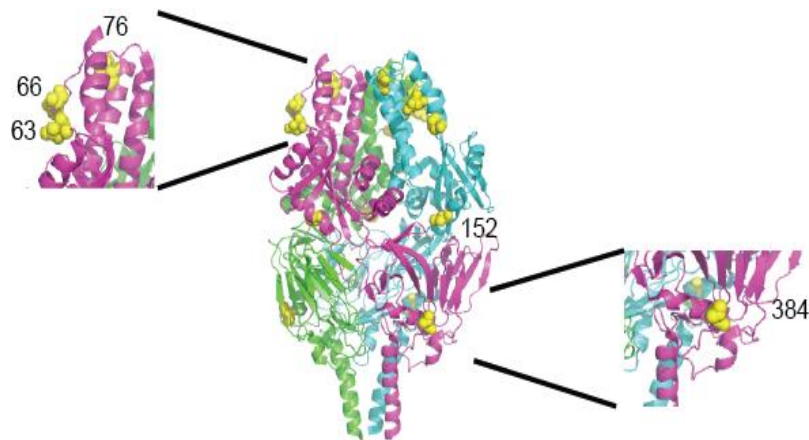


**Figure 12.** Side-view ribbon representation of the prefusion RSV F protein trimer (PDB 4JHW), colored by monomer. Yellow spheres highlight sequence differences between RSV strains A2 and 2-20 in one monomer. Inserts provide a close-up view of two areas with differing residues; a first set maps towards the top of the prefusion F structure (residues 63, 66, and 76), and residues 384 towards the lateral face of prefusion F. Residue 152 is also labeled

The relationship between viral load and disease in RSV pathogenesis is not defined. A previous study indicated that higher viral loads in infants are a predictor of greater disease severity (48, 49). Other studies, however, have shown no correlation between viral titers and disease severity (50, 51). In the mouse model of 2-20 and A2-2-20F, pathogenesis correlated with early viral load and not peak viral load. The cell tropism of clinical RSV strains may play a role in their differential pathogenesis. RSV has been shown to infect cells in both the bronchial and bronchiolar epithelium as well as alveolar cells in the lungs of RSV-infected children and mice (52, 53). RSV 2-20 viral antigen is localized to the airway epithelium at greater levels compared to A2 antigen day 1 post-infection

(13). A2 infection also resulted in less necrotic cell debris and lower viral load at this early time point. Peak viral load, although correlated with disease severity in some cases, may not be the most important factor in RSV airway pathogenesis. Early viral load may be responsible for driving disease that is not dependent on later peak viral loads (54). We hypothesize that RSV viral load localized to the airways, rather than peak viral load per se, drives airway pathogenesis. We speculate that elevated fusion activity may permit infection of the mouse airway epithelium. Host entry factors specific for airway and alveolar cells may impact airway penetration as well. RSV F has been shown to interact with nucleolin (55). However, we have not identified factors that specifically interact with 2-20 F in a cell type-dependent manner.

Previous studies reveal that neutrophils are prevalent bronchial infiltrates in human RSV infection (7, 9, 30). The neutrophil response occurs prior to the RSV-induced CD8<sup>+</sup> T cell response in infants (56). Depletion of neutrophils during influenza virus infection in mice results in higher virus titers in the lung and elevated mortality (57, 58). In the present study, however, neutrophil depletion did not affect viral load in RSV-infected mice. CD8<sup>+</sup> T cells have been shown to be important for RSV clearance in mice (59). We did not see any differences in CD8<sup>+</sup> T cell numbers in neutrophil-depleted mice (data not shown) but found that neutrophils affect the CD4<sup>+</sup> T cells IL-13 expression and TNF- $\alpha$  expression. Neutrophils have been linked to mucus plugging in severe RSV infection and asthma (6, 8, 23). Previous studies show that dysregulated or excessive neutrophil responses in the airways may contribute to disease during severe

influenza infections (60). Low, intermediate, or high virulence influenza strains differ in their ability to recruit neutrophils to airways. In severe influenza infection, neutrophils had a beneficial role in ultimately limiting disease (61). Neutrophils may be playing a similar damaging role in RSV infection. In lung bacterial infections, bacteria induce neutrophil sequestration and eventual damage (62). When neutrophils were depleted in BALB/cJ mice during RSV infection, we found few mucin positive cells in the airways. TNF- $\alpha$  expression was higher in RSV-infected, neutrophil-depleted mice compared to non-depleted, infected mice. Neutrophils are a source of TNF- $\alpha$  in the lungs (63), which in turn facilitates the recruitment of neutrophils during airway inflammation and has been implicated in stimulation of mucus factor MUC5AC expression (14, 64).

Increased concentrations of TNF- $\alpha$  and IL-13 have been measured in the BAL fluid of asthmatic patients following allergen stimulation (65). In a model of allergic asthma, IL-13 instillation results in TNF- $\alpha$  expression by neutrophils (66) and is necessary for mucus production (67). It has been shown that RSV infection promotes a T<sub>h</sub>2-type inflammatory response in the lung, subsequently inducing T<sub>h</sub>2-like effector phenotype in T<sub>reg</sub> cells and increasing susceptibility to asthma (68). BALB/cJ mouse infection with mucus-inducing strains RSV line 19 and 2-20 results in lung IL-13 expression (13, 14, 16). Neutrophils are seen in BAL samples from severe asthmatics but not from mild or moderate asthmatics (69). In a model of allergic asthma, IL-13 was shown to activate neutrophils (66, 70). It was also found that IL-13 administration induced substantial airway neutrophilia (71). In neutrophil-depleted, RSV-infected BALB/cJ mice, there was a drop in IL-

13<sup>+</sup> CD4 T cells compared to isotype-treated, RSV-infected mice. These results indicate that although IL-13 has been shown to act on neutrophils, neutrophils also modulate the IL-13 cellular immune response. Further elucidation of this pathway involving IL-13 and TNF- $\alpha$  may lead to therapies to combat RSV-infection-induced pulmonary mucus.

Neutrophils have long been associated with bronchiolitis. For the first time, we analyzed the role of neutrophils in a mouse model of RSV bronchiolitis. We have identified a novel pathway wherein the F protein affects the early immune response to RSV, including the neutrophil response, and subsequently influences downstream cytokine and mucus expression. Our data suggest that early viral load and damage influenced by the activity of the RSV F protein are related to the neutrophil and mucus responses.

#### **ACKNOWLEDGMENTS**

This work was supported by the following grants: NIH 1R01AI087798 and NIH 1U19AI095227. We thank the Emory Children's Pediatric Research Center flow cytometry core and immunology core, which are supported by Children's Healthcare of Atlanta (CHOA). We thank Naoyuki Kondo and Zene Matsuda for the DSP<sub>1-7</sub> and DSP<sub>8-11</sub> plasmids and Ursula Buchholz and Karl-Klaus Conzelmann for the BSR-T7/5 cells. We thank James Crowe, Jr. for Palivizumab. We also would like to thank Carla Shoffeitt for histology technical assistance.

## REFERENCES

1. **Leader, S., and K. Kohlhase.** 2003. Recent trends in severe respiratory syncytial virus (RSV) among US infants, 1997 to 2000. *J Pediatr* **143**:S127-132.
2. **Shay, D. K., R. C. Holman, R. D. Newman, L. L. Liu, J. W. Stout, and L. J. Anderson.** 1999. Bronchiolitis-associated hospitalizations among US children, 1980-1996. *JAMA* **282**:1440-1446.
3. **Thompson, W. W., D. K. Shay, E. Weintraub, L. Brammer, N. Cox, L. J. Anderson, and K. Fukuda.** 2003. Mortality associated with influenza and respiratory syncytial virus in the United States. *JAMA* **289**:179-186.
4. **Nakanishi, A., S. Morita, H. Iwashita, Y. Sagiya, Y. Ashida, H. Shirafuji, Y. Fujisawa, O. Nishimura, and M. Fujino.** 2001. Role of gob-5 in mucus overproduction and airway hyperresponsiveness in asthma. *Proc Natl Acad Sci U S A* **98**:5175-5180.
5. **Aherne, W., T. Bird, S. D. Court, P. S. Gardner, and J. McQuillin.** 1970. Pathological changes in virus infections of the lower respiratory tract in children. *J Clin Pathol* **23**:7-18.
6. **Bataki, E. L., G. S. Evans, and M. L. Everard.** 2005. Respiratory syncytial virus and neutrophil activation. *Clin Exp Immunol* **140**:470-477.
7. **Everard, M. L., A. Swarbrick, M. Wraitham, J. McIntyre, C. Dunkley, P. D. James, H. F. Sewell, and A. D. Milner.** 1994.

- Analysis of cells obtained by bronchial lavage of infants with respiratory syncytial virus infection. *Arch Dis Child* **71**:428-432.
8. **McNamara, P. S., B. F. Flanagan, L. M. Baldwin, P. Newland, C. A. Hart, and R. L. Smyth.** 2004. Interleukin 9 production in the lungs of infants with severe respiratory syncytial virus bronchiolitis. *Lancet* **363**:1031-1037.
  9. **Smith, P. K., S. Z. Wang, K. D. Dowling, and K. D. Forsyth.** 2001. Leucocyte populations in respiratory syncytial virus-induced bronchiolitis. *J Paediatr Child Health* **37**:146-151.
  10. **Miyamoto, M., O. Prause, M. Sjostrand, M. Laan, J. Lotvall, and A. Linden.** 2003. Endogenous IL-17 as a mediator of neutrophil recruitment caused by endotoxin exposure in mouse airways. *J Immunol* **170**:4665-4672.
  11. **Wang, S. Z., P. K. Smith, M. Lovejoy, J. J. Bowden, J. H. Alpers, and K. D. Forsyth.** 1998. The apoptosis of neutrophils is accelerated in respiratory syncytial virus (RSV)-induced bronchiolitis. *Clin Exp Immunol* **114**:49-54.
  12. **Busse, P. J., T. F. Zhang, K. Srivastava, B. P. Lin, B. Schofield, S. C. Sealfon, and X. M. Li.** 2005. Chronic exposure to TNF-alpha increases airway mucus gene expression in vivo. *J Allergy Clin Immunol* **116**:1256-1263.
  13. **Stokes, K. L., M. H. Chi, K. Sakamoto, D. C. Newcomb, M. G. Currier, M. M. Huckabee, S. Lee, K. Goleniewska, C. Pretto, J. V. Williams, A. Hotard, T. P. Sherrill, R. S. Peebles, Jr., and M. L.**

- Moore.** 2011. Differential pathogenesis of respiratory syncytial virus clinical isolates in BALB/c mice. *J Virol* **85**:5782-5793.
14. **Lukacs, N. W., R. M. Strieter, S. W. Chensue, M. Widmer, and S. L. Kunkel.** 1995. TNF-alpha mediates recruitment of neutrophils and eosinophils during airway inflammation. *J Immunol* **154**:5411-5417.
15. **Tekkanat, K. K., H. F. Maassab, D. S. Cho, J. J. Lai, A. John, A. Berlin, M. H. Kaplan, and N. W. Lukacs.** 2001. IL-13-induced airway hyperreactivity during respiratory syncytial virus infection is STAT6 dependent. *J Immunol* **166**:3542-3548.
16. **Moore, M. L., M. H. Chi, C. Luongo, N. W. Lukacs, V. V. Polosukhin, M. M. Huckabee, D. C. Newcomb, U. J. Buchholz, J. E. Crowe, Jr., K. Goleniewska, J. V. Williams, P. L. Collins, and R. S. Peebles, Jr.** 2009. A chimeric A2 strain of respiratory syncytial virus (RSV) with the fusion protein of RSV strain line 19 exhibits enhanced viral load, mucus, and airway dysfunction. *J Virol* **83**:4185-4194.
17. **Graham, B. S., M. D. Perkins, P. F. Wright, and D. T. Karzon.** 1988. Primary respiratory syncytial virus infection in mice. *J Med Virol* **26**:153-162.
18. **Buchholz, U. J., H. Granzow, K. Schuldt, S. S. Whitehead, B. R. Murphy, and P. L. Collins.** 2000. Chimeric bovine respiratory syncytial virus with glycoprotein gene substitutions from human respiratory syncytial virus (HRSV): effects on host range and evaluation as a live-attenuated HRSV vaccine. *J Virol* **74**:1187-1199.

19. **Collins, P. L., M. G. Hill, E. Camargo, H. Grosfeld, R. M. Chanock, and B. R. Murphy.** 1995. Production of infectious human respiratory syncytial virus from cloned cDNA confirms an essential role for the transcription elongation factor from the 5' proximal open reading frame of the M2 mRNA in gene expression and provides a capability for vaccine development. *Proc Natl Acad Sci U S A* **92**:11563-11567.
20. **Kondo, N., K. Miyauchi, F. Meng, A. Iwamoto, and Z. Matsuda.** 2010. Conformational changes of the HIV-1 envelope protein during membrane fusion are inhibited by the replacement of its membrane-spanning domain. *J Biol Chem* **285**:14681-14688.
21. **Cabantous, S., T. C. Terwilliger, and G. S. Waldo.** 2005. Protein tagging and detection with engineered self-assembling fragments of green fluorescent protein. *Nat Biotechnol* **23**:102-107.
22. **Ishikawa, H., F. Meng, N. Kondo, A. Iwamoto, and Z. Matsuda.** 2012. Generation of a dual-functional split-reporter protein for monitoring membrane fusion using self-associating split GFP. *Protein Eng Des Sel* **25**:813-820.
23. **McLellan, J. S., M. Chen, S. Leung, K. W. Graepel, X. Du, Y. Yang, T. Zhou, U. Baxa, E. Yasuda, T. Beaumont, A. Kumar, K. Modjarrad, Z. Zheng, M. Zhao, N. Xia, P. D. Kwong, and B. S. Graham.** 2013. Structure of RSV Fusion Glycoprotein Trimer Bound to a Prefusion-Specific Neutralizing Antibody. *Science*.
24. **Pettersen, E. F., T. D. Goddard, C. C. Huang, G. S. Couch, D. M. Greenblatt, E. C. Meng, and T. E. Ferrin.** 2004. UCSF Chimera--a



- visualization system for exploratory research and analysis. *J Comput Chem* **25**:1605-1612.
25. **Bruder, D., A. Srikiatkachorn, and R. I. Enelow.** 2006. Cellular immunity and lung injury in respiratory virus infection. *Viral Immunol* **19**:147-155.
  26. **Moore, M. L., and R. S. Peebles, Jr.** 2006. Respiratory syncytial virus disease mechanisms implicated by human, animal model, and in vitro data facilitate vaccine strategies and new therapeutics. *Pharmacol Ther* **112**:405-424.
  27. **Johnson, J. E., R. A. Gonzales, S. J. Olson, P. F. Wright, and B. S. Graham.** 2007. The histopathology of fatal untreated human respiratory syncytial virus infection. *Mod Pathol* **20**:108-119.
  28. **Rawling, J., B. Garcia-Barreno, and J. A. Melero.** 2008. Insertion of the two cleavage sites of the respiratory syncytial virus fusion protein in Sendai virus fusion protein leads to enhanced cell-cell fusion and a decreased dependency on the HN attachment protein for activity. *J Virol* **82**:5986-5998.
  29. **Low, K. W., T. Tan, K. Ng, B. H. Tan, and R. J. Sugrue.** 2008. The RSV F and G glycoproteins interact to form a complex on the surface of infected cells. *Biochem Biophys Res Commun* **366**:308-313.
  30. **Heidema, J., M. V. Lukens, W. W. van Maren, M. E. van Dijk, H. G. Otten, A. J. van Vught, D. B. van der Werff, S. J. van Gestel, M. G. Semple, R. L. Smyth, J. L. Kimpen, and G. M. van Bleek.** 2007. CD8+ T cell responses in bronchoalveolar lavage fluid and

- peripheral blood mononuclear cells of infants with severe primary respiratory syncytial virus infections. *J Immunol* **179**:8410-8417.
31. **Yu, K. L., X. A. Wang, R. L. Civiello, A. K. Trehan, B. C. Pearce, Z. Yin, K. D. Combrink, H. B. Gulgeze, Y. Zhang, K. F. Kadow, C. W. Cianci, J. Clarke, E. V. Genovesi, I. Medina, L. Lamb, P. R. Wyde, M. Krystal, and N. A. Meanwell.** 2006. Respiratory syncytial virus fusion inhibitors. Part 3: Water-soluble benzimidazol-2-one derivatives with antiviral activity in vivo. *Bioorg Med Chem Lett* **16**:1115-1122.
  32. **Daley, J. M., A. A. Thomay, M. D. Connolly, J. S. Reichner, and J. E. Albina.** 2008. Use of Ly6G-specific monoclonal antibody to deplete neutrophils in mice. *J Leukoc Biol* **83**:64-70.
  33. **Foley, S. C., and Q. Hamid.** 2007. Images in allergy and immunology: neutrophils in asthma. *J Allergy Clin Immunol* **119**:1282-1286.
  34. **Tanabe, T., K. Fujimoto, M. Yasuo, K. Tsushima, K. Yoshida, H. Ise, and M. Yamaya.** 2008. Modulation of mucus production by interleukin-13 receptor alpha2 in the human airway epithelium. *Clin Exp Allergy* **38**:122-134.
  35. **Wills-Karp, M., J. Luyimbazi, X. Xu, B. Schofield, T. Y. Neben, C. L. Karp, and D. D. Donaldson.** 1998. Interleukin-13: central mediator of allergic asthma. *Science* **282**:2258-2261.
  36. **Herlocher, M. L., M. Ewasyshyn, S. Sambhara, M. Gharaee-Kermani, D. Cho, J. Lai, M. Klein, and H. F. Maassab.** 1999.

- Immunological properties of plaque purified strains of live attenuated respiratory syncytial virus (RSV) for human vaccine. *Vaccine* **17**:172-181.
37. **Anderson, J. J., J. Norden, D. Saunders, G. L. Toms, and R. Scott.** 1990. Analysis of the local and systemic immune responses induced in BALB/c mice by experimental respiratory syncytial virus infection. *J Gen Virol* **71 ( Pt 7)**:1561-1570.
38. **Waning, D. L., C. J. Russell, T. S. Jardetzky, and R. A. Lamb.** 2004. Activation of a paramyxovirus fusion protein is modulated by inside-out signaling from the cytoplasmic tail. *Proc Natl Acad Sci U S A* **101**:9217-9222.
39. **Apte-Sengupta, S., S. Negi, V. H. Leonard, N. Oezguen, C. K. Navaratnarajah, W. Braun, and R. Cattaneo.** 2012. Base of the measles virus fusion trimer head receives the signal that triggers membrane fusion. *J Biol Chem* **287**:33026-33035.
40. **Zhang, L., M. E. Peeples, R. C. Boucher, P. L. Collins, and R. J. Pickles.** 2002. Respiratory syncytial virus infection of human airway epithelial cells is polarized, specific to ciliated cells, and without obvious cytopathology. *J Virol* **76**:5654-5666.
41. **Zhang, L., P. L. Collins, R. A. Lamb, and R. J. Pickles.** 2011. Comparison of differing cytopathic effects in human airway epithelium of parainfluenza virus 5 (W3A), parainfluenza virus type 3, and respiratory syncytial virus. *Virology* **421**:67-77.
42. **Villenave, R., S. Thavagnanam, S. Sarlang, J. Parker, I. Douglas, G. Skibinski, L. G. Heaney, J. P. McKaigue, P. V. Coyle, M. D.**

- Shields, and U. F. Power.** 2012. In vitro modeling of respiratory syncytial virus infection of pediatric bronchial epithelium, the primary target of infection in vivo. *Proc Natl Acad Sci U S A* **109**:5040-5045.
43. **Villenave, R., O. Touzelet, S. Thavagnanam, S. Sarlang, J. Parker, G. Skibinski, L. G. Heaney, J. P. McKaigue, P. V. Coyle, M. D. Shields, and U. F. Power.** 2010. Cytopathogenesis of Sendai virus in well-differentiated primary pediatric bronchial epithelial cells. *J Virol* **84**:11718-11728.
44. **Luque, L. E., O. A. Bridges, J. N. Mason, K. L. Boyd, A. Portner, and C. J. Russell.** 2010. Residues in the heptad repeat a region of the fusion protein modulate the virulence of Sendai virus in mice. *J Virol* **84**:810-821.
45. **Smith, E. C., M. R. Culler, L. M. Hellman, M. G. Fried, T. P. Creamer, and R. E. Dutch.** 2012. Beyond anchoring: the expanding role of the hendra virus fusion protein transmembrane domain in protein folding, stability, and function. *J Virol* **86**:3003-3013.
46. **Walker, J. A., and Y. Kawaoka.** 1993. Importance of conserved amino acids at the cleavage site of the haemagglutinin of a virulent avian influenza A virus. *J Gen Virol* **74 ( Pt 2)**:311-314.
47. **Lee, J. K., A. Prussia, J. P. Snyder, and R. K. Plemper.** 2007. Reversible inhibition of the fusion activity of measles virus F protein by an engineered intersubunit disulfide bridge. *J Virol* **81**:8821-8826.

48. **DeVincenzo, J. P., C. M. El Saleeby, and A. J. Bush.** 2005. Respiratory syncytial virus load predicts disease severity in previously healthy infants. *J Infect Dis* **191**:1861-1868.
49. **Houben, M. L., F. E. Coenjaerts, J. W. Rossen, M. E. Belderbos, R. W. Hofland, J. L. Kimpen, and L. Bont.** 2010. Disease severity and viral load are correlated in infants with primary respiratory syncytial virus infection in the community. *J Med Virol* **82**:1266-1271.
50. **Wright, P. F., W. C. Gruber, M. Peters, G. Reed, Y. Zhu, F. Robinson, S. Coleman-Dockery, and B. S. Graham.** 2002. Illness severity, viral shedding, and antibody responses in infants hospitalized with bronchiolitis caused by respiratory syncytial virus. *J Infect Dis* **185**:1011-1018.
51. **Legg, J. P., I. R. Hussain, J. A. Warner, S. L. Johnston, and J. O. Warner.** 2003. Type 1 and type 2 cytokine imbalance in acute respiratory syncytial virus bronchiolitis. *Am J Respir Crit Care Med* **168**:633-639.
52. **Taylor, G., E. J. Stott, M. Hughes, and A. P. Collins.** 1984. Respiratory syncytial virus infection in mice. *Infect Immun* **43**:649-655.
53. **Stott, E. J., and G. Taylor.** 1985. Respiratory syncytial virus. Brief review. *Arch Virol* **84**:1-52.
54. **DeVincenzo, J. P.** 2005. Factors predicting childhood respiratory syncytial virus severity: what they indicate about pathogenesis. *Pediatr Infect Dis J* **24**:S177-183, discussion S182.
55. **Tayyari, F., D. Marchant, T. J. Moraes, W. Duan, P. Mastrangelo, and R. G. Hegele.** 2011. Identification of nucleolin as a

- cellular receptor for human respiratory syncytial virus. *Nat Med* **17**:1132-1135.
56. **Lukens, M. V., A. C. van de Pol, F. E. Coenjaerts, N. J. Jansen, V. M. Kamp, J. L. Kimpen, J. W. Rossen, L. H. Ulfman, C. E. Tacke, M. C. Viveen, L. Koenderman, T. F. Wolfs, and G. M. van Bleek.** 2010. A systemic neutrophil response precedes robust CD8(+) T-cell activation during natural respiratory syncytial virus infection in infants. *J Virol* **84**:2374-2383.
57. **Fujisawa, H.** 2008. Neutrophils play an essential role in cooperation with antibody in both protection against and recovery from pulmonary infection with influenza virus in mice. *J Virol* **82**:2772-2783.
58. **Tate, M. D., A. G. Brooks, and P. C. Reading.** 2008. The role of neutrophils in the upper and lower respiratory tract during influenza virus infection of mice. *Respir Res* **9**:57.
59. **Cannon, M. J., P. J. Openshaw, and B. A. Askonas.** 1988. Cytotoxic T cells clear virus but augment lung pathology in mice infected with respiratory syncytial virus. *J Exp Med* **168**:1163-1168.
60. **Sakai, S., H. Kawamata, N. Mantani, T. Kogure, Y. Shimada, K. Terasawa, T. Sakai, N. Imanishi, and H. Ochiai.** 2000. Therapeutic effect of anti-macrophage inflammatory protein 2 antibody on influenza virus-induced pneumonia in mice. *J Virol* **74**:2472-2476.
61. **Tate, M. D., L. J. Ioannidis, B. Croker, L. E. Brown, A. G. Brooks, and P. C. Reading.** 2011. The role of neutrophils during mild and severe influenza virus infections of mice. *PLoS One* **6**:e17618.

62. **Craig, A., J. Mai, S. Cai, and S. Jeyaseelan.** 2009. Neutrophil recruitment to the lungs during bacterial pneumonia. *Infect Immun* **77**:568-575.
63. **Xing, Z., M. Jordana, H. Kirpalani, K. E. Driscoll, T. J. Schall, and J. Gauldie.** 1994. Cytokine expression by neutrophils and macrophages in vivo: endotoxin induces tumor necrosis factor-alpha, macrophage inflammatory protein-2, interleukin-1 beta, and interleukin-6 but not RANTES or transforming growth factor-beta 1 mRNA expression in acute lung inflammation. *Am J Respir Cell Mol Biol* **10**:148-153.
64. **Smirnova, M. G., J. P. Birchall, and J. P. Pearson.** 2000. TNF-alpha in the regulation of MUC5AC secretion: some aspects of cytokine-induced mucin hypersecretion on the in vitro model. *Cytokine* **12**:1732-1736.
65. **Luttmann, W., T. Matthiesen, H. Matthys, and J. C. Virchow, Jr.** 1999. Synergistic effects of interleukin-4 or interleukin-13 and tumor necrosis factor-alpha on eosinophil activation in vitro. *Am J Respir Cell Mol Biol* **20**:474-480.
66. **Shim, J. J., K. Dabbagh, I. F. Ueki, T. Dao-Pick, P. R. Burgel, K. Takeyama, D. C. Tam, and J. A. Nadel.** 2001. IL-13 induces mucin production by stimulating epidermal growth factor receptors and by activating neutrophils. *Am J Physiol Lung Cell Mol Physiol* **280**:L134-140.
67. **Walter, D. M., J. J. McIntire, G. Berry, A. N. McKenzie, D. D. Donaldson, R. H. DeKruyff, and D. T. Umetsu.** 2001. Critical role

- for IL-13 in the development of allergen-induced airway hyperreactivity. *J Immunol* **167**:4668-4675.
68. **Krishnamoorthy, N., A. Khare, T. B. Oriss, M. Raundhal, C. Morse, M. Yarlagadda, S. E. Wenzel, M. L. Moore, R. S. Peebles, Jr., A. Ray, and P. Ray.** 2012. Early infection with respiratory syncytial virus impairs regulatory T cell function and increases susceptibility to allergic asthma. *Nat Med* **18**:1525-1530.
69. **Wenzel, S. E., S. J. Szefler, D. Y. Leung, S. I. Sloan, M. D. Rex, and R. J. Martin.** 1997. Bronchoscopic evaluation of severe asthma. Persistent inflammation associated with high dose glucocorticoids. *Am J Respir Crit Care Med* **156**:737-743.
70. **Zaitse, M., Y. Hamasaki, M. Matsuo, A. Kukita, K. Tsuji, M. Miyazaki, R. Hayasaki, E. Muro, S. Yamamoto, I. Kobayashi, T. Ichimaru, O. Kohashi, and S. Miyazaki.** 2000. New induction of leukotriene A(4) hydrolase by interleukin-4 and interleukin-13 in human polymorphonuclear leukocytes. *Blood* **96**:601-609.
71. **Pope, S. M., E. B. Brandt, A. Mishra, S. P. Hogan, N. Zimmermann, K. I. Matthaei, P. S. Foster, and M. E. Rothenberg.** 2001. IL-13 induces eosinophil recruitment into the lung by an IL-5- and eotaxin-dependent mechanism. *J Allergy Clin Immunol* **108**:594-601.



## CHAPTER 4: DISCUSSION

Despite the prevalence and morbidity of RSV in the United States and worldwide, an RSV vaccine still does not exist. The only available therapy is a humanized monoclonal antibody against the RSV F protein. This therapy is very expensive and only administered to high risk infants as defined by American Academy of Pediatrics (AAP) criteria (1). Unfortunately, those populations most at risk for severe RSV disease also represent difficult groups to immunize.

There are several major obstacles that stand in the way of successful RSV vaccine development. RSV causes yearly epidemics of respiratory infection. The peak of RSV illness is in infants 2-6 months of age. This early age of infection plays a role in development of severe disease because infection occurs when both the pulmonary and immune systems are immature (2). Infants under 6 months of age had significantly worse secretory antibody responses than older infants in two studies (3, 4). The IgA response may be important for viral clearance but is not correlated with neutralization activity (4). Neutralizing antibody responses against the surface glycoproteins F and G in animals are protective (5, 6), but poor immune protection is observed in infants. Despite the fact that infants have been shown to develop sufficient levels of neutralizing antibodies (7), this response is short-lived. In infants under six months of age, maternal antibody provides partial protection but may also interfere with the immunogenicity of live virus vaccines and vectors (8).

RSV's ability to evade or modulate innate immune response is a hindrance for successful vaccine development. The NS1 and NS2 are able to inhibit IFN-associated genes through IFN-regulatory factor 3 (IRF3) and signal transducer and activator of transcription 2 (STAT2) (9, 10). RSV can induce suppressor of cytokine signaling (SOCS) molecules to affect the type I IFN response (11), as well as activate and suppress signaling through several TLRs (12-14). RSV has mechanisms to inhibit TLR signaling through both myeloid differentiation factor 88 (MyD88) and mitochondrial antiviral signaling protein (MAVS) (15) as well as interfering with RIG-I signaling that would increase IFN production (16). For an infant whose innate immune response is already subdued, the loss of IFN can be a significant problem. The lack of this initial immune response may result in the spread of RSV from the upper airways to the lower respiratory tract.

RSV reinfection throughout life is also a significant obstacle to understanding the RSV immune response. Despite effective clearance of RSV in most cases, the virus is able to reinfect people multiple times. About half of children are reinfected during their second year of life (17), and children and adults are reinfected every three to ten years (18). Viruses that traditionally cause repeated infections, such as HIV and influenza, have significant genetic and antigenic diversity. Conversely, RSV is not particularly diverse and has highly conserved neutralizing antibody antigenic sites (2). It has been suggested that initial RSV infection alters the adaptive immune effector and memory responses. The reason for the failure of the FI-RSV vaccine has been purported to be a skewing of the helper T cell response towards  $T_H2$ . Upon rechallenge after vaccination, the  $T_H2$

skewing results in disease pathology (19). Reinfection following an initial natural infection may also cause a similar immune skewing.

The ambiguity of mechanisms of severe RSV disease in humans further poses an obstacle to the development of rational RSV therapies. The goal of our work was to better understand the airway mucus response in RSV infection. In the preceding chapters, we investigated how a clinical strain infection of BALB/c mice mirrors severe RSV infection in humans and the immune mechanisms of this illness, offering a useful model that is suitable for examining both innate and adaptive immune responses. Using the RSV strain 2-20 BALB/c model of severe RSV infection, we showed that the early innate immune response affects later adaptive T cell responses to RSV infection. Specifically, early higher viral RSV loads and pulmonary damage in BALB/c mice is linked to later Th2 cytokine response, airway mucin expression, and airway dysfunction. Depletion of neutrophils resulted in a decrease in TNF- $\alpha$  levels, IL-13+ CD4 T cells, and airway mucin expression. Therefore, neutrophils (innate response) affect the mucin T cell responses in RSV.

The RSV clinical isolates studied were isolated from both upper respiratory tract infections and lower respiratory tract infections and exhibited varying phenotypes in mice. Weight loss is commonly used as a marker of disease severity. The clinical isolates displayed differing weight loss patterns (Chapter 2 Fig. 1). RSV long and line 19 did not show any significant weight loss compared to mock. Considering their drastically different mucus expression patterns, it was

interesting that these two groups had similar patterns. On the other hand, these strains are closely related in terms of sequence; therefore, the region of the virus genome responsible for weight loss may be the same in these two strains.

Infection with A2001/2-20 and A2001/3-12, two clinical strains that are closely related sequence-wise, exhibited distinctive weight loss patterns. 3-12 showed only early weight loss while 2-20 infection resulted in a pattern of both early and late bimodal weight loss (Chapter 2, Fig. 1). These strains also differ in their IL-13 production (Chapter 2 Fig. 3), gob-5 expression (Chapter 2 Fig. 4), mucus expression (Chapter 2 Fig. 9). Table 1 summarizes the differences between A2, 3-12, and 2-20 below. Discrete amino acid differences within the genomes of these viruses may therefore be responsible for virulence differences. Interestingly, 2-20 and 3-12 exhibited similar viral loads (Chapter 2 Fig. 6), bronchiolar antigen staining (Chapter 2 Fig. 7), and histopathology (Chapter 2 Fig. 8) one day post-infection. These results suggest that the reasons for dissimilar mucus expression between 3-12 and 2-20 differ from those for line 19 and long. Additionally, infection with a chimeric virus expressing the line 19 fusion (F) protein in an A2 background resulted in significantly higher viral load in BALB/c mice compared to both the A2 and line 19 parent viruses (20). In this particular case, there may be a link between viral load and disease severity. In infants, peak viral load has been linked to disease severity in some studies (21). Peak viral load, however, does not seem to play a role in disease severity in 2-20 infection.

**Table 1: Comparison of RSV Clinical Isolate Characteristics**

	A2	3-12	2-20
<b>Disease Severity</b>	Low	Low	High
<b>Mucus</b>	No	No	Yes
<b>IL-13 protein</b>	Low	Low	High
<b>Passage Number</b>	Unknown (high)	11	11

We sought to examine both the role of the RSV fusion (F) protein as well as the role of neutrophils in mucus expression. The immune response to RSV is complex. Host factors include young age, prematurity, and underlying cardiopulmonary or immunosuppressive conditions (22). Virulence factors, however, are less defined. In the BALB/c mouse model, disease severity has previously been shown to be strain specific. Line 19, a subgroup A strain, was shown to induce more mucin, gob5 and MUC5AC mRNA and protein levels, IL-13 expression, and AHR compared to another group A strain (23). Interestingly, the F glycoprotein of RSV line 19 has only 6 amino acid differences compared to non-mucogenic strain RSV long, indicating small sequence differences may be important in pathogenesis (20). A number of studies have shown a correlation between the genome of RSV and the severity of illness in humans (24-27). One study reported that infection with group A RSV strains was associated with more severe illness compared to group B RSV strains among hospitalized infants (27), while another study linked RSV illness with a specific clade rather than subtype (24). These results suggest that strain sequence contributes to RSV disease.

The research outlined in Chapter 3 provides a basis for increased RSV 2-20 strain-induced disease severity in BALB/c mice compared to the A2 strain. The chimeric virus approach allows the specific study of a particular RSV gene and the elucidation of a molecular basis for pathogenesis differences. Our data showed that the F glycoprotein of RSV 2-20 plays a role in mucus expression. A2-2-20F showed a similar phenotype to its parent virus 2-20 versus the other parent virus, RSV A2. A2-2-20F resulted in a higher day one post-infection viral load (Chapter 3 Fig. 1), more interstitial pneumonia and necrotic cell debris within the airways (Chapter 3 Fig. 2), more mucin expression (Chapter 3 Fig. 3), and increased lung neutrophil infiltration (Chapter 3 Fig. 5) similar to RSV 2-20. Table 1 below summarizes these differences. Interestingly, the recombinant virus showed a slightly more severe phenotype than its parent virus 2-20. Because A2-2-20F expresses both A2 and 2-20 proteins, it most likely contains regions from each parent virus that contribute to increased virulence.

**Table 2: Comparison of Chimeric and Parent RSV Strains**

	A2	A2001/2-20	A2-2-20F
<b>Viral Load</b>	Highest on d 4 p.i.	Higher than A2 on d 1 p.i.	Higher than A2 on d 1 p.i.
<b>Weight loss</b>	Early only	bimodal	Similar to 2-20 (data not shown)
<b>Histologic features (d 1 p.i.)</b>	Less interstitial pneumonia (IP), perivascular edema (PE), and airway necrotic cell debris	PE, airway necrotic cell debris, bronchiolar luminal debris	Greater IP than A2 airway necrotic cell debris
<b>PAS Positivity</b>	Not significant compared to mock	Significantly more than mock and A2	Significantly more than mock and A2
<b><i>In vitro</i> fusion activity</b>	No boost with A2 G	Boost with 2-20 G	Boost with A2 G

There are 15 amino acid differences between the RSV A2 and 2-20 F proteins (Fig. 2). Five of these residues are not present in the mature protein because they are part of the signal peptide that directs the FO precursor to the ER. The last three residues, 519, 524, and 574, are located near the membrane and may influence protein interactions with membrane lipids. For example, a tryptophan-rich motif in the membrane-proximal region of HIV type 1 gp41 protein is important for glycoprotein-mediated fusion (28). Residues 63, 66, and 76 form a cluster at the tip of the DIII domain that may be important in the protein's metastability (29). In paramyxovirus fusion, the F is thought to initially fold into a metastable form that subsequently undergoes discrete conformational changes to a lower energy state (30). Amino acid 124 is present within a 27 amino acid long peptide, pep27, which is flanked by two furin cleavage sites that allows for its cleavage and secretion. These two cleavage sites are also present in the closely related bovine RSV (31). In bovine RSV, pep27 is secreted by infected cells and has homology to substance P, a peptide hormone (32). The pep27 cleaved from human RSV, however, does not contain this motif, and its function in human RSV remains unknown. Residues 103 and 152 putatively cluster around the area containing pep27 and amino acid 27. This may represent an area of interest in the RSV F protein. Lastly, residue 384 is present where the head and stalk regions of the protein meet. Residues in this area were previously shown to be important for metastability and fusion in the measles virus. Introduction of a disulfide bond at the intersection of the F head and stalk domains abolished fusion (33). Stabilizing reactions in this region in RSV A2 may decrease fusion activity compared to 2-20.

A2	1	MELLILKANAITTILTAVLFCFASGONITEEFYQSTCSAVSKGYLSALRT
2-20	1	MELPILKTNAITTILAAVTLCFASSONITEEFYQSTCSAVSKGYLSALRT
A2	51	GWYTSVITIELSNIKKNCNGTDAKIKLIKQELDKYKNAVTELOLLMQST
2-20	51	GWYTSVITIELSTIKENKNCNGTDAKIKLIKQELDKYKNAVTELOLLMQST
A2	101	PATNNRARRELPRFMNYTLNNAKKTNVTLSSKKRKRFLGFLGVSASIAS
2-20	101	PAANNRARRELPRFMNYTLNNAKKNVTLSSKKRKRFLGFLGVSASIAS
A2	151	GVAVSKVLHLEGEVNKIKSALLSTNKAVVSLNGVSVLTSKVLDLKNYID
2-20	151	GVAVSKVLHLEGEVNKIKSALLSTNKAVVSLNGVSVLTSKVLDLKNYID
A2	201	KQLLPVVKQSCSISNIETVIEFQQKNRLLIETREFSVNAGVTTPVSTY
2-20	201	KQLLPVVKQSCSISNIETVIEFQQKNRLLIETREFSVNAGVTTPVSTY
A2	251	MLTNSELLSLINDMPITNDQKKLMSNNVQIVRQQSYSIMSIIKEEVLAYV
2-20	251	MLTNSELLSLINDMPITNDQKKLMSNNVQIVRQQSYSIMSIIKEEVLAYV
A2	301	VQLPLYGVIDTPCWKLHTSPLCTTNTKEGSNICLRTDRGWYCDNAGSVS
2-20	301	VQLPLYGVIDTPCWKLHTSPLCTTNTKEGSNICLRTDRGWYCDNAGSVS
A2	351	FFPQAETCKVQSNRVFCDTMNSLTLPSEVNLCNVIDIFNPKYDCKIMTSKT
2-20	351	FFPQAETCKVQSNRVFCDTMNSLTLPSEVNLCNVIDIFNPKYDCKIMTSKT
A2	401	DVSSSVITSLGAIVSCYGKTKCTASNKNRGIKTF SNGCDYVSNKGVDTV
2-20	401	DVSSSVITSLGAIVSCYGKTKCTASNKNRGIKTF SNGCDYVSNKGVDTV
A2	451	SVGNTLYYVVKQEGKSLYVKGEPIINFYDPLVFPSEFDASISQVNEKIN
2-20	451	SVGNTLYYVVKQEGKSLYVKGEPIINFYDPLVFPSEFDASISQVNEKIN
A2	501	QSLAFIRKSDELLHVNVAVKSTTNIMITTIIVIIVILLSLIAVGLLLYC
2-20	501	QSLAFIRKSDELLHVNVAVKSTTKIMITTIIVIIVILLSLIAVGLLLYC
A2	551	KARSTPVTLSKDQLSGINNIAFSN
2-20	551	KARSTPVTLSKDQLSGINNIAFSS

**Figure 1.** Sequence alignment of A2 and 2-20 F proteins. This alignment was generated using T-Coffee (34) and BOXSHADE.



The observed increase in pathogenesis of A2-2-20F and 2-20 may also be due to the interaction of the F and G proteins. The level of 2-20 F-induced fusion increased when it was co-transfected with either 2-20 G or A2 G. Co-transfection of A2 F with its cognate G did not result in increased fusion compared to F alone (Chapter 3, Fig. 4). These proteins form a complex on the surface of infected cells (35). Membrane fusion of several paramyxoviruses is initiated by a complex of the fusion and attachment proteins. The binding of the attachment protein to the cell surface receptor induces a conformational change in the fusion protein, which mediates fusion activity (30). The G protein mediates attachment because antibodies to G block RSV cell binding while F antibodies do not (36). Recently, nucleolin was identified as a functional cell receptor for RSV. Nucleolin was shown to interact with F, however, not G as expected (37). Thus, nucleolin may be important for RSV entry, although the wide cell type distribution of nucleolin suggests this protein does not determine tropism. Surface glycosaminoglycans (GAGs), specifically heparan sulfates, which interact with G have been shown to be important for RSV infection (38, 39). A RSV G deletion virus showed that this protein is not required for RSV replication *in vitro*, but deletion did result in attenuated viral load and pathogenesis *in vivo* (40). Therefore, although not explicitly required for replication, G has an important function in replication. Our data show that, in the *in vitro* fusion assay, the function of F depends on its interaction with G for RSV 2-20 glycoprotein. Two non-mutually exclusive hypotheses could explain this. First G and F directly interact to promote fusion. Second, the ability of G to attach to cells brings F and its target membrane in proximity to promote fusion.

Stability of pre-fusion F during virus-to-cell fusion may also be affected by RSV F and G interactions. Specifically, this hypothesized G-F interaction may be important because paramyxoviruses have evolved separate receptor-binding proteins that trigger F proteins after binding to the target cell. Mutations that disrupt the interactions between the attachment and fusion proteins decrease membrane fusion (41, 42). Paramyxoviruses have also evolved metastable F proteins that couple the energy released from refolding to the work of membrane fusion (43). This energy barrier must be able to prevent nonspecific activation but also be small enough to actually allow triggering once binding has occurred (44). Several F protein residues have been shown to be important for maintenance of this kinetic barrier. Mutations in these residues lead to both increased activation and indiscriminant activation of the F protein (45). The thermal stability of the RSV F protein may be related to the kinetic barrier required for paramyxovirus fusion. Virus stocks of A2, 2-20, and A2-2-20F were thawed and exposed to 48°C, 50°C, 52°C, and 54°C for 10 minutes. The infectivity of heat-treated stocks was determined by plaque assay. RSV A2 infectivity was much more heat-resistant than both 2-20 and A2-2-20F. At 48°C, A2-2-20F showed an intermediate phenotype between its parent viruses (Fig. 1A and B). These results indicate that the stability of A2 may prevent some fusion activity (Chapter 3 Fig. 4).

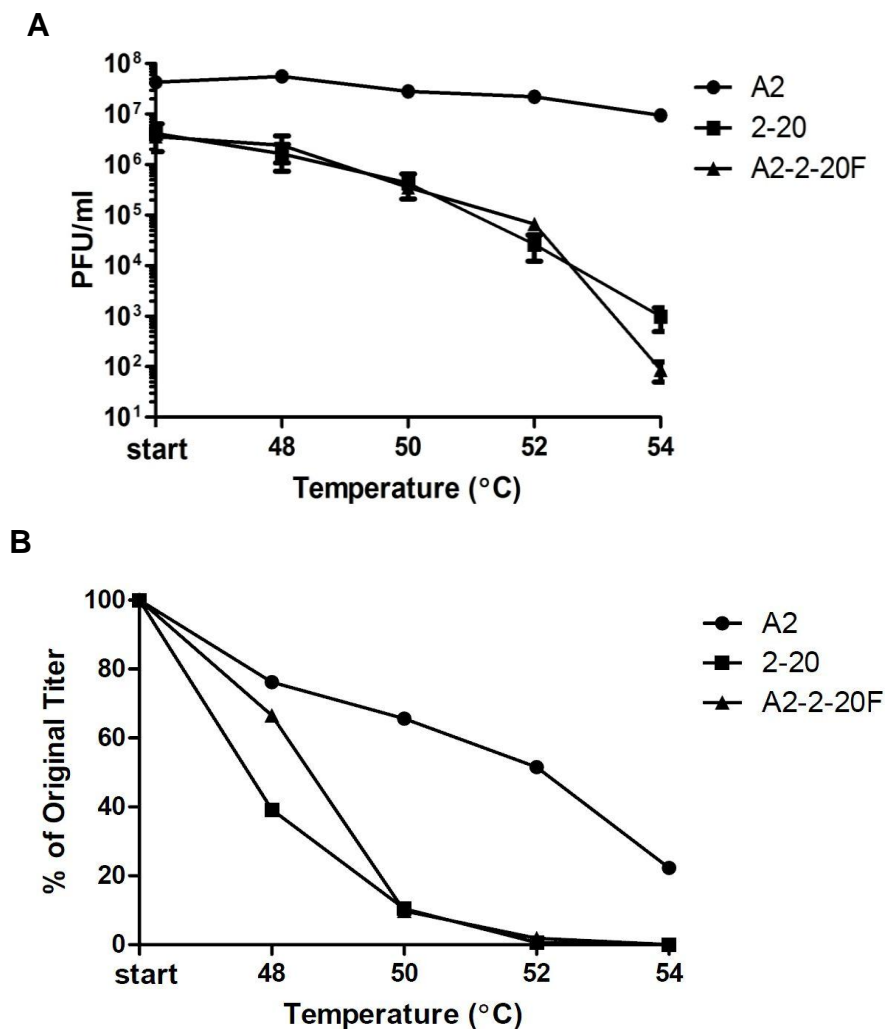


**Figure 2.** Thermostability of RSV Strains. RSV stocks were thawed and exposed to indicated temperatures for 10 minutes. Infectious yields of heat-treated stocks was then determined through plaque assay. (A) Virus titrations after heat treatment. (B) The % loss of infectivity of RSV A2, 2-20, and A2-2-20F after heat treatment, based on the original titer.

Our data demonstrates that that the early neutrophil response to RSV infection influences the later T cell response. When neutrophils were depleted in RSV-infected mice, we observed decreased airway mucin expression compared to

isotype-treated mice (Chapter 3 Fig. 9), less TNF- $\alpha$  production (Chapter 3 Fig. 10), and less IL-13<sup>+</sup> CD4 T cells (Chapter 3 Fig. 11) compared to isotype-treated controls. The precise mechanism by which neutrophil influence the RSV-induced mucus response is unknown. In a murine model of the parasite schistosomiasis japonica, greater granulomatous inflammation was seen in mice deficient in IL-4 and IL-13 compared to wild-type mice. Because increased IFN- $\gamma$  was not observed, the inflammation was likely not due to a T<sub>h</sub>1/T<sub>h</sub>2 imbalance. These findings indicate that IL-13 suppresses excessive neutrophil recruitment and cytokine production (46). In our model, IL-13 may be made in response to lung neutrophil infiltration during RSV infection. Early neutrophil levels were significantly higher than those seen at later time points (Chapter 3 Fig. 6). We also did not observe an effect on IFN- $\gamma$ <sup>+</sup> CD8 T cells in our model. Neutrophils are potent producers of chemokines that recruit further immune cells to the site of infection. Preliminary data indicates that A2-2-20F infection results in increased MIP-1 $\alpha$  expression (data not shown). TNF- $\alpha$  administration resulted in increased neutrophil infiltration as well as MIP-1 $\alpha$  upregulation in a mouse model of acute inflammation using the murine air pouch (47). MIP-1 $\alpha$  has been shown to regulate CD4<sup>+</sup> T cell chemotaxis in *Pseudomonas aeruginosa* corneal infection (48). Therefore, chemokine production during the neutrophil response may affect the subsequent T cell response. Further experiments will have to be performed in order to determine the exact mechanism at work in this TNF- $\alpha$  and IL-13 pathway.

One caveat of our chosen RSV pathogenesis model is that mice have important genetic and structural differences compared to humans. Mice, however, offer a tractable system in which to study the interplay of host and viral factors for disease. The study of host genetics and RSV pathogenesis in humans has been limited to specific individual genes thought to be involved in the regulation of the immune response. There have been polymorphisms in over 30 genes associated with RSV pathogenesis (49). Examples include innate immune genes such as IFNA5 and nitric oxide synthase 2 (NOS2A) (50). Polymorphisms in neutrophil-related genes have also been implicated in severe RSV disease. For example, specific polymorphisms in the receptor CCR5 have been associated with severe bronchiolitis. CCR5 is the receptor for chemokine that recruit immune cells such as T cells and neutrophils (51). A forward genetics study found that a particular gene that conferred susceptibility to herpesviruses in mice correlated with clinical data from humans (52, 53). Forward genetics of strain variability in the mouse model may help to identify RSV susceptibility genes with clinical correlates in humans.

We have shown the mucus over-production lead to RSV pathogenesis (Chapters 2 and 3). Excess mucous secretion is a key feature of lung disease such as asthma and chronic obstructive pulmonary disease (COPD) (54, 55). Mucus, however, is a necessary for protection of the airways. There are considerable benefits to having low levels of mucus in the airways, including the ability to trap and eliminated inhaled particles and to desiccation of airway surfaces (56). In Gob-5 deficient mice, significant BAL inflammation was observed as compared with

wild-type mice (57). It is unclear how Gob-5 or MUC5AC deficiency would affect RSV clearance. Therapies to target mucin over-production may be useful but one must be careful not to cause below baseline mucus levels.

In BALB/c mice, RSV symptoms such as breathing difficulty and mucin expression occur either during or after viral clearance. CD4+ and CD8+ T cells are recruited during viral clearance (Figure 3). Therefore, therapies to target immune responses rather than induce viral clearance may be useful in some cases. A thorough understanding of the mechanisms by which RSV infection induces mucus and the role of various immune system cells in this system will provide an opportunity for specific therapies to combat mucin over-production and mucin-induced airway obstruction in RSV. The current study has highlighted the importance of particular strains in RSV-induced mucin expression.

Therefore, the choice of strain for RSV pathogenesis studies is important, as well as the strain employed in vaccine challenge studies. Additionally, as previously stated, the failure of animal models to fully recapitulate acute RSV pathogenesis has been a critical shortcoming in the RSV field. We purport that RSV 2-20 is a suitable model for the study of severe RSV disease in an animal model.

Examining variation among the F and G proteins of RSV is also relevant for vaccine strategies because variation in these proteins affects neutralizing antibody sites important for vaccine efficacy. A recently published crystal structure the RSV prefusion F revealed neutralizing antigenic sites unique to the prefusion form (58). Sequence differences between strains may affect these particular sites.

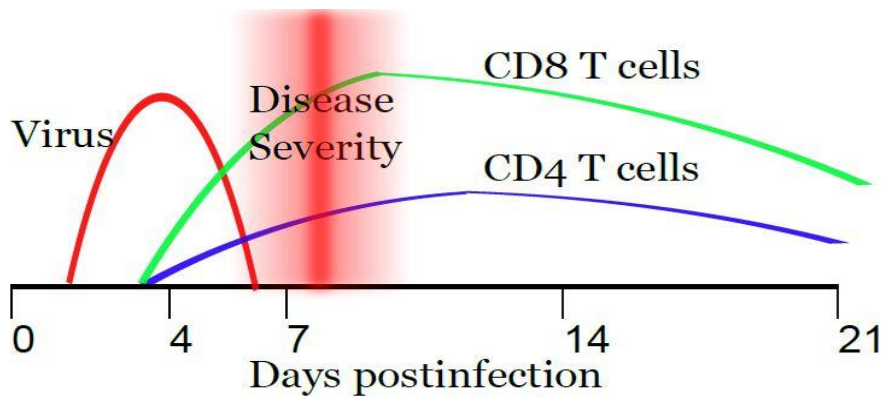


Figure 3. Overview of the T cell events in viral clearance and disease. Virus peaks on approximately day four post-infection. Virus is eliminated between days 5 and 8, during which CD4 and CD8 T cells are recruited (59).

We have shown that both viral proteins and the host immune system play a role in mucus production during RSV infection. Sequence differences within the F protein resulted in epithelial damage in infected mice, a vigorous neutrophil response, and robust mucin expression. Additional research is needed to completely understand the complicated interplay between virus and host in RSV infection. Elucidating determinants of RSV airway pathology may have future implications for RSV treatment.

## REFERENCES

1. **Jafri, H. S.** 2003. Treatment of respiratory syncytial virus: antiviral therapies. *Pediatr Infect Dis J* **22**:S89-92; discussion S92-83.
2. **Graham, B. S.** 2011. Biological challenges and technological opportunities for respiratory syncytial virus vaccine development. *Immunol Rev* **239**:149-166.
3. **Kaul, T. N., R. C. Welliver, D. T. Wong, R. A. Udwadia, K. Riddlesberger, and P. L. Ogra.** 1981. Secretory antibody response to respiratory syncytial virus infection. *Am J Dis Child* **135**:1013-1016.
4. **McIntosh, K., H. B. Masters, I. Orr, R. K. Chao, and R. M. Barkin.** 1978. The immunologic response to infection with respiratory syncytial virus in infants. *J Infect Dis* **138**:24-32.
5. **Walsh, E. E., J. J. Schlesinger, and M. W. Brandriss.** 1984. Protection from respiratory syncytial virus infection in cotton rats by passive transfer of monoclonal antibodies. *Infect Immun* **43**:756-758.
6. **Walsh, E. E., C. B. Hall, M. Briselli, M. W. Brandriss, and J. J. Schlesinger.** 1987. Immunization with glycoprotein subunits of respiratory syncytial virus to protect cotton rats against viral infection. *J Infect Dis* **155**:1198-1204.
7. **Shinoff, J. J., K. L. O'Brien, B. Thumar, J. B. Shaw, R. Reid, W. Hua, M. Santosham, and R. A. Karron.** 2008. Young infants can develop protective levels of neutralizing antibody after infection with respiratory syncytial virus. *J Infect Dis* **198**:1007-1015.



8. **Anderson, L. J., P. R. Dormitzer, D. J. Nokes, R. Rappuoli, A. Roca, and B. S. Graham.** 2013. Strategic priorities for respiratory syncytial virus (RSV) vaccine development. *Vaccine* **31 Suppl 2**:B209-215.
9. **Lo, M. S., R. M. Brazas, and M. J. Holtzman.** 2005. Respiratory syncytial virus nonstructural proteins NS1 and NS2 mediate inhibition of Stat2 expression and alpha/beta interferon responsiveness. *J Virol* **79**:9315-9319.
10. **Spann, K. M., K. C. Tran, and P. L. Collins.** 2005. Effects of nonstructural proteins NS1 and NS2 of human respiratory syncytial virus on interferon regulatory factor 3, NF-kappaB, and proinflammatory cytokines. *J Virol* **79**:5353-5362.
11. **Hashimoto, K., K. Ishibashi, K. Ishioka, D. Zhao, M. Sato, S. Ohara, Y. Abe, Y. Kawasaki, Y. Sato, S. Yokota, N. Fujii, R. S. Peebles, Jr., M. Hosoya, and T. Suzutani.** 2009. RSV replication is attenuated by counteracting expression of the suppressor of cytokine signaling (SOCS) molecules. *Virology* **391**:162-170.
12. **Murawski, M. R., G. N. Bowen, A. M. Cerny, L. J. Anderson, L. M. Haynes, R. A. Tripp, E. A. Kurt-Jones, and R. W. Finberg.** 2009. Respiratory syncytial virus activates innate immunity through Toll-like receptor 2. *J Virol* **83**:1492-1500.
13. **Rallabhandi, P., R. L. Phillips, M. S. Boukhvalova, L. M. Pletneva, K. A. Shirey, T. L. Gioannini, J. P. Weiss, J. C. Chow, L. D. Hawkins, S. N. Vogel, and J. C. Blanco.** 2012. Respiratory

syncytial virus fusion protein-induced toll-like receptor 4 (TLR4) signaling is inhibited by the TLR4 antagonists Rhodobacter sphaeroides lipopolysaccharide and eritoran (E5564) and requires direct interaction with MD-2. *MBio* **3**.

14. **Lukacs, N. W., J. J. Smit, S. Mukherjee, S. B. Morris, G. Nunez, and D. M. Lindell.** 2010. Respiratory virus-induced TLR7 activation controls IL-17-associated increased mucus via IL-23 regulation. *J Immunol* **185**:2231-2239.
15. **Bhoj, V. G., Q. Sun, E. J. Bhoj, C. Somers, X. Chen, J. P. Torres, A. Mejias, A. M. Gomez, H. Jafri, O. Ramilo, and Z. J. Chen.** 2008. MAVS and MyD88 are essential for innate immunity but not cytotoxic T lymphocyte response against respiratory syncytial virus. *Proc Natl Acad Sci U S A* **105**:14046-14051.
16. **Ling, Z., K. C. Tran, and M. N. Teng.** 2009. Human respiratory syncytial virus nonstructural protein NS2 antagonizes the activation of beta interferon transcription by interacting with RIG-I. *J Virol* **83**:3734-3742.
17. **Henderson, F. W., A. M. Collier, W. A. Clyde, Jr., and F. W. Denny.** 1979. Respiratory-syncytial-virus infections, reinfections and immunity. A prospective, longitudinal study in young children. *N Engl J Med* **300**:530-534.
18. **Hall, C. B., E. E. Walsh, C. E. Long, and K. C. Schnabel.** 1991. Immunity to and frequency of reinfection with respiratory syncytial virus. *J Infect Dis* **163**:693-698.

19. **Openshaw, P. J.** 1995. Immunity and immunopathology to respiratory syncytial virus. The mouse model. *Am J Respir Crit Care Med* **152**:S59-62.
20. **Moore, M. L., M. H. Chi, C. Luongo, N. W. Lukacs, V. V. Polosukhin, M. M. Huckabee, D. C. Newcomb, U. J. Buchholz, J. E. Crowe, Jr., K. Goleniewska, J. V. Williams, P. L. Collins, and R. S. Peebles, Jr.** 2009. A chimeric A2 strain of respiratory syncytial virus (RSV) with the fusion protein of RSV strain line 19 exhibits enhanced viral load, mucus, and airway dysfunction. *J Virol* **83**:4185-4194.
21. **DeVincenzo, J. P., C. M. El Saleeby, and A. J. Bush.** 2005. Respiratory syncytial virus load predicts disease severity in previously healthy infants. *J Infect Dis* **191**:1861-1868.
22. **Parrott, R. H., H. W. Kim, J. O. Arrobio, D. S. Hodes, B. R. Murphy, C. D. Brandt, E. Camargo, and R. M. Chanock.** 1973. Epidemiology of respiratory syncytial virus infection in Washington, D.C. II. Infection and disease with respect to age, immunologic status, race and sex. *Am J Epidemiol* **98**:289-300.
23. **Lukacs, N. W., M. L. Moore, B. D. Rudd, A. A. Berlin, R. D. Collins, S. J. Olson, S. B. Ho, and R. S. Peebles, Jr.** 2006. Differential immune responses and pulmonary pathophysiology are induced by two different strains of respiratory syncytial virus. *Am J Pathol* **169**:977-986.
24. **Martinello, R. A., M. D. Chen, C. Weibel, and J. S. Kahn.** 2002. Correlation between respiratory syncytial virus genotype and severity of illness. *J Infect Dis* **186**:839-842.

25. **Hall, C. B., E. E. Walsh, K. C. Schnabel, C. E. Long, K. M. McConnochie, S. W. Hildreth, and L. J. Anderson.** 1990. Occurrence of groups A and B of respiratory syncytial virus over 15 years: associated epidemiologic and clinical characteristics in hospitalized and ambulatory children. *J Infect Dis* **162**:1283-1290.
26. **Scott, P. D., R. Ochola, M. Ngama, E. A. Okiro, D. J. Nokes, G. F. Medley, and P. A. Cane.** 2004. Molecular epidemiology of respiratory syncytial virus in Kilifi district, Kenya. *J Med Virol* **74**:344-354.
27. **Walsh, E. E., K. M. McConnochie, C. E. Long, and C. B. Hall.** 1997. Severity of respiratory syncytial virus infection is related to virus strain. *J Infect Dis* **175**:814-820.
28. **Salzwedel, K., J. T. West, and E. Hunter.** 1999. A conserved tryptophan-rich motif in the membrane-proximal region of the human immunodeficiency virus type 1 gp41 ectodomain is important for Env-mediated fusion and virus infectivity. *J Virol* **73**:2469-2480.
29. **Yin, H. S., X. Wen, R. G. Paterson, R. A. Lamb, and T. S. Jardetzky.** 2006. Structure of the parainfluenza virus 5 F protein in its metastable, prefusion conformation. *Nature* **439**:38-44.
30. **Dutch, R. E., T. S. Jardetzky, and R. A. Lamb.** 2000. Virus membrane fusion proteins: biological machines that undergo a metamorphosis. *Biosci Rep* **20**:597-612.
31. **Begona Ruiz-Arguello, M., L. Gonzalez-Reyes, L. J. Calder, C. Palomo, D. Martin, M. J. Saiz, B. Garcia-Barreno, J. J. Skehel, and J. A. Melero.** 2002. Effect of proteolytic processing at two distinct

- sites on shape and aggregation of an anchorless fusion protein of human respiratory syncytial virus and fate of the intervening segment. *Virology* **298**:317-326.
32. **Zimmer, G., M. Rohn, G. P. McGregor, M. Schemann, K. K. Conzelmann, and G. Herrler.** 2003. Virokinin, a bioactive peptide of the tachykinin family, is released from the fusion protein of bovine respiratory syncytial virus. *J Biol Chem* **278**:46854-46861.
33. **Lee, J. K., A. Prussia, J. P. Snyder, and R. K. Plemper.** 2007. Reversible inhibition of the fusion activity of measles virus F protein by an engineered intersubunit disulfide bridge. *J Virol* **81**:8821-8826.
34. **Notredame, C., D. G. Higgins, and J. Heringa.** 2000. T-Coffee: A novel method for fast and accurate multiple sequence alignment. *J Mol Biol* **302**:205-217.
35. **Low, K. W., T. Tan, K. Ng, B. H. Tan, and R. J. Sugrue.** 2008. The RSV F and G glycoproteins interact to form a complex on the surface of infected cells. *Biochem Biophys Res Commun* **366**:308-313.
36. **Levine, S., R. Klaiber-Franco, and P. R. Paradiso.** 1987. Demonstration that glycoprotein G is the attachment protein of respiratory syncytial virus. *J Gen Virol* **68 ( Pt 9)**:2521-2524.
37. **Tayyari, F., D. Marchant, T. J. Moraes, W. Duan, P. Mastrangelo, and R. G. Hegele.** 2011. Identification of nucleolin as a cellular receptor for human respiratory syncytial virus. *Nat Med* **17**:1132-1135.

38. **Techarpornkul, S., P. L. Collins, and M. E. Peeples.** 2002. Respiratory syncytial virus with the fusion protein as its only viral glycoprotein is less dependent on cellular glycosaminoglycans for attachment than complete virus. *Virology* **294**:296-304.
39. **Feldman, S. A., S. Audet, and J. A. Beeler.** 2000. The fusion glycoprotein of human respiratory syncytial virus facilitates virus attachment and infectivity via an interaction with cellular heparan sulfate. *J Virol* **74**:6442-6447.
40. **Karron, R. A., D. A. Buonagurio, A. F. Georgiu, S. S. Whitehead, J. E. Adamus, M. L. Clements-Mann, D. O. Harris, V. B. Randolph, S. A. Udem, B. R. Murphy, and M. S. Sidhu.** 1997. Respiratory syncytial virus (RSV) SH and G proteins are not essential for viral replication in vitro: clinical evaluation and molecular characterization of a cold-passaged, attenuated RSV subgroup B mutant. *Proc Natl Acad Sci U S A* **94**:13961-13966.
41. **Deng, R., Z. Wang, P. J. Mahon, M. Marinello, A. Mirza, and R. M. Iorio.** 1999. Mutations in the Newcastle disease virus hemagglutinin-neuraminidase protein that interfere with its ability to interact with the homologous F protein in the promotion of fusion. *Virology* **253**:43-54.
42. **Gravel, K. A., and T. G. Morrison.** 2003. Interacting domains of the HN and F proteins of newcastle disease virus. *J Virol* **77**:11040-11049.
43. **Russell, C. J., T. S. Jardetzky, and R. A. Lamb.** 2001. Membrane fusion machines of paramyxoviruses: capture of intermediates of fusion. *EMBO J* **20**:4024-4034.

44. **Russell, C. J., T. S. Jardetzky, and R. A. Lamb.** 2004. Conserved glycine residues in the fusion peptide of the paramyxovirus fusion protein regulate activation of the native state. *J Virol* **78**:13727-13742.
45. **Paterson, R. G., C. J. Russell, and R. A. Lamb.** 2000. Fusion protein of the paramyxovirus SV5: destabilizing and stabilizing mutants of fusion activation. *Virology* **270**:17-30.
46. **Inoue, D., M. Yamaya, H. Kubo, T. Sasaki, M. Hosoda, M. Numasaki, Y. Tomioka, H. Yasuda, K. Sekizawa, H. Nishimura, and H. Sasaki.** 2006. Mechanisms of mucin production by rhinovirus infection in cultured human airway epithelial cells. *Respir Physiol Neurobiol* **154**:484-499.
47. **Tessier, P. A., P. H. Naccache, I. Clark-Lewis, R. P. Gladue, K. S. Neote, and S. R. McColl.** 1997. Chemokine networks in vivo: involvement of C-X-C and C-C chemokines in neutrophil extravasation in vivo in response to TNF-alpha. *J Immunol* **159**:3595-3602.
48. **Kernacki, K. A., R. P. Barrett, S. McClellan, and L. D. Hazlett.** 2001. MIP-1alpha regulates CD4+ T cell chemotaxis and indirectly enhances PMN persistence in *Pseudomonas aeruginosa* corneal infection. *J Leukoc Biol* **70**:911-919.
49. **Miyairi, I., and J. P. DeVincenzo.** 2008. Human genetic factors and respiratory syncytial virus disease severity. *Clin Microbiol Rev* **21**:686-703.
50. **Janssen, R., L. Bont, C. L. Siezen, H. M. Hodemaekers, M. J. Ermers, G. Doornbos, R. van 't Slot, C. Wijmenga, J. J. Goeman,**

- J. L. Kimpen, H. C. van Houwelingen, T. G. Kimman, and B. Hoebe.** 2007. Genetic susceptibility to respiratory syncytial virus bronchiolitis is predominantly associated with innate immune genes. *J Infect Dis* **196**:826-834.
51. **Hull, J., K. Rowlands, E. Lockhart, C. Moore, M. Sharland, and D. Kwiatkowski.** 2003. Variants of the chemokine receptor CCR5 are associated with severe bronchiolitis caused by respiratory syncytial virus. *J Infect Dis* **188**:904-907.
52. **Casrouge, A., S. Y. Zhang, C. Eidenschenk, E. Jouanguy, A. Puel, K. Yang, A. Alcais, C. Picard, N. Mahfoufi, N. Nicolas, L. Lorenzo, S. Plancoulaine, B. Senechal, F. Geissmann, K. Tabeta, K. Hoebe, X. Du, R. L. Miller, B. Heron, C. Mignot, T. B. de Villemeur, P. Lebon, O. Dulac, F. Rozenberg, B. Beutler, M. Tardieu, L. Abel, and J. L. Casanova.** 2006. Herpes simplex virus encephalitis in human UNC-93B deficiency. *Science* **314**:308-312.
53. **Tabeta, K., K. Hoebe, E. M. Janssen, X. Du, P. Georgel, K. Crozat, S. Mudd, N. Mann, S. Sovath, J. Goode, L. Shamel, A. A. Herskovits, D. A. Portnoy, M. Cooke, L. M. Tarantino, T. Wiltshire, B. E. Steinberg, S. Grinstein, and B. Beutler.** 2006. The Unc93b1 mutation 3d disrupts exogenous antigen presentation and signaling via Toll-like receptors 3, 7 and 9. *Nat Immunol* **7**:156-164.
54. **Dunnill, M. S.** 1960. The pathology of asthma, with special reference to changes in the bronchial mucosa. *J Clin Pathol* **13**:27-33.



55. **Vestbo, J.** 2005. Chronic mucus hypersecretion, exacerbations and natural history of COPD. *Exp Lung Res* **31 Suppl 1**:63-65.
56. **Williams, O. W., A. Sharafkhaneh, V. Kim, B. F. Dickey, and C. M. Evans.** 2006. Airway mucus: From production to secretion. *Am J Respir Cell Mol Biol* **34**:527-536.
57. **Long, A. J., J. P. Sypek, R. Askew, S. C. Fish, L. E. Mason, C. M. Williams, and S. J. Goldman.** 2006. Gob-5 contributes to goblet cell hyperplasia and modulates pulmonary tissue inflammation. *Am J Respir Cell Mol Biol* **35**:357-365.
58. **McLellan, J. S., M. Chen, S. Leung, K. W. Graepel, X. Du, Y. Yang, T. Zhou, U. Baxa, E. Yasuda, T. Beaumont, A. Kumar, K. Modjarrad, Z. Zheng, M. Zhao, N. Xia, P. D. Kwong, and B. S. Graham.** 2013. Structure of RSV Fusion Glycoprotein Trimer Bound to a Prefusion-Specific Neutralizing Antibody. *Science*.
59. **Openshaw, P. J., and J. S. Tregoning.** 2005. Immune responses and disease enhancement during respiratory syncytial virus infection. *Clin Microbiol Rev* **18**:541-555.